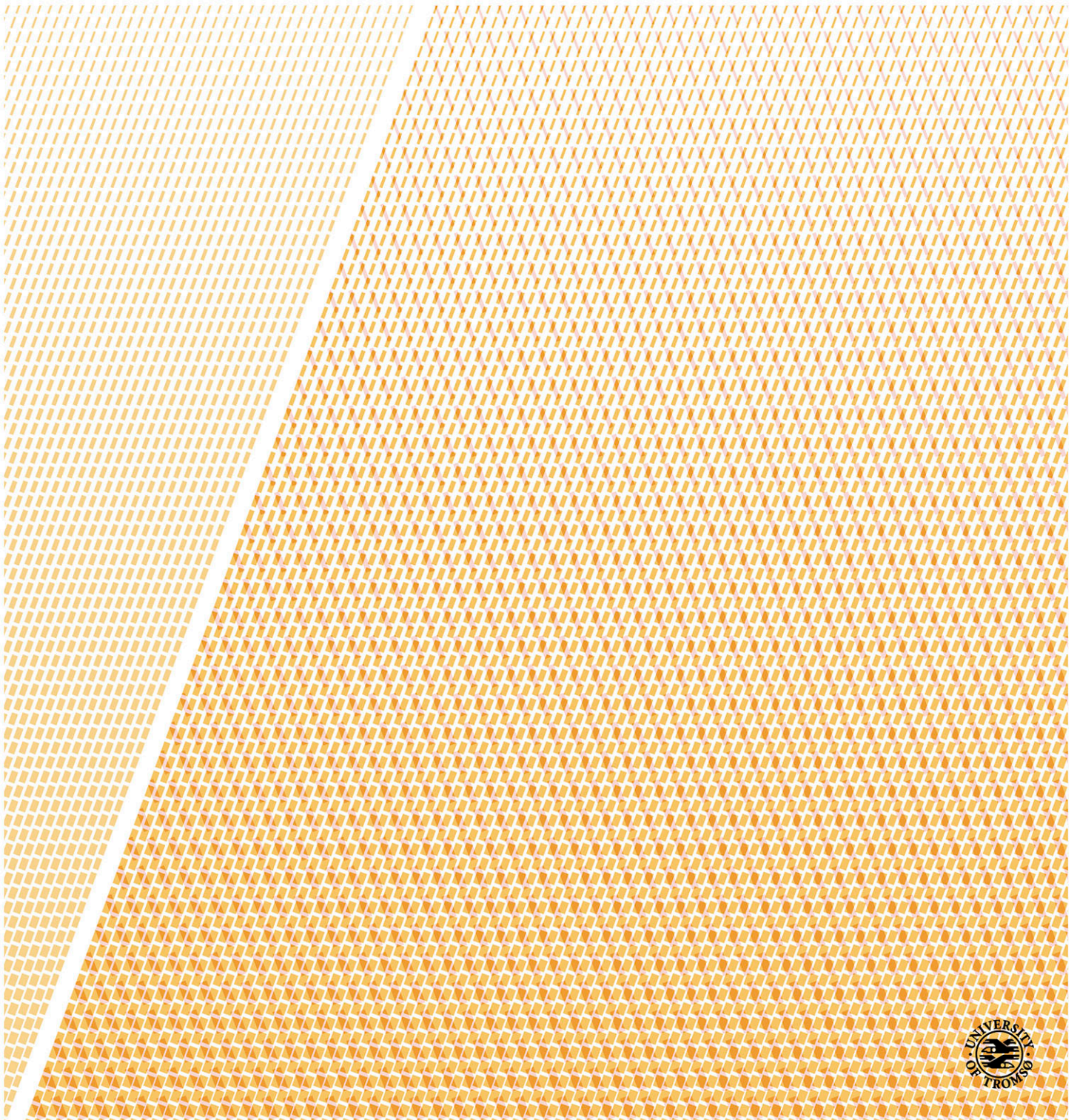


Expression and functional properties of selected miRNAs in human cancer tissue and cancer cell lines

A study of expression and function of miR-143, miR-145 and miR-126 in breast cancer and non-small cell lung cancer

Charles Walquist Johannessen

A dissertation for the degree of Philosophiae Doctor – November 2018



Expression and functional properties of selected miRNAs in human cancer tissue and cancer cell lines

**A study of expression and function of miR-143, miR-145 and miR-126 in breast cancer
and non-small cell lung cancer**

Doctoral Thesis

Charles Walquist Johannessen



Translational Cancer Research Group

Department of Medical Biology

Faculty of Health Science

UiT – The Arctic University of Norway

Acknowledgements

The work presented in this thesis was carried out at the Translational Cancer Research Group, Department of Medical Biology, Faculty of Health Science, UiT – The Arctic University of Norway, Tromsø between 2014 and 2018. I would like to thank the Northern Norway Regional Health Authority for financing this work.

First, I would like to express my deep gratitude to my main supervisor, Line Moi. Thank you for your inspired guidance, valuable suggestions, insightful criticism, encouragement and support throughout this thesis. Also, to my co-supervisor, professor Lill-Tove Rasmussen Busund, thank you for your invaluable and vast knowledge. Your expert advice has, no doubt, greatly improved the depth of my research. And to my co-supervisor, Yuri Kiselev, the person putting me on the path of science in the first place. Your enthusiasm, work ethics, rigorous attitude and dedication to scientific research has made a great impression on me, and I am sure it will continue to benefit my future life and career.

I would also like to thank professor Eiliv Lund, together with the rest of the members of the Norwegian Women and Cancer study, for their good cooperation and support of my work.

Thank you, Mona Irene Pedersen, for your excellent technical support, and kind and supporting words when I needed them. Thank you, Mehrdad Rakaee, my office partner and good friend. Our laughs and non-scientific discussions were always a welcome break, and highly valued.

I would like to thank all my co-authors and fellow group members who have contributed to this work. It has been a privilege and pleasure to collaborate with, what I must consider, the best of the best.

Thank you to my family and friends, especially May Wenche and Kristian. Your encouraging words during numerous coffee breaks and “fredagsgrøt” have been important motivators.

Finally, to my beautiful wife and daughters. I am so incredible grateful for your unconditioned love and support during this period. You give my life purpose, and I love you more than anything.

Tromsø, 2018

Charles W. Johannessen

Summary

MicroRNAs (miRNAs) are small non-coding RNAs (ncRNAs) involved in the regulation of gene expression, and they are often seen dysregulated in cancer. For this reason, it is of great scientific interest to study these ncRNAs to better understand their distribution in human tissues and their mode of function. Based on a comprehensive miRNA microarray from 108 breast cancers in the Norwegian Woman and Cancer Study and 44 healthy controls, this thesis sought to investigate tissue expression and functional properties of the miRNA cluster miR-143/145 in breast and lung cancer tissues and cell lines, as well as miR-126 in breast cancer (BC) tissue and cell lines.

Our analysis found the miR-143/145 cluster to be downregulated in tumor samples from both breast and lung, as well as in their corresponding cancer cell lines. The transfection of miR-143 into a number of cancer cell lines from both breast and lung, promoted proliferation in some, whilst having opposite or no effect in others. In contrast, all cell lines suffered inhibition in both proliferation and migration when transfected with miR-145.

In BC tissue, expression of miR-143 and miR-145 was lower in malignant compared to benign breast tissue, and lower in the more aggressive tumors. Interestingly, miR-145 was mainly expressed in the myoepithelial cells of benign breast tissue, and at the subcellular level located to the nuclei. In lung cancer tissue, expression of the miR-143/145 cluster was found to correlate with expression of several sex steroid hormone receptors. Also, stromal expression of miR-143 was an independent positive prognostic factor in female patients, whereas stromal expression of miR-145 was associated with improved disease specific survival for male patients.

Both miR-126-3p and its passenger strand, miR-126-5p, was verified as downregulated in BCs as well as in all tested BC cell lines. The passenger strand had a strong proliferation promoting

effect in the most aggressive BC cell line, whilst having the opposite effect in the other cell lines. The introduction of miR-126-3p resulted in decreased proliferation and invasion in all BC cell lines. In BC tissue, expression of miR-126-5p was significantly higher in high grade tumors, and both miR-126 strands were downregulated in lymph node positive BCs when compared to tumors with no nodal involvement.

This thesis depicts interesting findings, and contributes to a better understanding of context-specific expression patterns, functions and prognostic impacts of the three selected miRNAs.

List of papers

Paper I

Charles Johannessen, Line Moi, Yury Kiselev, Mona Irene Pedersen, Stig Manfred Dalen, Tonje Braaten, Lill-Tove Busund.

Expression and function of the miR-143/145 cluster *in vitro* and *in vivo* in human breast cancer

PLoS One. 2017 Oct 26;12(10):e0186658. doi: 10.1371/journal.pone.0186658.

Paper II

Charles Johannessen, Yury Kiselev, Mona Irene Pedersen, Stig Manfred Dalen, Lill-Tove Rasmussen Busund, Line Moi.

Different functional roles and expression of miR-126-3p and miR-126-5p in breast cancer cell lines and tissues

Manuscript

Paper III

Kaja Skjefstad, Charles Johannessen, Thea Grindstad, Thomas Kilvaer, Erna-Elise Paulsen, Mona Pedersen, Tom Donnem, Sigve Andersen, Roy Bremnes, Elin Richardsen, Samer Al-Saad, Lill-Tove Busund.

A gender specific improved survival related to stromal miR-143 and miR-145 expression in non-small cell lung cancer

Sci Rep. 2018 Jun 4;8(1):8549. doi: 10.1038/s41598-018-26864-w.

List of abbreviations

3'UTR	3'untranslated region
ADC	Adenocarcinoma
BC	Breast cancer
BL	Basal-like
bp	Base pair
CAF	Cancer associated fibroblast
CK	Cytokeratin
DCIS	Ductal carcinoma <i>in situ</i>
DNA	Deoxyribonucleic acid
dsRBD	Double-stranded RNA binding domain
EGFR	Epidermal growth factor receptor
ER	Estrogen receptor
EXP5	Exportin 5
HER2	Human epidermal growth factor receptor 2
IHC	Immunohistochemistry
ISH	<i>In situ</i> hybridization
MeSH	Medical subject heading search
miRNA	MicroRNA
ncRNA	Non-coding RNA
NOS	Not otherwise specified
NOWAC	Norwegian women and cancer study
NSCLC	Non-small cell lung cancer
NST	No special type
p63	Transformation-related protein 63
PR	Progesterone receptor
Pre-miRNA	Precursor miRNA
Pri-miRNA	Primary miRNA
qPCR	Quantitative polymerase chain reaction
RISC	RNA-induced silencing complex
RNA	Ribonucleic acid
RNA pol II	RNA polymerase II
rRNA	Ribosomal RNA
SCC	Squamous cell carcinoma
SCLC	Small cell lung cancer
TMA	Tissue microarray
TN	Triple-negative
TNBC	Triple-negative breast cancer
TRBP	TAR RNA-binding protein
tRNA	Transfer RNA
TTF-1	Thyroid transcription factor-1
WTS	Whole-tissue section

Contents

Acknowledgements	I
Summary	II
List of papers	IV
List of abbreviations.....	V
1. Background	1
1.1 Breast cancer	1
1.1.1 Classification.....	3
1.2 Non-small cell lung cancer.....	9
1.2.1 Classification.....	10
1.3 MicroRNA.....	13
1.3.1 MiRNA biogenesis.....	14
1.3.2 The role of miRNAs in cancer	17
2. Aims of the study	19
3. Summary of results.....	21
4. General discussion.....	25
4.1 Materials and methods	25
4.1.1 Patient cohorts	25
4.1.2 Tissue microarray	26
4.1.3 Immunohistochemistry.....	27
4.1.4 <i>In situ</i> hybridization	28
4.1.5 Human cell lines.....	29
4.2 Discussion of main results.....	30
4.2.1 Paper I	30
4.2.2 Paper II.....	34
4.2.3 Paper III.....	37
5. Conclusions and future perspectives	39
6. References	41

1. Background

1.1 Breast cancer

Worldwide, there are reported more than 1.6 million new cases of breast cancer (BC) every year, and the annual BC death rate is in excess of 500,000 [1]. This makes BC the most diagnosed cancer in the female population, where it contributes to 25% of all new cancer cases, and 15% of all cancer related deaths [1]. The five year survival rate of BC is 89% [2], but once metastases to distant organs occur, the five year survival rate drops below 25% [3].

Although metastatic BC rarely presents at the initial time of diagnosis, as many as 30% of patients diagnosed with early stage BC will later develop recurrent advanced disease or metastasis [4, 5]. The majority of BC metastases occur in the liver, bone, lung or central nervous system [6]. Although there has been some controversy regarding the effects of mammography [7], public screening programs are considered important for early detection and prevention of BC [8].

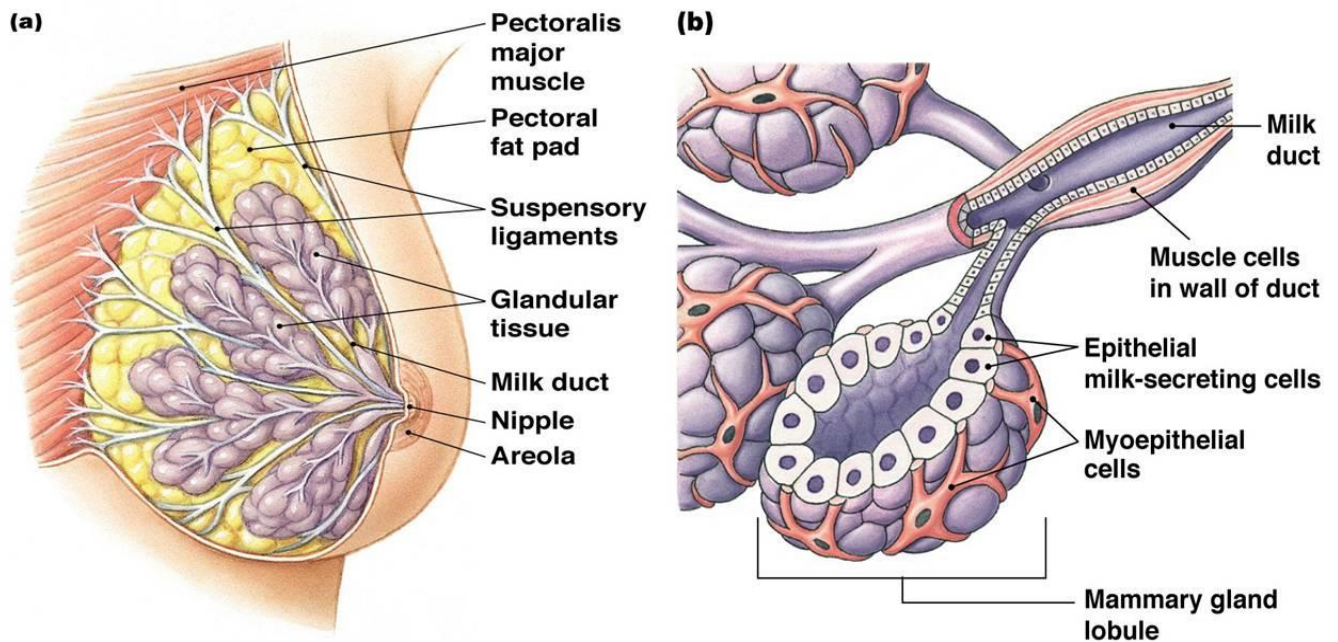


Figure 1: Anatomy and histology of the breast. Alvarado, 2016.

The mammary gland (figure 1) consists of several different cell types [9], and is a complex organ. The epithelial cells form the ductal network of the glands which are bilayered structures comprised of luminal cells (milk secreting epithelial cells) and basal cells [10]. The luminal cells form the ducts and the secretory alveoli, and makes up the inner layer of the glands' bilayered structure, whilst the basal cells form the outer layer which consists mainly of myoepithelial cells [10]. The function of the alveoli and the luminal cells is to secrete milk containing water and nutrients, whereas the contraction by the myoepithelial cells directs the milk through the ductal pathways [10, 11]. A relatively newly discovered cell type in this cellular landscape is the mammary stem cells which have been described as lineage-restricted cells with the capacity to differentiate into either luminal cells or myoepithelial cells [12, 13].

Precursor lesions of BC are annotated ductal carcinoma *in situ* (DCIS), and consist of clusters of neoplastic cells confined to the milk duct. It is estimated that up to 40% of DCIS cases progress into invasive carcinoma of no special type (NST), where cancer cells breach the basement membrane and infiltrate the surrounding tissue [14, 15]. Noteworthy, hereditary BC accounts for approximately 5-10% of all BC cases, and is primarily caused by mutations in one of the genes coding for the tumor suppressor proteins BRCA1 or BRCA2. Mutations in either of these genes are very potent cancer predictors, and women carrying these mutations have a 40-80% chance of developing BC before the age of 80 [16, 17].

1.1.1 Classification

BC is a highly heterogeneous disease composed of a diverse collection of molecular subtypes, which can be determined by gene expression patterns or immunohistochemistry (IHC) [18-21]. The identification of each tumor's molecular subtype is of great value, as each subtype has biological and clinical features [20] which are associated with prognosis and direct choice of treatment [22]. It is established that the different gene expression patterns observed in BC account for this heterogeneity [19]. The histopathological features of BC include characteristics such as histological morphology, receptor status, tumor size, tumor grade and nodal involvement. With the knowledge of both the molecular subtype and the histopathological status, the metastatic predisposition of the primary tumor may be determined [22, 23]. With the access to whole-genome profiling, one has been able to categorize BC into four general molecular subtypes. These subtypes are the luminal A, luminal B, human epidermal growth factor receptor 2 positive (HER2+) and the triple-negative (TN)/basal-like (BL) BCs [19, 24, 25]. Routinely, the classification of the tumors molecular subtype is basically based on the expression of relevant immunohistochemically stained receptors, and the expression of the proliferative marker Ki67. An illustration of immunohistochemical staining patterns for BCs with different receptor status is presented in figure 2.

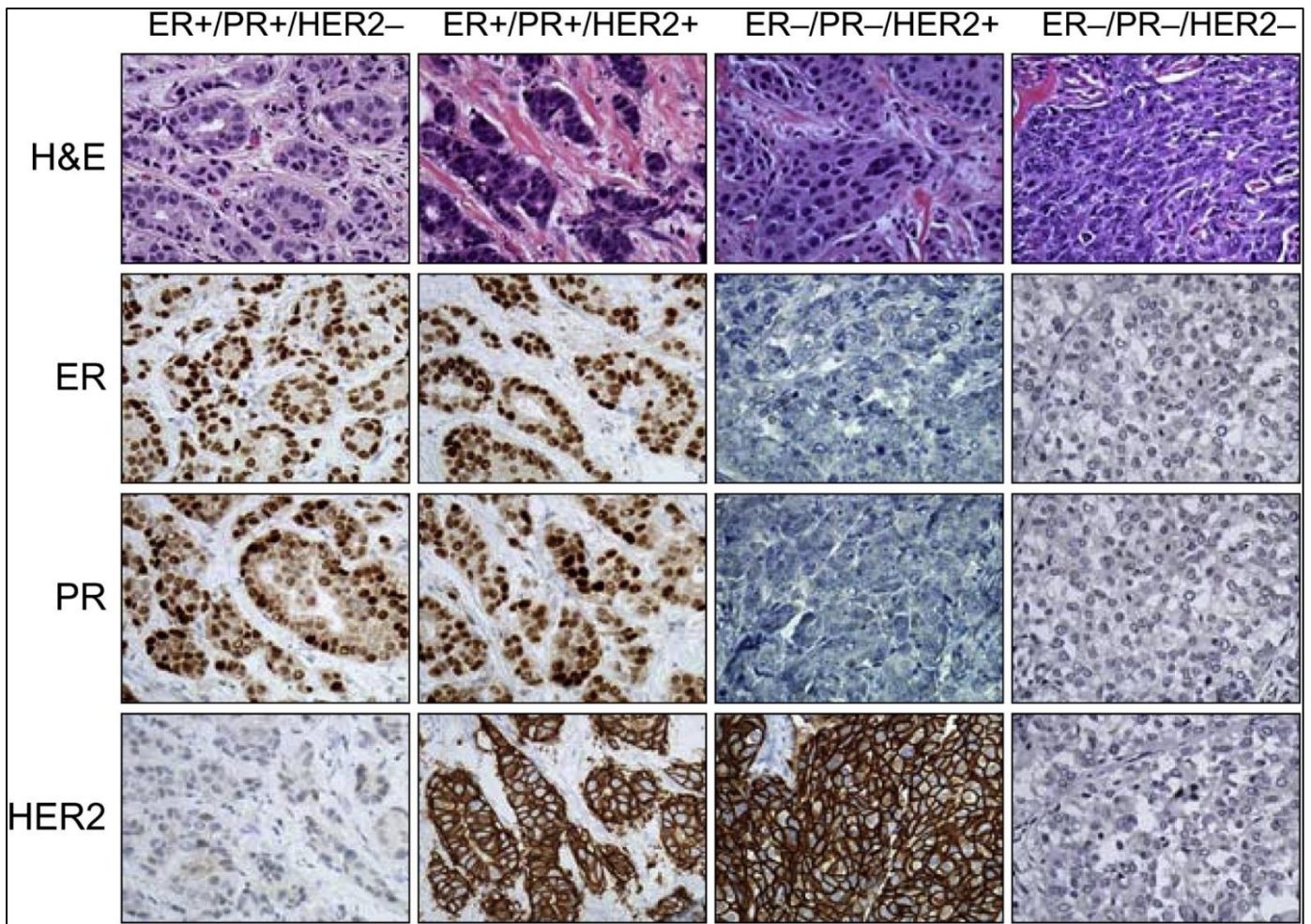


Figure 2: Representative immunohistochemical expression of ER, PR and HER2 in different subtypes of invasive BC.
 Rivenbark et al., 2013.

The luminal BCs are so named because their molecular profile has a similar gene expression to the normal luminal epithelium of the breast, and they are typically estrogen receptor positive (ER+) and progesterone receptor positive (PR+). The luminal A tumors display high expression of ER, low expression of HER2 and low expression of proliferation promoting genes [26, 27]. Luminal B tumors exhibit ER expression at lower levels compared to the luminal A subgroup, they can be either HER2+ or HER2-, and they typically have a higher expression of the proliferation-associated protein, Ki67 [27, 28]. The luminal BCs comprise the largest subgroup of BCs, where the luminal B cancers account for approximately 40% of all BCs [29], thus making it the largest individual subgroup. Due to the higher expression of ER and the lower

expression of proliferation markers in the luminal A tumors, this subgroup has a better prognosis than patients in the luminal B subgroup, with an overall survival rate 10 years after diagnosis of 70% vs 54%, respectively [22]. Notably, when further subgrouping the luminal B subgroup into luminal B/HER2+ and luminal B/HER2-, there is a significant difference in the overall survival rate at 10 years after diagnosis of 46% vs 54%, respectively [22]. Combined, however, the luminal BCs have a better prognosis compared to the non-luminal subgroups, which primarily is a result of their positive ER-status, hence allowing for targeted hormonal therapy [30].

The molecular subgroup HER2+ constitutes approximately 15-20% of all BC cases, where the *HER2* gene copy number can be as high as 50, resulting in a protein overexpression close to a 100-fold [31]. HER2 is a transmembrane receptor protein and is one of the four membrane receptor tyrosine kinases (RTKs) in the epidermal growth factor receptor family, first identified in rat neuroblastomas as a protein capable of transforming a mouse fibroblasts cell line into malignancy [32]. This family of receptors is important in communication between cell-cell and cell-stroma via signal transducers known as ligands. HER2 is a co-receptor for many ligands, and whilst the HER2 receptor has no known ligand of its own, the receptor forms heterodimers with other receptors of the HER family when activated by their ligand(s) [33]. Dysregulation of HER2, on both gene and protein level, is associated with a worse prognosis in both the lymph node-negative and lymph node-positive BC patients [34]. Adjuvant treatment of HER2+ BC with trastuzumab, a monoclonal antibody targeting the extracellular domain of the HER2 protein, has proven beneficial to patient outcome, with a 34% reduction in risk of death after two years [35]. Currently, adjuvant treatment with trastuzumab is the standard care of treatment for HER2+ tumors.

The TN/BL subgroup is highly heterogeneous, is immunohistochemically defined as BCs not overexpressing HER2, and is both ER and PR negative. It is considered an especially aggressive subtype, in particular affecting the younger female population, and targeted therapeutic options are limited to clinical trials [36]. The terms TN and BL are often used as synonyms, and although most TN cancers are of a BL phenotype, and most tumors expressing basal-markers are TN, this is not always the case [37, 38]. In fact, studies have revealed that 70-90% of TN cancer are of a BL subtype, and 50-80% of molecular BL tumors are TN [38-40]. However, pooling the TN and the BL cancers into one subgroup is sensible, as they exhibit great similarities in that they affect younger patients, are more likely to present as interval cancers, and they are significantly more aggressive than tumors in other subclasses [41, 42].

The TNBCs account for 10-20% of all BCs, depending on the methods and thresholds used to evaluate ER, PR and HER2 expression [41]. There are histological subtypes which are typically TN, but the TN cancers as a group lack distinctive histological characteristics [43]. With their expression of epidermal growth factor receptor (EGFR) together with cytokeratins 5, 14 and 17, their genomic characteristics are similar to the normal myoepithelial (basal) cells of the breast [44], and interestingly, the gene expression patterns of myoepithelial mammary cells are similar to those found in squamous cell carcinoma of the lung [45].

As a result of the tumors' negative receptor status, the TNBC patients benefit from neither endocrine therapy, nor trastuzumab (HER2 antagonist). The current backbone in TNBC management is treatment with cytotoxic chemotherapy, where TNBCs have a higher pathologic complete response rate when compared to hormone receptor-positive BC treated with neoadjuvant chemotherapy [46]. Still, however, patients harboring the TN subtype have a worse outcome after chemotherapy compared to patients with BC of other subtypes [44, 47].

The highly heterogeneous nature of TNBC argues for personalized treatment strategies targeting molecular tumor-specific sites. This is further substantiated by the fact that the response rate of TNBC patients treated with chemotherapy is 40% or less [43]. Indeed, there are currently several ongoing clinical trials investigating the potential for targeted therapy for TNBC. These targets include, but are not limited to, the androgen receptor (phase II), the AKT-pathway (phase II) and poly (ADP-ribose) polymerase PARP (phase III) [36]. The future of treating TNBCs may be brighter, as the treatment regime shifts towards more personalized, molecular targeted therapies.

1.2 Non-small cell lung cancer

Worldwide, lung cancer is the leading cause of cancer related death, and annually 1.8 million new lung cancer cases are reported [48]. Additionally, it is also one of the cancers with the highest death rate, with just short of 1.6 million people dying each year [48]. It is estimated that approximately 80-90% of all lung cancer cases in high-income countries are directly related to smoking [49], and although lung cancer incidence in men is slowly declining due to fewer smokers, the incidence in women continues to rise, also in Norway [50] (figure 3).

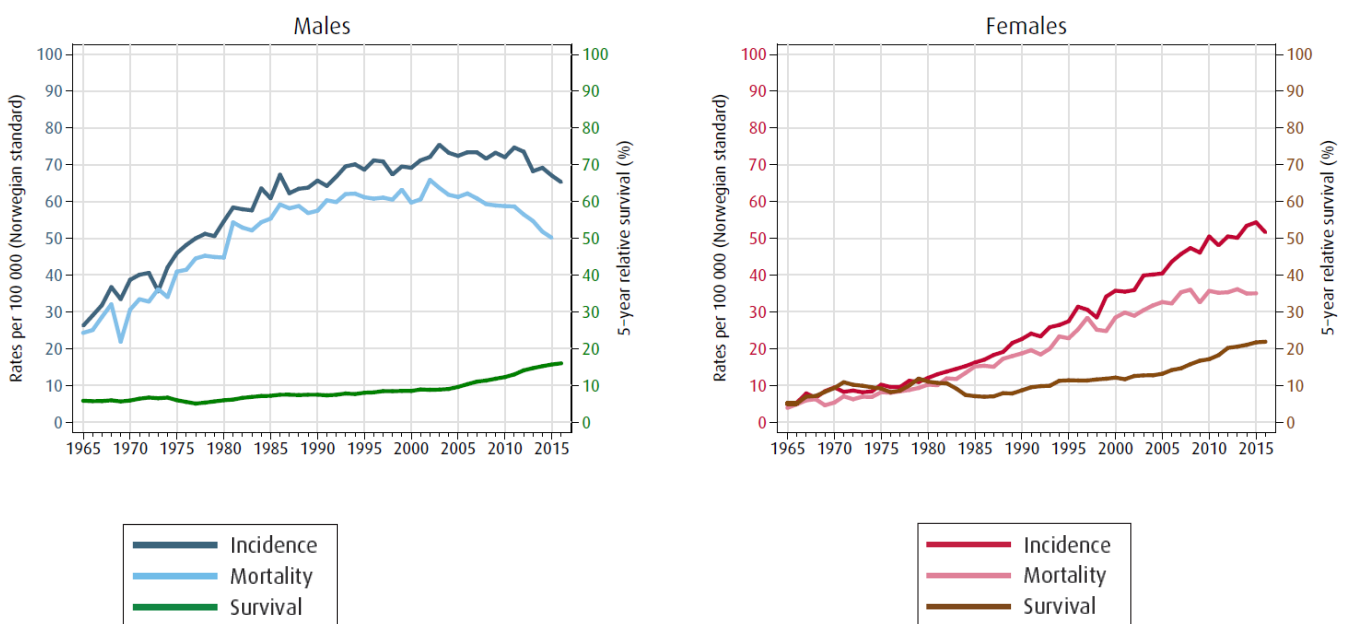


Figure 3: Incidence and mortality rates in lung cancer patients from 1965-2015.

(Adapted from www.kreftregisteret.no; Cancer in Norway 2016)

Lung cancer is a disease that presents great challenges, as 70% of lung cancer patients have advanced stage at the time of diagnosis [58]. Metastases to distant organs are responsible for 70% of all lung cancer deaths, regardless of histological subtype, and the most frequent sites for metastases include bone, brain, adrenal glands and liver [59]. An obvious way to decrease lung cancer mortality (in addition to reducing smoking in the population) is through achieving early diagnosis, and hence treatment, by screening programs. However, studies involving chest radiographs and sputum cytology for early detection did not significantly reduce lung

cancer mortality [60]. On the other hand, patients in high-risk groups participating in The American National Lung Screening Trial had significantly lower mortality, but there are still unanswered questions in regards to over-diagnosis and over-treatment [60, 61].

1.2.1 Classification

Histologically and clinically, lung cancer is typically classified into two major groups: Small cell lung cancer (SCLC) and non-small cell lung cancer (NSCLC). SCLC accounts for approximately 15% of all diagnosed lung cancers and is a very aggressive type of cancer, generally observed in smokers [51].

NSCLC is the largest group and accounts for approximately 85% of all lung cancer cases, and is further classified into subgroups [52]. The classification of NSCLCs was recently revised by the 2015 WHO Classification of Lung Tumors, and consist of squamous cell carcinoma (SCC), adenocarcinoma (ADC) and NSCLC not otherwise specified (NOS) [53]. ADC is the most common subtype observed in never-smokers [54], it typically forms glandular structures, and the production of mucus is sometimes observed. SCCs are typically more aggressive than ADCs, and can be keratinizing, non-keratinizing or display a low differentiated basaloid morphology, somewhat similar to that of TNBCs [45, 55].

Previous classification of NSCLC was based on light microscopy of hematoxylin and eosin stained tissue samples, and focused mainly on morphology. However, new IHC analyses have been applied to classify subgroups more accurately. These analyses include the thyroid transcription factor-1 (TTF-1), which is expressed by pneumocytes and is primarily associated with ADCs [53]. Similarly, the transformation-related protein 63 (p63), its isoform p40, and cytokeratin 5/6 (CK 5/6) are predominantly expressed in the bronchial epithelium and are

typically associated with SCCs [53]. On rare occasions (3% of cases), if no distinct IHC staining pattern is evident to indicate either ADC or SCC, then the NOS subtype is applied, and merely as a diagnosis of exclusion [53].

The histological and molecular distinction between ADC and SCC is crucial when it comes to therapeutic decisions and to predicting the clinical course, especially for patients with advanced-stage disease [56]. In Norway, the recent availability of targeted treatments has resulted in the screening of all non-SCCs for mutations in both the EGFR and the anaplastic lymphoma kinase (ALK) gene at the time of diagnosis. In addition, the list of potential future candidates for targeted treatment of NSCLC is still growing, and include KRAS, BRAF, HER2, RET, ROS1, MET, PIK3CA, NTRK [57].

1.3 MicroRNA

In the early era of DNA research, 3% of genes were considered to be protein-coding while the other 97% was considered little more than 'junk' DNA [58]. However, decades later, our understanding of the human transcriptome has changed fundamentally. Not too long ago, the Encyclopedia of DNA Elements (ENCODE) project reported that as much as 75% of the human genome is transcribed into RNA, which is a big statement to the fact that non-coding RNAs (ncRNAs) comprise the majority of the human transcriptome [59, 60]. The first ncRNAs were discovered in the 1950s, and they include the ribosomal RNA (rRNA) and the transfer RNA (tRNA). Since then, a vast variety of various ncRNAs have been described, where microRNAs (miRNAs) are the best described class of short ncRNAs [61, 62].

The first miRNA, named *lin-4*, was initially described in the transparent nematode *Caenorhabditis elegans*, and was reported as a small RNA with antisense complementarity to the mRNA transcript of the gene *lin-14* [63]. Today, more than 2500 human miRNAs later, we understand that the regulation and dysregulation of miRNAs are involved in virtually all types of cellular processes, both benign and malignant, as miRNAs' involvement in a vast number of different intracellular processes has been revealed [64-69].

The mature miRNA is typically 22 nucleotides in length and is normally processed by the two RNase III proteins Droscha and Dicer [70]. In RNA silencing, the miRNA sequence function as a guide by base pairing with the complementary 3'untranslated region (3'UTR) of its target mRNA, and when united with the AGO proteins, this ultimately results in either translational repression, mRNA deadenylation or mRNA degradation [70].

1.3.1 MiRNA biogenesis

The genes encoding miRNAs are typically located within intergenic regions, but approximately 30% of miRNA genes are positioned within introns or exons of protein-coding genes [71]. It is not unusual that miRNA loci are positioned in relative close proximity to each other, making a polycistronic transcription unit, often referred to as a miRNA cluster [72]. The miRNA cluster is generally subject to a common promoter region, and is hence cotranscribed. However, subsequent differentiated processing and regulation at the posttranscriptional level is common [72, 73]. The miRNA genes that reside in the introns or exons of protein-coding genes often share promoter with their host gene, but it has been shown that different miRNA genes can have several start sites for transcription, which is also the case for intragenic miRNA, whose promoter site can be distinct from the promoters of their host genes [74].

The vast majority of miRNAs are transcribed by RNA polymerase II (RNA pol II). This is apparent when considering the length of the primary miRNA (pri-miRNA) transcript, which is more than 1 kb longer than a typical RNA pol III transcript [75]. In addition, the pri-miRNA transcript contains sequences of uridine residues, which terminate transcription by RNA pol III [76]. Transcriptional regulation of miRNAs is typically directed by various factors, like the transcription factors p53, MYC, ZEB1 and ZEB2, as well as epigenetic factors, like DNA methylation and histone modification [73, 77, 78].

Transcribed pri-miRNA is typically >1 kb long and forms a specific hairpin-shaped stem-loop secondary structure where the mature miRNA sequence is embedded. Typically, a pri-miRNA consists of the mature miRNA-containing stem (33-35 bp), the terminal loop, and a single-stranded RNA segment at both the 5' and 3' side [73]. The nuclear maturation process of pri-miRNA is in essence initiated by the nuclear RNase III protein Drosha in collaboration with the DiGeorge syndrome chromosomal region 8 (DGCR8) protein. The RNA binding protein

DGCR8 identifies and binds pri-miRNA and the central part of the Drosha protein. Together, these proteins form the Microprocessor complex, which process the 5' and the 3' strand of the pri-miRNA into an approximately 65 bp hairpin-shaped RNA structure called precursor miRNA (pre-miRNA) [79, 80]. The pre-miRNA is subsequently exported into the cytoplasm, where maturation can be completed. The export of pre-miRNA is aided by the protein exportin 5 (EXP5), whose interaction with the GTP-binding nuclear protein RAN·GTP forms a transporter complex [81]. Upon reaching the cytoplasm through the nuclear pore, the GTP is hydrolyzed and the pre-miRNA/EXP5/RAN·GTP-complex is disassembled, resulting in the release of pre-miRNA into the cell's cytosol [82, 83].

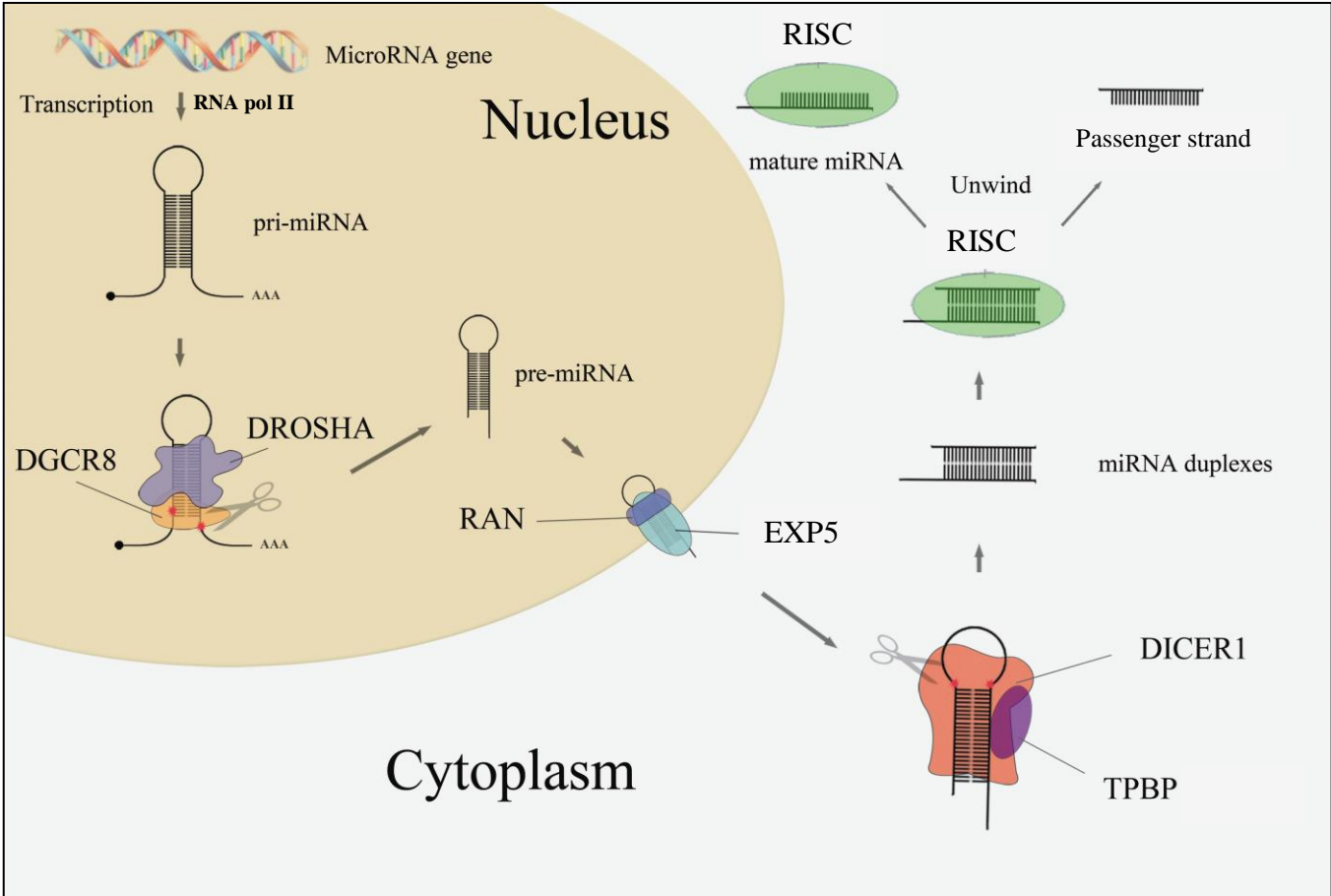


Figure 4: miRNA pathway. An illustration of the miRNA pathway from transcribed pri-miRNA to translational repression. Modified from He et al., 2016.

Once the pre-miRNA is released into the cytosol, the RNase III endonuclease Dicer carries out the next step in miRNA maturation. Dicer recognizes the 5' phosphate and the 3' overhang close to the terminal loop, and cleaves the double stranded pre-miRNA at this site, producing a roughly 22 bp long RNA duplex often referred to as a miRNA:miRNA* complex [73, 76, 84]. There are many different factors and pathways regulating the activity of Dicer, the most recognized being by the TAR RNA-binding protein (TRBP). TRBP contains three double-stranded RNA binding domains (dsRBDs) and is involved in the modulation of several pre-miRNAs, as well as in regulating the length of mature miRNAs [85, 86].

Next, the miRNA:miRNA* complex is loaded into the RNA induced silencing complex (RISC) to finalize the miRNA maturation. The catalytic component of the human RISC complex is the Ago2 protein, who is essential in both binding miRNA and in releasing Dicer [87]. Ago2 is a protein with endonuclease activity, and it cleaves the 3' arm of the miRNA before it is processed by Dicer, a course that is believed to aid in determining the mature lead miRNA strand [87, 88]. Selection of the miRNA lead strand is based on the relative thermodynamic stability of the two ends of the small RNA duplex, and the lead strand is generally the one with the more relatively unstable terminus at the 5' side [73, 89]. In addition, the Ago2 protein selects the lead strand based on the first nucleotide sequence, and the lead strand presenting a U at nucleotide position 1 is typically selected [90].

The Arg2, using the lead miRNA as a guide, then directs the RISC complex to downregulate target genes. Based on the complementarity between the 3'UTR of the target mRNA and the RISC incorporated miRNA, gene expression is post-transcriptionally repressed by either translational repression, mRNA degradation or mRNA deadenylation [70, 91]. An illustration of the canonical miRNA pathway is presented in figure 4 [92].

1.3.2 The role of miRNAs in cancer

Ever since the first publication describing the deletion of the *miR-15* and *miR-16* loci in the majority of samples from patients with B-cell chronic lymphocytic leukemia [93], a large number of papers describing dysregulation of numerous different miRNAs in a vast diversity of cancers has been published [94]. In general, the mechanisms involved in miRNA dysregulation are chromosomal abnormalities, alterations in transcriptional control, epigenetic changes and defects in the miRNA biogenesis [95].

The deletion of the *miR-15* and *miR-16* loci was the first reported miRNA dysregulation due to a chromosomal abnormality (deletion). Similarly, the 5q33 region, harboring the *miR-143/145* gene cluster, is commonly deleted in lung cancer, resulting in reduced expression of both these miRNAs [96]. In contrast, duplication of the *miR-17-92* gene cluster has been reported in both B-cell lymphomas and lung cancer, resulting in overexpression of these miRNAs [97, 98]. It has become evident that both deletions and duplications (amplifications) of specific genomic regions, as well as chromosomal translocations, contribute to abnormal miRNA expression.

The expression of pri-miRNAs is subject to dysregulation similar to protein-coding genes. During tumorigenesis, alterations in tumor suppressors or oncogenic factors functioning as transcriptional activators or suppressors, will affect the expression of pri-miRNAs. One of these alterations involves the oncogenic miR-17-92 cluster, which is upregulated in several different cancers [99]. MYC stimulates expression of the miR-17-92 cluster, which in turn promotes tumorigenesis by regulating the post transcriptional expression of E2F1, THBS1, CTGF and other transcripts important for cell cycle progression and angiogenesis [94, 100]. Conversely, the miR-200 family is regularly reported as downregulated in human tumors. The miR-200 family is involved in targeting important transcription factors involved in suppression of epithelial genes in order to facilitate the epithelial-mesenchymal transition, which is key to

invasion and metastasis [101]. There are many transcription factors associated with cancer that regulate expression of miRNAs, making transcriptional dysregulation a crucial mechanism in altered miRNA expression in cancer.

Modifications of histones and DNA control the chromatin structure of the chromosome, and these epigenetic changes have an important role in regulating expression of both protein coding RNA and ncRNA. The gene promoters of miRNAs, as well as promoters for most genes, have a relatively high content of CpG islands, and these are frequently hypermethylated in tumor suppressor miRNAs, resulting in an epigenetic silencing of these miRNAs [102]. Histone modification is another epigenetic change, and has been reported to cooperate with DNA methylation to suppress the expression of tumor suppressor miRNAs in cancer [103]. Together, these epigenetic mechanisms play important parts in repressing tumor suppressive miRNAs in cancer.

In miRNA biogenesis, the two RNase III proteins Drosha and Dicer are frequently downregulated in various cancers, and this downregulation is associated with poor patient outcome [104]. For example, the expression of *DROSHA* is regulated by the proto-oncogenic transcription factor MYC, which may lead to decreased pri-miRNA processing [105]. Also, downregulation of *DROSHA* has been reported in context with hypoxia, and this process was facilitated by direct binding of the hypoxia-responsive transcription factors ETS1 and ELK1 to the promoter of *DROSHA* [106]. Likewise, the expression of *DICER* is also subject to dysregulation in cancer, a process that is highly diverse. The transcription factor Tap63 activates *DICER* expression by direct promoter binding to its promoter, but this transcription factor is frequently lost in cancer, leading to downregulation of *DICER*. Another pathway in which *DICER* is downregulated is through direct binding to its 3'UTR by specific miRNAs, an effect highly influenced by hypoxia [106, 107].

2. Aims of the study

The overall aim of this study was to explore functions and expression patterns of carefully selected miRNAs in breast cancer and lung cancer. To this end, we investigated expression in tissue samples from both breast- and lung cancer patients, alongside functional studies on cancer cell lines representing both organ systems. Expression of miRNA was evaluated using miRNA microarray, qPCR and ISH, and functional studies included experiments eligible for the study of cell proliferation and cell migration.

More specifically, the objectives of the study were to evaluate expression patterns and functional properties of the miR-143/145 cluster in BC and NSCLC. Also, expression and function of the miR-126-3p, and its passenger strand, miR-126-5p, was investigated in BC tissue and BC cell lines.

3. Summary of results

Paper I

Expression and function of the miR-143/145 cluster *in vitro* and *in vivo* in human breast cancer

Vast numbers of miRNAs are dysregulated in cancer, and the miRNA cluster miR-143/145 is among them. In this paper, we sought to investigate the functional properties and expression of the miR-143/145 cluster both *in vivo* and *in vitro* in human breast cancer. For the functional studies we used three different BC cell lines corresponding to the major subtypes of BC: ER+, HER2+ and TN. In addition to analyzing expression, we also studied how the cell lines' ability to proliferate and migrate/invade was affected when transfected with either miR-143 mimic, miR-145 mimic, or miR-143 mimic and miR-145 mimic in combination. For the *in vivo* part, the cellular and subcellular expression of miR-143 and miR-145 was evaluated in full histological slides from both benign and malignant breast tissue. Patient samples were stratified according to molecular subtype, tumor grade and receptor status, and expression patterns of miR-143 and miR-145 were analyzed accordingly.

Results from a comprehensive miRNA microarray study on breast cancer tissue revealed both miR-143 and miR-145 to be downregulated in BC tumors when compared to benign breast tissue. These results were later verified by RT-qPCR. Similar, expression of both miR-143 and miR-145 were downregulated in all tested BC cell lines.

In vitro, miR-143 promoted proliferation of the ER+ and the TN BC cell line, whereas having no significant effect on the proliferation properties of the HER2+ cell line. In contrast, all BC cell lines suffered proliferation inhibition when transfected with miR-145. The cotransfection with miR-143 and miR-145 resulted in inhibited proliferation similar to that of miR-145 alone

in all BC cell lines. All BC cell lines suffered inhibition of invasion when transfected with either miR-143, miR-145 or miR-143 and miR-145. *In vivo*, the expression of miR-143 and miR-145 was lower in malignant compared to benign breast tissue, and lower in the more aggressive tumors with higher tumor grade, loss of ER and the basal-like phenotype. The collected ISH data also contributed very interesting findings regarding cellular and subcellular distribution of the studied miRNAs, especially for the miR-145. Staining patterns of miR-143 were primarily cytoplasmatic and predominantly found in luminal cells of benign breast tissue. In contrast, miR-145 was mainly expressed in the myoepithelial cells of benign breast tissue, and sub-cellularly located to the nuclei.

Paper II

Different functional roles and expression of miR-126-3p and miR-126-5p in breast cancer cell lines and tissues

In the literature, miR-126 is described as a tumor suppressor in various cancers, and is involved in regulation of metastatic processes in BCs. In this paper, we were interested in investigating expression and functional properties of both the miR-126-3p and its passenger strand, miR-126-5p. The study explored the effects of transfecting miR-126-3p mimic, miR-126-5p mimic, or miR-126-3p mimic and miR-126-5p mimic in combination on proliferation and invasion in BC cell lines representing the major subtypes of BC. Expression of miR-126-3p and miR-126-5p in tissue samples were investigated using *in situ* hybridization and tissue miRNA microarrays and PCR.

Results from the miRNA microarray revealed both miR-126-3p and miR-126-5p to be downregulated in BC tumors when compared to benign breast tissue. Results were verified by

qPCR. Likewise, expression of both miR-126 strands were downregulated in all our tested BC cell lines when compared to the non-cancerous breast cell line MCF-10A. Transfection of miR-126-3p resulted in decreased proliferation and invasion in all BC cell lines. Transfection of miR-126-5p decreased proliferation in the ER+ and the HER2+ BC cell lines, whereas having a strong opposite effect in the TN BC cell line, dramatically increasing proliferation potential. *In vivo*, expression of miR-126-5p was significantly higher in high grade tumors and in stroma and tumor cells of luminal B, HER2+ and TN tumors when compared to luminal A tumors. In addition, both miR-126 strands were downregulated in lymph node positive BCs when compared to tumors with no nodal involvement.

Paper III

A gender specific improved survival related to stromal miR-143 and miR-145 expression in non-small cell lung cancer

In addition to the BC cohort (paper I), the miRNA cluster miR-143/145 was investigated in a large retrospective study including 553 NSCLC patients. Tissue was collected from primary lung tumors and metastatic lymph nodes, and tissue microarrays were subsequently constructed from these. Functional studies to evaluate proliferation and migration after transfection of either miR-143 mimic, miR-145 mimic, or miR-143 mimic and miR-145 mimic in combination, were performed using different NSCLC cell lines representing adenocarcinomas, squamous cell carcinomas and large cell carcinomas. Expression of miR-143 and miR-145 in tissue samples was investigated using *in situ* hybridization and tissue miRNA microarrays.

Expression of both miR-143 and miR-145 was downregulated in all NSCLC cell lines included in this study. In contrast, ISH-results from patient samples demonstrated significantly increased

expression of miR-143/miR-145 in tumor cells and adjoining stromal cells when compared to non-malignant tissue. Migration studies were performed on the NSCLC cell lines representing adenocarcinoma and large cell carcinoma. Both cell lines displayed a notable decrease in migration potential when transfected with either miR-143 or miR-145. Proliferation was evaluated in NSCLC cell lines representing adenocarcinoma, squamous cell carcinoma and large cell carcinoma. Both the adenocarcinoma cell line and the large cell carcinoma cell line experienced proliferation inhibition when transfected with either miR-143, miR-145, or miR-143 and miR-145 in combination. In contrast, the squamous cell carcinoma cell line displayed increased proliferation when transfected with miR-143, whilst displaying inhibition of proliferation when transfected with miR-145. When combining miR-143 and miR-145, the proliferation rate of the squamous cell carcinoma cell line was not significantly different to the negative control. *In vivo*, expression of the miR-143/145 cluster was found to correlate with expression of several sex steroid hormone receptors, including progesterone receptor, androgen receptor and estrogen receptor beta. In addition, stromal expression of miR-143 was an independent positive prognostic factor in female patients in both univariate and multivariate analysis, whereas stromal expression of miR-145 was associated with improved disease specific survival for male patients in both univariate and multivariate analysis.

4. General discussion

The main focus of this work has been to investigate functional properties and expression patterns of selected miRNAs in breast cancer tissue. In **paper III** we investigate the same miRNAs as in **paper I**, but in NSCLC. Results for each paper are discussed within the respective papers. In the first part of the discussion (4.1), selected materials and methods will be briefly presented and discussed, and in the second part (4.2) the major findings in each paper will be discussed.

4.1 Materials and methods

4.1.1 Patient cohorts

Patients in the BC cohort were collected from the NOWAC postgenome cohort [108], and included participants diagnosed with BC during the years 2004-2010. A total of 102 BC surgery specimens and 38 benign breast specimens were included in the miRNA microarray, and the data from the miRNA microarray analysis were used in the planning and design of **papers I and II**. The histological grading was based on the modified criteria by Elston and Ellis [109], and the molecular subtyping of tumors were based on the expression of ER, PR, HER2 and Ki67 in consensus with guidelines provided by the St Gallen International Expert Consensus and previous publications [29, 110].

The large NSCLC cohort, which is a part of **paper III**, comprises 553 resected patients with stage I-IIIb NSCLC. The cohort includes patients who underwent surgical resection at the Nordland Central Hospital (NS), Bodø and the University Hospital of North Norway (UNN), Tromsø from 1990-2011 [111, 112], and includes complete medical records with follow-up data up until October 1, 2013 [113].

The most common histological subtype of NSCLC has shifted during the last years from SCC towards ADC. This shift contributes to our data being not quite representative of the current situation, as the SCC subtype had a higher frequency in the early material (1990-2004), which contains 335 of the 553 patients in the NSCLC cohort [111, 112]. The enrollment of patients and the collection of clinical data used in this study was done over a time period spanning more than 20 years. During this period, there have been several alterations in how lung cancer was treated, with the most important one being the implementation of adjuvant chemotherapy in 2005. Moreover, criteria for diagnosing and subtyping NSCLC have also changed during the follow up period. The changes in treatment regimens and criteria for diagnosing and subtyping that have been implemented since the start of data collection present a challenge for this retrospective study, as the longitudinal data may not have been treated adequately homogeneously, resulting in skewed results. However, to counter any discrepancies due to updated criteria and to minimize test-retest variations, all tumor material was systematically examined by an experienced pathologist whenever new criteria for NSCLC classification were applied.

4.1.2 Tissue microarray

The process of constructing a tissue microarray (TMA) involves systematically transferring cylinders of small representative tissue from a ‘donor’ block, usually a whole-tissue section (WTS) block, into an empty ‘recipient’ paraffin block [114]. One ‘recipient’ block may hold several hundred cores, allowing several samples from numerous patients in the same ‘recipient’ block [115].

Compared to WTSs, TMAs saves both time and tissue, as one slide containing TMAs can hold close to 800 cores. Another very important advantage of using TMAs, is the elimination of

batch-to-batch variability. To analyze the same amount of samples using WTSs, one would have to prepare slides from hundreds of patients, and the staining process would have to be performed in numerous batches, greatly increasing the chance for batch-to-batch variability [116]. The pathologist(s) that would subsequently evaluate and analyze the samples to identify the relevant tumor compartments, would be facing a very time consuming task, complicating the standardization of staining.

In regards to challenges using TMA, the question of whether a 0.6-1.0 mm core is representative for the heterogeneity of the total tumor is often raised. Studies have, however, revealed that there can be a correlation of more than 90% when comparing the expression of certain biomarkers in TMA and WTS [117, 118], and a recent study provides additional evidence of reliability in determining biomarkers using TMA when using more than one tissue core [119]. It is, however, important to also consider the limitations of WTS, as one single WTS contains a small fragment of the total tumor volume, hence representing a small part of the tumor, and may not itself be representative for large heterogenic tumors.

4.1.3 Immunohistochemistry

IHC is a method for the detection of antigens within cells or tissue sections (usually WTSs or TMAs) using specific antibodies against the antigen of interest. Next, the antibody-antigen complex is visualized by staining. This is a versatile technique, and can be used to assess the expression of numerous antigens, including proteins, amino acids and infectious agents. IHC is an important tool in routine diagnostics, as well as in basal research [120].

The advantages of IHC are many, and include cost effectiveness and *in situ* assessment of distribution and localization of cellular components of interest. It is a well-established method around the world, and IHC analysis can be performed on archived tissue, decades old.

Factors contributing to the challenges of IHC include adequate fixation, tissue processing and antigen retrieval. If tissues are not adequately fixated, decomposition of tissue and its markers may occur, and insufficient antigen retrieval may contribute to false negative results. Other analytical factors include selecting antibody with sufficient specificity, antibody concentration for adequate visualization, incubation conditions, and selection of secondary antibodies and mode of detection.

4.1.4 *In situ* hybridization

ISH is a method used to detect specific nucleotide sequences, like DNA and RNA, in tissue samples or in individual cells. A probe with a specific nucleotide sequence is hybridized to its target RNA or DNA, and subsequently visualized microscopically.

A great advantage when using ISH for the detection of miRNAs, is the visualization of both expression levels and the ability to pinpoint cellular localization. However, miRNAs are small in size, the sequence between related miRNAs may be very similar, resulting in unspecific hybridization, and they may be tissue specific. Other challenges are similar to those for IHC, and include probe specificity, probe concentration, incubation conditions and mode of detection. Probe specificity is important to avoid unspecific hybridization (false positive), whereas correct probe concentration is important to ensure a representative view of expression.

4.1.5 Human cell lines

Human immortalized cancer cell lines are widely used as a substitute for primary cells to investigate the biology of human cancers. They are cost effective, easy to use, they divide practically eternally, hence producing an unlimited supply of material, and they bypass ethical concerns often associated with animal studies. In addition, they comprise a very pure population of cells, absent of stromal and immune cells, contributing to consistency and reproducibility of results. However, this also produces a challenge, as cell lines are cultivated in absence of a normal tumor microenvironment, lacking the stromal compartment. Also, cell lines are highly manipulated and their original phenotype, functions and responsiveness may, to a great extent, have been lost [121]. Additionally, high passage numbers can inflict both genotypic and phenotypic variations, and genetic drift may over time cause heterogeneity in cell cultures [121].

It is important to realize that cell lines do not mirror primary cells, which in turn do not mirror source tissue either, and caution should be made when/if conclusions are drawn from cell line experiments. It is also important to recognize that both primary cells and cell lines are usually cultured in the absence of their normal environment, again urging for the use of caution when ascribing function in the body/model based on results from cell culture experiments alone.

4.2 Discussion of main results

4.2.1 Paper I

In the first paper we present functional properties and expression patterns of the miRNA cluster miR-143/145 in BC. The findings are based on results from functional studies, miRNA microarray, RT-qPCR and ISH. A miRNA cluster is miRNAs whose genes are localized in close proximity to each other on the DNA, resulting in their simultaneous transcription under the control of a common promoter. The correlation in expression between miR-143 and miR-145 was highly significant ($R=0.88$, $p<0.001$), suggesting their cotranscription.

We found the miR-143/145 cluster to be significantly downregulated in tumor cells when compared to benign cells, both in tissue samples collected from the BC cohort and in BC cell lines. Downregulation of the miR-143/145 cluster has been previously published for both BC and other cancer tissues [113, 122-126], but together with miRNA microarray and RT-qPCR, our study also verified expression in BC by ISH.

Results from the miRNA microarray indicated that expression of the miR-143/145 cluster was higher in ER+ tumors than in ER- tumors, and this result was later verified by RT-qPCR (**paper I, table 4**). Partly due to their sensitivity to endocrine therapy targeting the ER, ER+ BCs are generally considered among the least aggressive subtypes. In fact, increased expression of both miR-143 and miR-145 was observed consistently in the least aggressive subtypes (**paper I, tables 3 and 5**). This finding is in line with previous studies describing miR-143 and miR-145 as tumor suppressor miRNAs [127-129].

Functions of miRNAs are complex, and not yet fully understood, as is exemplified by publications reporting adverse effects of miR-143 and miR-145. Dimitrova et al. reported the stromal expression of miR-143 and miR-145 to stimulate neoangiogenesis, and in turn facilitate

tumor expansion in the lung [130]. Also, Donnarumma et al. reported increased levels of miR-143 in exosomes from cancer associated fibroblasts, and that exosome mediated delivery to BC cells could promote further BC progression [131].

Results from the functional studies performed for **paper I** were interesting and somewhat surprising. The miR-143, which is conventionally considered a tumor suppressor [128, 132, 133], displayed evidence of tumor promoting characteristics. The functional studies in **paper I** included three different BC cell lines, representing the major subtypes of BC. When transfecting these with the miR-143 mimic, both the ER+ and the TN BC cell line experienced increased proliferation. Proliferation in the HER2+ cell line did not significantly change from the negative control after transfection with the miR-143 mimic. These findings confirm the presence of a dualism in the function of miRNAs, and that environment and cellular context may be more important than expected.

Interestingly when considering the proliferation experiments, the miR-143 mimic had inhibitory effect on the cells' ability to invade in all three BC cell lines. In addition, all three BC cell lines suffered inhibition of both proliferation and invasion when transfected with the miR-145 mimic. The inhibitory effect on proliferation presented as very potent (**paper I, figures 2a-c**), and these results are in accordance with most of previous publications on miR-145 [134-139]. Cotransfecting miR-143 and miR-145 in equal concentration, resulted in an inhibition of both proliferation and invasion in all three BC cell lines, which is in line with previous publications [140-142]. The magnitude of the effect was similar to that of the cells transfected with miR-145 alone. This translates into two deductions: 1) the proliferation promoting properties of miR-143 in the ER+ and the TN BC cell lines were not able to significantly halt the inhibitory effects of miR-145, and 2) the cotransfection of miR-143 and miR-145 did not in synergy contribute to significantly lower the cells invasive potential when

compared to cells transfected with either miR-143 or miR-145 alone (**paper I, figure 2d**). Different results in different BC cell lines may be explained by the target genes that are active in operating the oncogenic phenotype at any given time, and the miRNAs that are there to regulate them.

A very interesting finding in **paper I** was the subcellular miR-145 distribution in the nuclei of myoepithelial cells (**paper I, figure 7**). Mature miRNAs located to the nucleus are gaining more and more interest, and in a very recent review by Liu et al. they summarize existing evidence of nuclear miRNAs [143]. The list of nuclear mature miRNAs is ever growing, and a relevant selection is presented in table 1.

In addition to nuclear enrichment of mature miRNAs, which presence is in divergence to earlier beliefs, new and surprising functions of miRNAs are also starting to emerge. Recent publications have reported that nuclear miRNAs probably are involved in upregulation of transcription via interactions between miRNAs and gene promoters and enhancers [144]. Interestingly, Xiao et al. recently published a research article describing miRNAs as epigenetic gene activators, and that a subset of miRNAs is capable of activating transcription by means of association with active genetic enhancers [145]. Further, they demonstrated that miR-24-1 function as an alternative mediator for transcriptional gene activation by facilitating the remodeling of chromatin at enhancer regions [145].

Table 1: Profiling of nuclear microRNAs. Adapted from [143].

Cell line	Method	Result
Human nasopharyngeal carcinoma (NPC) 5-8F cell line	Deep sequencing	Among 339 nuclear and 324 cytoplasmic miRNAs, 300 of them overlap.
HCT116 human colorectal carcinoma cell	Microarray	The overall average of nuclear ratio of miRNAs is 0.471 ± 0.15 .
	RT-PCR	MiR-16, miR-19b, miR-200b, miR-222, miR-29b, miR-29c are highly expressed in the nucleus.
	Northern blot	MiR-19b, miR-195 are highly expressed in the nucleus.
HeLa	RT-qPCR array	11 miRNAs are highly expressed in the nucleolus.
	In situ Hybridization	MiR191, miR-484, miR-574-3p and miR-193b are highly expressed in the nucleolus
The human breast cancer cell line MCF-7, MDA-MB-231 and the human mammary epithelial cell line MCF-10A (normal breast cells)	Microarray	Nuclear/cytoplasmic ratios of numerous miRNAs vary considerably across different cell lines

4.2.2 Paper II

Based on results from miRNA microarray on the BC cohort and previous work performed by our research group, we wanted to investigate the miR-126. Downregulation of miR-126 is previously reported in malignant breast tissue, and is associated with metastatic progression in BC cells, mainly through upregulation of key functions such as cell proliferation, migration, and survival [146, 147]. In order to gain more insight into functions and expression, we decided to include the passenger strand, miR-126-5p, into our inquiry.

We found endogenous expression of both miR-126-3p (lead strand) and miR-126-5p (passenger strand) to be significantly downregulated in tumor cells when compared to benign cells, both in tissue samples collected from the BC cohort and in BC cell lines representing the major subtypes of BC: ER+, HER2+ and TN.

Endogenous expression of miR-126-3p is considered to be tumor suppressive [148-151], and this is supported by our findings in the functional experiments, where all three BC cell lines suffered both reduced proliferation and reduced invasive capacity when transfected with the miR-126-3p mimic (**paper II, figures 3 and 4**). Surprisingly, the TN BC cell line experienced a very potent increase in proliferation when transfected with miR-126-5p, whilst the ER+ and the HER2+ BC cell lines suffered inhibition of proliferation when transfected with the same miRNA. Invasion potential was also increased in the TN BC cell line when transfected with miR-126-5p, but the magnitude of the response was not as obvious as it was for the proliferation experiment. These findings are not in line with previous publications, where the passenger strand, miR-126-5p, is reported to work in synergy with the lead strand, miR-126-3p, to facilitate a tumor suppressor phenotype [151, 152]. However, there are several reports supporting our findings in the TN BC cell line, and they put miR-126-5p in association with tumor supporting properties such as drug resistance and poor prognosis in acute myeloid

leukemia (AML) patients [153], promotion and protection of endothelial proliferation by inhibition of Dlk1 and SetD5 [154, 155], and induction of proliferation and angiogenesis in non-tumorigenic cells via the PI3K/AKT and MAPK/ERK pathways [156]. Other pathways described in association with miR-126-5p and enhanced tumor progression, include the NOTCH pathway, the Akt signaling pathway and the IGF-1 signaling pathway [157-159].

Expression analysis using TMA revealed that stromal levels of miR-126-5p were significantly associated with both molecular subtype and histological grade, and the highest levels of miR-126-5p were found in the more aggressive subtypes of BC. In this context it is also relevant to point out the correlation between miR-126-5p and the proliferation marker Ki67, at $R=0.24$, $p=0.055$. Although not statistically significant at the $p\leq 0.05$ level, it is worth considering in this setting. In the clinical tissue material analyzed by microarray and RT-qPCR, expression of miR-126-3p and miR126-5p was lower in BCs with nodal involvement (**paper II, figure 5**). As previously described, miR-126 is associated with metastases, and has been demonstrated as a negative regulator of the metastatic process in BC, in part by suppressing tumor growth *in vitro* using highly metastatic BC cell lines [146]. Knockdown of miR-126 has also been proven to lead to formation of metastases with high blood vessel density due to increased recruitment of endothelial cells to the metastatic cells [160].

The passenger strands of miRNAs are typically degraded after processing, and are consequently less abundant compared to their lead strand [161], and this is also evident in our study when analyzing results from microarray and PCR. Interestingly, when comparing endogenous levels of lead strand miRNA with endogenous levels of passenger strand miRNA in the non-cancerous breast cell line MCF-10A, the ER+ BC cell line, the HER2+ BC cell line and the TN BC cell line, we discovered an incremental shift in the miR-126-3p/miR-126-5p expression pattern, revealing miR-126-5p to be the more abundant strand in the TN BC cell line (**paper II, figure**

2). It is possible that mechanisms responsible for targeting the passenger strand for degradation are either corrupted, or in some way modified, allowing the accumulation of the passenger strand (**paper II, figure 8**). Consequently, a larger part of the mature passenger strand is eligible to interact with the RISC-complex to exhibit a more potent biological response in the TN BC cell line, which represents the most aggressive BC subtype.

There was a strong link between molecular subtype, tumor grade and expression of miR-126-5p in the tumor stromal compartments. Several studies have described considerable crosstalk between tumor and stroma via exosomal transfer of miRNAs [162-164] where microvesicles containing miRNAs derived from cancer cells convert fibroblast into cancer associated fibroblasts (CAFs) with tumor-promoting properties. Together with functional studies on miR-126-5p, the increased expression in stroma of more advanced BCs tells an interesting story. This work has provided valuable insight into the duplicity of miRNA function, emphasized by mature miR-126 having both potent tumor suppressor and tumor driver functions with opposite effects of the two different miR-126 strands in TN BC.

4.2.3 Paper III

Herein, we present results on functional studies, expression patterns, and prognostic significance in regards to the same miRNA cluster as in **paper I**, namely the miR-143/145 cluster. The work in this paper was performed on a NSCLC cohort comprising 553 patients and NSCLC cell lines. My involvement in this work was primarily on the design and implementation of the functional studies, and the subsequent interpretation and discussion of the results obtained from these studies.

The results from this work revealed stromal expression of miR-143 to be a positive prognostic marker in the female population, and it was also demonstrated that stromal expression of miR-145 is a positive prognostic marker in the male population. Previous publications have reported comparable findings, where low expression of miR-145 was associated with poor outcome in NSCLC and prostate cancer [165, 166]. However, there are reports of miR-143/145 expression having a negative impact on survival for patients with esophageal cancer [167] and bladder cancer [168], suggesting that impact of the expression patterns is tissue-specific. There are indications implying that expression of certain miRNAs may be gender specific, in addition to tissue-specific, and Duttagupta et al. have observed a subset of miRNAs to be differentially expressed in men and women [169]. This is interesting, and in line with our results, where stromal expression of miR-143 was associated with positive prognosis in women, and stromal expression of miR-145 was associated with positive prognosis in men.

The functional experiments were performed on NSCLC cell lines representing adenocarcinoma, squamous cell carcinoma and large-cell lung cancer. Cell lines were transfected with either miR-143 mimic, miR-145 mimic or miR-143 and miR-145 in equal concentrations. All cell lines suffered a significant loss in their capacity to both proliferate and migrate when introduced to miR-145. The adenocarcinoma cell line and the large-cell lung cancer cell line displayed

similar behavior when introduced to either miR-143 alone, or miR-143 and miR-145 in combination and in equal concentrations, although the effect was less prominent for the miR-143 transfected cells. When the squamous cell carcinoma cell line was transfected with miR-143, the proliferation was significantly increased, indicating miR-143 to promote tumor growth in this cell line. This is a very interesting observation when considering the results from the BC study on miR-143 and miR-145. In **paper I** we demonstrated that miR-143 was a potent tumor promoting factor in the ER+ and the TN BC cell lines (paper I, figures 2a and 2c). We have yet to explain why miR-143 has this effect on these cell lines, but it is noteworthy that basal cells and squamous cells share many cellular signatures [45, 55]. It is possible that the proliferation promoting properties of miR-143 in these two cell lines from different organs are a direct result of their cellular similarities, perhaps arguing for cell-type specific miRNAs rather than, or in addition to, tissue-specific miRNAs. Unfortunately, we were not able to get the squamous lung cancer cell line to migrate, so there are no results for this experiment. It would have been interesting to observe if the miR-143 has an inhibitory effect on migration in the squamous cell lung carcinoma cell line, like it had in the TN BC cell line, or if it would promote migration as it promotes proliferation.

As we observed for BC cell lines in **paper I**, the miR-143/145 cluster has a two-faced function in NSCLC cell lines as well, probably ascribed to cellular context. In order to increase our understanding into this duplicity, future experiments should focus on deciphering cellular pathways and miRNA targets in cells with different subtype, but within the same tissue, and also from cells in various tissues.

5. Conclusions and future perspectives

The discovery of miRNAs in the early 1990s was groundbreaking, and a MeSH search (medical subject heading search) today, revealed close to 60 000 entries regarding miRNAs in the PubMed database. In the majority of publications their described function appears to be pretty obvious: To act as post-transcriptional inhibitors of translation, targeting specific mRNAs via interactions with endonucleases. Today, however, we have come to realize that the actual picture is far more complicated. New pathways and mechanisms of action are frequently being described for both well-known and newly discovered miRNAs. Very recently (August 2018), Dragomir et al. published a SnapShot in Cell, describing unconventional functions of miRNAs, including miRNAs directly activating transcription and miRNAs coding for proteins [170]. These are modes of action quite opposite to the central/old dogma of miRNA biogenesis and function, and will likely maneuver future miRNA research into new directions.

The main focus of this thesis has been on investigating functions and tissue expression of selected miRNAs identified as dysregulated in BC. We have determined that the miR-143/145 cluster generally function as a tumor suppressor, which is in accordance with the general consensus, but that this function is dependent on (at least) cellular context. The functional dualism observed for the miR-143 in both BC cell lines and NSCLC cell lines, emphasizes the need for more specific research into pathways and functions of miRNAs. Adding to this story, are the results from the paper describing miR-126. Again, we encounter results contradicting the general consensus, and again we observe a dualism in function which is unsuspected.

One of the major questions of the future is whether or not miRNAs can be effective players in targeted therapy, e.g. as miRNA replacement therapy in cancer treatment. Indeed, interesting research has depicted certain miRNAs to prevent development of drug resistance when used in multi-targeted treatment [171, 172], and the first miRNA treatment eligible for clinical trial,

MesomiR-1, quite recently completed phase I, and preliminary results are promising [173]. But as this thesis accentuates, caution should be exercised when navigating the miRNA landscape in search for new therapeutics, as their functional duality may become a concern.

Hopefully, the future development of new technologies will help shed light on the complex role of miRNA function in human cells. It is my sincere belief that, guided by miRNAs, the future holds promise of increased accuracy of diagnosis and treatment options for many malignancies.

6. References

1. Ferlay J, Soerjomataram I, Dikshit R, Eser S, Mathers C, Rebelo M, Parkin DM, Forman D, Bray F: **Cancer incidence and mortality worldwide: sources, methods and major patterns in GLOBOCAN 2012.** *Int J Cancer* 2015, **136**(5):E359-386.
2. DeSantis C, Ma J, Bryan L, Jemal A: **Breast cancer statistics, 2013.** *CA Cancer J Clin* 2014, **64**(1):52-62.
3. Siegel R, Naishadham D, Jemal A: **Cancer statistics, 2013.** *CA Cancer J Clin* 2013, **63**(1):11-30.
4. Berman AT, Thukral AD, Hwang WT, Solin LJ, Vapiwala N: **Incidence and patterns of distant metastases for patients with early-stage breast cancer after breast conservation treatment.** *Clin Breast Cancer* 2013, **13**(2):88-94.
5. Redig AJ, McAllister SS: **Breast cancer as a systemic disease: a view of metastasis.** *J Intern Med* 2013, **274**(2):113-126.
6. Gerratana L, Fanotto V, Bonotto M, Bolzonello S, Minisini AM, Fasola G, Puglisi F: **Pattern of metastasis and outcome in patients with breast cancer.** *Clin Exp Metastasis* 2015, **32**(2):125-133.
7. Autier P, Boniol M, Gavin A, Vatten LJ: **Breast cancer mortality in neighbouring European countries with different levels of screening but similar access to treatment: trend analysis of WHO mortality database.** *BMJ* 2011, **343**:d4411.
8. **Cancer in Norway 2015 - Cancer incidence, prevalence, mortality and survival in Norway.** In. Oslo: Cancer registry of Norway - Institute of population-based cancer research; 2015.
9. Alvarado A: **Anatomy and histology of the breast - Mammary gland [image].** In. <http://humanbiologylab.pbworks.com/w/page/104941359/Histology%20of%20the%20Mammary%20Gland>; [Accessed 15 June 2018] 2016.
10. Watson CJ, Khaled WT: **Mammary development in the embryo and adult: a journey of morphogenesis and commitment.** *Development* 2008, **135**(6):995-1003.
11. Visvader JE: **Keeping abreast of the mammary epithelial hierarchy and breast tumorigenesis.** *Genes Dev* 2009, **23**(22):2563-2577.
12. Van Keymeulen A, Rocha AS, Ousset M, Beck B, Bouvencourt G, Rock J, Sharma N, Dekoninck S, Blanpain C: **Distinct stem cells contribute to mammary gland development and maintenance.** *Nature* 2011, **479**(7372):189-193.
13. Bland P, Howard BA: **Mammary lineage restriction in development.** *Nat Cell Biol* 2018, **20**(6):637-639.
14. Sanders ME, Schuyler PA, Simpson JF, Page DL, Dupont WD: **Continued observation of the natural history of low-grade ductal carcinoma in situ reaffirms proclivity for local recurrence even after more than 30 years of follow-up.** *Mod Pathol* 2015, **28**(5):662-669.
15. Micalizzi DS, Maheswaran S: **On the trail of invasive cells in breast cancer.** *Nature* 2018, **554**(7692):308-309.
16. Schubert EL, Lee MK, Mefford HC, Argonza RH, Morrow JE, Hull J, Dann JL, King MC: **BRCA2 in American families with four or more cases of breast or ovarian cancer: recurrent and novel mutations, variable expression, penetrance, and the possibility of families whose cancer is not attributable to BRCA1 or BRCA2.** *Am J Hum Genet* 1997, **60**(5):1031-1040.
17. Fackenthal JD, Olopade OI: **Breast cancer risk associated with BRCA1 and BRCA2 in diverse populations.** *Nat Rev Cancer* 2007, **7**(12):937-948.

18. Park S, Koo JS, Kim MS, Park HS, Lee JS, Lee JS, Kim SI, Park BW: **Characteristics and outcomes according to molecular subtypes of breast cancer as classified by a panel of four biomarkers using immunohistochemistry.** *Breast* 2012, **21**(1):50-57.
19. Perou CM, Sorlie T, Eisen MB, van de Rijn M, Jeffrey SS, Rees CA, Pollack JR, Ross DT, Johnsen H, Akslen LA *et al*: **Molecular portraits of human breast tumours.** *Nature* 2000, **406**(6797):747-752.
20. Sorlie T, Tibshirani R, Parker J, Hastie T, Marron JS, Nobel A, Deng S, Johnsen H, Pesich R, Geisler S *et al*: **Repeated observation of breast tumor subtypes in independent gene expression data sets.** *Proc Natl Acad Sci U S A* 2003, **100**(14):8418-8423.
21. Rivenbark AG, O'Connor SM, Coleman WB: **Molecular and cellular heterogeneity in breast cancer: challenges for personalized medicine.** *Am J Pathol* 2013, **183**(4):1113-1124.
22. Kennecke H, Yerushalmi R, Woods R, Cheang MC, Voduc D, Speers CH, Nielsen TO, Gelmon K: **Metastatic behavior of breast cancer subtypes.** *J Clin Oncol* 2010, **28**(20):3271-3277.
23. Sihto H, Lundin J, Lundin M, Lehtimäki T, Ristimäki A, Holli K, Sillanpää L, Kataja V, Turpeenniemi-Hujanen T, Isola J *et al*: **Breast cancer biological subtypes and protein expression predict for the preferential distant metastasis sites: a nationwide cohort study.** *Breast Cancer Res* 2011, **13**(5):R87.
24. Sotiriou C, Neo SY, McShane LM, Korn EL, Long PM, Jazaeri A, Martiat P, Fox SB, Harris AL, Liu ET: **Breast cancer classification and prognosis based on gene expression profiles from a population-based study.** *Proc Natl Acad Sci U S A* 2003, **100**(18):10393-10398.
25. Stephens PJ, Tarpey PS, Davies H, Van Loo P, Greenman C, Wedge DC, Nik-Zainal S, Martin S, Varela I, Bignell GR *et al*: **The landscape of cancer genes and mutational processes in breast cancer.** *Nature* 2012, **486**(7403):400-404.
26. Fan C, Oh DS, Wessels L, Weigelt B, Nuyten DS, Nobel AB, van't Veer LJ, Perou CM: **Concordance among gene-expression-based predictors for breast cancer.** *N Engl J Med* 2006, **355**(6):560-569.
27. Hashmi AA, Aijaz S, Khan SM, Mahboob R, Irfan M, Zafar NI, Nisar M, Siddiqui M, Edhi MM, Faridi N *et al*: **Prognostic parameters of luminal A and luminal B intrinsic breast cancer subtypes of Pakistani patients.** *World J Surg Oncol* 2018, **16**(1):1.
28. Voduc KD, Cheang MC, Tyldesley S, Gelmon K, Nielsen TO, Kennecke H: **Breast cancer subtypes and the risk of local and regional relapse.** *J Clin Oncol* 2010, **28**(10):1684-1691.
29. Vasconcelos I, Hussainzada A, Berger S, Fietze E, Linke J, Siedentopf F, Schoenegg W: **The St. Gallen surrogate classification for breast cancer subtypes successfully predicts tumor presenting features, nodal involvement, recurrence patterns and disease free survival.** *Breast* 2016, **29**:181-185.
30. Burstein HJ, Temin S, Anderson H, Buchholz TA, Davidson NE, Gelmon KE, Giordano SH, Hudis CA, Rowden D, Solky AJ *et al*: **Adjuvant endocrine therapy for women with hormone receptor-positive breast cancer: american society of clinical oncology clinical practice guideline focused update.** *J Clin Oncol* 2014, **32**(21):2255-2269.
31. Gutierrez C, Schiff R: **HER2: biology, detection, and clinical implications.** *Arch Pathol Lab Med* 2011, **135**(1):55-62.

32. Shih C, Padhy LC, Murray M, Weinberg RA: **Transforming genes of carcinomas and neuroblastomas introduced into mouse fibroblasts.** *Nature* 1981, **290**(5803):261-264.
33. Rubin I, Yarden Y: **The basic biology of HER2.** *Ann Oncol* 2001, **12 Suppl 1**:S3-8.
34. Ross JS, Slodkowska EA, Symmans WF, Pusztai L, Ravdin PM, Hortobagyi GN: **The HER-2 receptor and breast cancer: ten years of targeted anti-HER-2 therapy and personalized medicine.** *Oncologist* 2009, **14**(4):320-368.
35. Krishnamurti U, Silverman JF: **HER2 in breast cancer: a review and update.** *Adv Anat Pathol* 2014, **21**(2):100-107.
36. Vidula N, Bardia A: **Targeted therapy for metastatic triple negative breast cancer: The next frontier in precision oncology.** *Oncotarget* 2017, **8**(63):106167-106168.
37. Rakha EA, Tan DS, Foulkes WD, Ellis IO, Tutt A, Nielsen TO, Reis-Filho JS: **Are triple-negative tumours and basal-like breast cancer synonymous?** *Breast Cancer Res* 2007, **9**(6):404; author reply 405.
38. Bertucci F, Finetti P, Cervera N, Esterni B, Hermitte F, Viens P, Birnbaum D: **How basal are triple-negative breast cancers?** *Int J Cancer* 2008, **123**(1):236-240.
39. Cheang MC, Martin M, Nielsen TO, Prat A, Voduc D, Rodriguez-Lescure A, Ruiz A, Chia S, Shepherd L, Ruiz-Borrego M *et al*: **Defining breast cancer intrinsic subtypes by quantitative receptor expression.** *Oncologist* 2015, **20**(5):474-482.
40. Prat A, Adamo B, Cheang MC, Anders CK, Carey LA, Perou CM: **Molecular characterization of basal-like and non-basal-like triple-negative breast cancer.** *Oncologist* 2013, **18**(2):123-133.
41. Badve S, Dabbs DJ, Schnitt SJ, Baehner FL, Decker T, Eusebi V, Fox SB, Ichihara S, Jacquemier J, Lakhani SR *et al*: **Basal-like and triple-negative breast cancers: a critical review with an emphasis on the implications for pathologists and oncologists.** *Mod Pathol* 2011, **24**(2):157-167.
42. Prat A, Lluch A, Albanell J, Barry WT, Fan C, Chacon JI, Parker JS, Calvo L, Plazaola A, Arcusa A *et al*: **Predicting response and survival in chemotherapy-treated triple-negative breast cancer.** *Br J Cancer* 2014, **111**(8):1532-1541.
43. Bianchini G, Balko JM, Mayer IA, Sanders ME, Gianni L: **Triple-negative breast cancer: challenges and opportunities of a heterogeneous disease.** *Nat Rev Clin Oncol* 2016, **13**(11):674-690.
44. Foulkes WD, Smith IE, Reis-Filho JS: **Triple-negative breast cancer.** *N Engl J Med* 2010, **363**(20):1938-1948.
45. Chung CH, Bernard PS, Perou CM: **Molecular portraits and the family tree of cancer.** *Nat Genet* 2002, **32 Suppl**:533-540.
46. Schmadeka R, Harmon BE, Singh M: **Triple-negative breast carcinoma: current and emerging concepts.** *Am J Clin Pathol* 2014, **141**(4):462-477.
47. Liedtke C, Mazouni C, Hess KR, Andre F, Tordai A, Mejia JA, Symmans WF, Gonzalez-Angulo AM, Hennessy B, Green M *et al*: **Response to neoadjuvant therapy and long-term survival in patients with triple-negative breast cancer.** *J Clin Oncol* 2008, **26**(8):1275-1281.
48. Torre LA, Bray F, Siegel RL, Ferlay J, Lortet-Tieulent J, Jemal A: **Global cancer statistics, 2012.** *CA Cancer J Clin* 2015, **65**(2):87-108.
49. Stewart BW, Wild C, International Agency for Research on Cancer, World Health Organization: **World cancer report 2014.** Lyon-France, Geneva-Switzerland: International Agency for Research on Cancer. WHO Press.; 2014.
50. Siegel RL, Miller KD, Jemal A: **Cancer statistics, 2016.** *CA Cancer J Clin* 2016, **66**(1):7-30.

51. Herbst RS, Heymach JV, Lippman SM: **Lung cancer**. *N Engl J Med* 2008, **359**(13):1367-1380.
52. Molina JR, Yang P, Cassivi SD, Schild SE, Adjei AA: **Non-small cell lung cancer: epidemiology, risk factors, treatment, and survivorship**. *Mayo Clin Proc* 2008, **83**(5):584-594.
53. Travis WD, Brambilla E, Nicholson AG, Yatabe Y, Austin JHM, Beasley MB, Chirieac LR, Dacic S, Duhig E, Flieder DB *et al*: **The 2015 World Health Organization Classification of Lung Tumors: Impact of Genetic, Clinical and Radiologic Advances Since the 2004 Classification**. *J Thorac Oncol* 2015, **10**(9):1243-1260.
54. Sun S, Schiller JH, Gazdar AF: **Lung cancer in never smokers--a different disease**. *Nat Rev Cancer* 2007, **7**(10):778-790.
55. Davidson MR, Gazdar AF, Clarke BE: **The pivotal role of pathology in the management of lung cancer**. *J Thorac Dis* 2013, **5 Suppl 5**:S463-478.
56. Thomas A, Liu SV, Subramaniam DS, Giaccone G: **Refining the treatment of NSCLC according to histological and molecular subtypes**. *Nat Rev Clin Oncol* 2015, **12**(9):511-526.
57. Hirsch FR, Scagliotti GV, Mulshine JL, Kwon R, Curran WJ, Jr., Wu YL, Paz-Ares L: **Lung cancer: current therapies and new targeted treatments**. *Lancet* 2017, **389**(10066):299-311.
58. International Human Genome Sequencing C: **Finishing the euchromatic sequence of the human genome**. *Nature* 2004, **431**(7011):931-945.
59. Consortium EP: **An integrated encyclopedia of DNA elements in the human genome**. *Nature* 2012, **489**(7414):57-74.
60. Djebali S, Davis CA, Merkel A, Dobin A, Lassmann T, Mortazavi A, Tanzer A, Lagarde J, Lin W, Schlesinger F *et al*: **Landscape of transcription in human cells**. *Nature* 2012, **489**(7414):101-108.
61. Palazzo AF, Lee ES: **Non-coding RNA: what is functional and what is junk?** *Front Genet* 2015, **6**:2.
62. Bartel DP: **MicroRNAs: target recognition and regulatory functions**. *Cell* 2009, **136**(2):215-233.
63. Lee RC, Feinbaum RL, Ambros V: **The *C. elegans* heterochronic gene *lin-4* encodes small RNAs with antisense complementarity to *lin-14***. *Cell* 1993, **75**(5):843-854.
64. Calin GA, Croce CM: **MicroRNA signatures in human cancers**. *Nat Rev Cancer* 2006, **6**(11):857-866.
65. Zhang C: **MicroRNAs: role in cardiovascular biology and disease**. *Clin Sci (Lond)* 2008, **114**(12):699-706.
66. Tan L, Yu JT, Tan L: **Causes and Consequences of MicroRNA Dysregulation in Neurodegenerative Diseases**. *Mol Neurobiol* 2015, **51**(3):1249-1262.
67. Nieto-Diaz M, Esteban FJ, Reigada D, Munoz-Galdeano T, Yunta M, Caballero-Lopez M, Navarro-Ruiz R, Del Aguila A, Maza RM: **MicroRNA dysregulation in spinal cord injury: causes, consequences and therapeutics**. *Front Cell Neurosci* 2014, **8**:53.
68. Iorio MV, Croce CM: **Causes and consequences of microRNA dysregulation**. *Cancer J* 2012, **18**(3):215-222.
69. Gross N, Kropp J, Khatib H: **MicroRNA Signaling in Embryo Development**. *Biology (Basel)* 2017, **6**(3).
70. Huntzinger E, Izaurralde E: **Gene silencing by microRNAs: contributions of translational repression and mRNA decay**. *Nat Rev Genet* 2011, **12**(2):99-110.

71. Bartel DP: **MicroRNAs: genomics, biogenesis, mechanism, and function.** *Cell* 2004, **116**(2):281-297.
72. Lee Y, Jeon K, Lee JT, Kim S, Kim VN: **MicroRNA maturation: stepwise processing and subcellular localization.** *EMBO J* 2002, **21**(17):4663-4670.
73. Ha M, Kim VN: **Regulation of microRNA biogenesis.** *Nat Rev Mol Cell Biol* 2014, **15**(8):509-524.
74. Monteys AM, Spengler RM, Wan J, Tecedor L, Lennox KA, Xing Y, Davidson BL: **Structure and activity of putative intronic miRNA promoters.** *RNA* 2010, **16**(3):495-505.
75. Lee Y, Kim M, Han J, Yeom KH, Lee S, Baek SH, Kim VN: **MicroRNA genes are transcribed by RNA polymerase II.** *EMBO J* 2004, **23**(20):4051-4060.
76. Vishnoi A, Rani S: **MiRNA Biogenesis and Regulation of Diseases: An Overview.** *Methods Mol Biol* 2017, **1509**:1-10.
77. Krol J, Loedige I, Filipowicz W: **The widespread regulation of microRNA biogenesis, function and decay.** *Nat Rev Genet* 2010, **11**(9):597-610.
78. Davis-Dusenbery BN, Hata A: **Mechanisms of control of microRNA biogenesis.** *J Biochem* 2010, **148**(4):381-392.
79. Lee Y, Ahn C, Han J, Choi H, Kim J, Yim J, Lee J, Provost P, Radmark O, Kim S *et al*: **The nuclear RNase III Drosha initiates microRNA processing.** *Nature* 2003, **425**(6956):415-419.
80. Ohtsuka M, Ling H, Doki Y, Mori M, Calin GA: **MicroRNA Processing and Human Cancer.** *J Clin Med* 2015, **4**(8):1651-1667.
81. Bohnsack MT, Czaplinski K, Gorlich D: **Exportin 5 is a RanGTP-dependent dsRNA-binding protein that mediates nuclear export of pre-miRNAs.** *RNA* 2004, **10**(2):185-191.
82. Lund E, Guttinger S, Calado A, Dahlberg JE, Kutay U: **Nuclear export of microRNA precursors.** *Science* 2004, **303**(5654):95-98.
83. Okada C, Yamashita E, Lee SJ, Shibata S, Katahira J, Nakagawa A, Yoneda Y, Tsukihara T: **A high-resolution structure of the pre-microRNA nuclear export machinery.** *Science* 2009, **326**(5957):1275-1279.
84. Hutvagner G, McLachlan J, Pasquinelli AE, Balint E, Tuschl T, Zamore PD: **A cellular function for the RNA-interference enzyme Dicer in the maturation of the let-7 small temporal RNA.** *Science* 2001, **293**(5531):834-838.
85. Lee HY, Doudna JA: **TRBP alters human precursor microRNA processing in vitro.** *RNA* 2012, **18**(11):2012-2019.
86. Fukunaga R, Han BW, Hung JH, Xu J, Weng Z, Zamore PD: **Dicer partner proteins tune the length of mature miRNAs in flies and mammals.** *Cell* 2012, **151**(3):533-546.
87. Diederichs S, Haber DA: **Dual role for argonautes in microRNA processing and posttranscriptional regulation of microRNA expression.** *Cell* 2007, **131**(6):1097-1108.
88. Sanghvi VR, Steel LF: **The cellular TAR RNA binding protein, TRBP, promotes HIV-1 replication primarily by inhibiting the activation of double-stranded RNA-dependent kinase PKR.** *J Virol* 2011, **85**(23):12614-12621.
89. Khvorova A, Reynolds A, Jayasena SD: **Functional siRNAs and miRNAs exhibit strand bias.** *Cell* 2003, **115**(2):209-216.
90. Hu HY, Yan Z, Xu Y, Hu H, Menzel C, Zhou YH, Chen W, Khaitovich P: **Sequence features associated with microRNA strand selection in humans and flies.** *BMC Genomics* 2009, **10**:413.

91. Hutvagner G, Zamore PD: **A microRNA in a multiple-turnover RNAi enzyme complex.** *Science* 2002, **297**(5589):2056-2060.
92. He J, Zhao J, Zhu W, Qi D, Wang L, Sun J, Wang B, Ma X, Dai Q, Yu X: **MicroRNA biogenesis pathway genes polymorphisms and cancer risk: a systematic review and meta-analysis.** *PeerJ* 2016, **4**:e2706.
93. Calin GA, Dumitru CD, Shimizu M, Bichi R, Zupo S, Noch E, Aldler H, Rattan S, Keating M, Rai K *et al*: **Frequent deletions and down-regulation of micro- RNA genes miR15 and miR16 at 13q14 in chronic lymphocytic leukemia.** *Proc Natl Acad Sci U S A* 2002, **99**(24):15524-15529.
94. Lin S, Gregory RI: **MicroRNA biogenesis pathways in cancer.** *Nat Rev Cancer* 2015, **15**(6):321-333.
95. Peng Y, Croce CM: **The role of MicroRNAs in human cancer.** *Signal Transduct Target Ther* 2016, **1**:15004.
96. Calin GA, Croce CM: **MicroRNAs and chromosomal abnormalities in cancer cells.** *Oncogene* 2006, **25**(46):6202-6210.
97. Hayashita Y, Osada H, Tatematsu Y, Yamada H, Yanagisawa K, Tomida S, Yatabe Y, Kawahara K, Sekido Y, Takahashi T: **A polycistronic microRNA cluster, miR-17-92, is overexpressed in human lung cancers and enhances cell proliferation.** *Cancer Res* 2005, **65**(21):9628-9632.
98. Mavrakis KJ, Wolfe AL, Oricchio E, Palomero T, de Keersmaecker K, McJunkin K, Zuber J, James T, Khan AA, Leslie CS *et al*: **Genome-wide RNA-mediated interference screen identifies miR-19 targets in Notch-induced T-cell acute lymphoblastic leukaemia.** *Nat Cell Biol* 2010, **12**(4):372-379.
99. Mogilyansky E, Rigoutsos I: **The miR-17/92 cluster: a comprehensive update on its genomics, genetics, functions and increasingly important and numerous roles in health and disease.** *Cell Death Differ* 2013, **20**(12):1603-1614.
100. O'Donnell KA, Wentzel EA, Zeller KI, Dang CV, Mendell JT: **c-Myc-regulated microRNAs modulate E2F1 expression.** *Nature* 2005, **435**(7043):839-843.
101. Gregory PA, Bert AG, Paterson EL, Barry SC, Tsykin A, Farshid G, Vadas MA, Khew-Goodall Y, Goodall GJ: **The miR-200 family and miR-205 regulate epithelial to mesenchymal transition by targeting ZEB1 and SIP1.** *Nat Cell Biol* 2008, **10**(5):593-601.
102. Lujambio A, Calin GA, Villanueva A, Ropero S, Sanchez-Cespedes M, Blanco D, Montuenga LM, Rossi S, Nicoloso MS, Faller WJ *et al*: **A microRNA DNA methylation signature for human cancer metastasis.** *Proc Natl Acad Sci U S A* 2008, **105**(36):13556-13561.
103. Guil S, Esteller M: **DNA methylomes, histone codes and miRNAs: tying it all together.** *Int J Biochem Cell Biol* 2009, **41**(1):87-95.
104. Karube Y, Tanaka H, Osada H, Tomida S, Tatematsu Y, Yanagisawa K, Yatabe Y, Takamizawa J, Miyoshi S, Mitsudomi T *et al*: **Reduced expression of Dicer associated with poor prognosis in lung cancer patients.** *Cancer Sci* 2005, **96**(2):111-115.
105. Wang X, Zhao X, Gao P, Wu M: **c-Myc modulates microRNA processing via the transcriptional regulation of Drosha.** *Sci Rep* 2013, **3**:1942.
106. Rupaimoole R, Slack FJ: **MicroRNA therapeutics: towards a new era for the management of cancer and other diseases.** *Nat Rev Drug Discov* 2017, **16**(3):203-222.

107. Martello G, Rosato A, Ferrari F, Manfrin A, Cordenonsi M, Dupont S, Enzo E, Guzzardo V, Rondina M, Spruce T *et al*: **A MicroRNA targeting dicer for metastasis control.** *Cell* 2010, **141**(7):1195-1207.
108. Dumeaux V, Borresen-Dale AL, Frantzen JO, Kumle M, Kristensen VN, Lund E: **Gene expression analyses in breast cancer epidemiology: the Norwegian Women and Cancer postgenome cohort study.** *Breast Cancer Res* 2008, **10**(1):R13.
109. Elston CW, Ellis IO: **Pathological prognostic factors in breast cancer. I. The value of histological grade in breast cancer: experience from a large study with long-term follow-up.** *Histopathology* 1991, **19**(5):403-410.
110. Coates AS, Winer EP, Goldhirsch A, Gelber RD, Gnant M, Piccart-Gebhart M, Thurlimann B, Senn HJ, Panel M: **Tailoring therapies--improving the management of early breast cancer: St Gallen International Expert Consensus on the Primary Therapy of Early Breast Cancer 2015.** *Ann Oncol* 2015, **26**(8):1533-1546.
111. Skjefstad K, Richardsen E, Donnem T, Andersen S, Kiselev Y, Grindstad T, Hald SM, Al-Shibli K, Bremnes RM, Busund LT *et al*: **The prognostic role of progesterone receptor expression in non-small cell lung cancer patients: Gender-related impacts and correlation with disease-specific survival.** *Steroids* 2015, **98**:29-36.
112. Skjefstad K, Grindstad T, Khanehkenari MR, Richardsen E, Donnem T, Kilvaer T, Andersen S, Bremnes RM, Busund LT, Al-Saad S: **Prognostic relevance of estrogen receptor alpha, beta and aromatase expression in non-small cell lung cancer.** *Steroids* 2016, **113**:5-13.
113. Skjefstad K, Johannessen C, Grindstad T, Kilvaer T, Paulsen EE, Pedersen M, Donnem T, Andersen S, Bremnes R, Richardsen E *et al*: **A gender specific improved survival related to stromal miR-143 and miR-145 expression in non-small cell lung cancer.** *Sci Rep* 2018, **8**(1):8549.
114. Kononen J, Bubendorf L, Kallioniemi A, Barlund M, Schraml P, Leighton S, Torhorst J, Mihatsch MJ, Sauter G, Kallioniemi OP: **Tissue microarrays for high-throughput molecular profiling of tumor specimens.** *Nat Med* 1998, **4**(7):844-847.
115. Lin F, Prichard J: **Tissue Microarray.** In: *Handbook of practical immunohistochemistry: frequently asked questions*, Second edition. edn. New York ; Heidelberg: Springer; 2015.
116. Camp RL, Neumeister V, Rimm DL: **A decade of tissue microarrays: progress in the discovery and validation of cancer biomarkers.** *J Clin Oncol* 2008, **26**(34):5630-5637.
117. Camp RL, Charette LA, Rimm DL: **Validation of tissue microarray technology in breast carcinoma.** *Lab Invest* 2000, **80**(12):1943-1949.
118. Gillett CE, Springall RJ, Barnes DM, Hanby AM: **Multiple tissue core arrays in histopathology research: a validation study.** *J Pathol* 2000, **192**(4):549-553.
119. Pohl M, Olsen KE, Holst R, Ditzel HJ, Hansen O: **Tissue microarrays in non-small-cell lung cancer: reliability of immunohistochemically-determined biomarkers.** *Clin Lung Cancer* 2014, **15**(3):222-230 e223.
120. Matos LL, Trufelli DC, de Matos MG, da Silva Pinhal MA: **Immunohistochemistry as an important tool in biomarkers detection and clinical practice.** *Biomark Insights* 2010, **5**:9-20.
121. Kaur G, Dufour JM: **Cell lines: Valuable tools or useless artifacts.** *Spermatogenesis* 2012, **2**(1):1-5.
122. Zheng T, Zhang X, Wang Y, Yu X: **Predicting associations between microRNAs and target genes in breast cancer by bioinformatics analyses.** *Oncol Lett* 2016, **12**(2):1067-1073.

123. Navon R, Wang H, Steinfeld I, Tsalenko A, Ben-Dor A, Yakhini Z: **Novel rank-based statistical methods reveal microRNAs with differential expression in multiple cancer types.** *PLoS One* 2009, **4**(11):e8003.
124. Iorio MV, Ferracin M, Liu CG, Veronese A, Spizzo R, Sabbioni S, Magri E, Pedriali M, Fabbri M, Campiglio M *et al*: **MicroRNA gene expression deregulation in human breast cancer.** *Cancer Res* 2005, **65**(16):7065-7070.
125. Michael MZ, SM OC, van Holst Pellekaan NG, Young GP, James RJ: **Reduced accumulation of specific microRNAs in colorectal neoplasia.** *Mol Cancer Res* 2003, **1**(12):882-891.
126. Yuan DZ, Lei Y, Zhao D, Pan JL, Zhao YB, Nie L, Liu M, Long Y, Zhang JH, Yue LM: **Progesterone-Induced miR-145/miR-143 Inhibits the Proliferation of Endometrial Epithelial Cells.** *Reprod Sci* 2018:1933719118768687.
127. Liu J, Mao Y, Zhang D, Hao S, Zhang Z, Li Z, Li B: **RETRACTED: MiR-143 inhibits tumor cell proliferation and invasion by targeting STAT3 in esophageal squamous cell carcinoma.** *Cancer Lett* 2016, **373**(1):97-108.
128. Xu YF, Li YQ, Guo R, He QM, Ren XY, Tang XR, Jia WH, Kang TB, Zeng MS, Sun Y *et al*: **Identification of miR-143 as a tumour suppressor in nasopharyngeal carcinoma based on microRNA expression profiling.** *Int J Biochem Cell Biol* 2015, **61**:120-128.
129. Yu X, Zhang X, Dhakal IB, Beggs M, Kadlubar S, Luo D: **Induction of cell proliferation and survival genes by estradiol-repressed microRNAs in breast cancer cells.** *BMC Cancer* 2012, **12**:29.
130. Dimitrova N, Gocheva V, Bhutkar A, Resnick R, Jong RM, Miller KM, Bendor J, Jacks T: **Stromal Expression of miR-143/145 Promotes Neoangiogenesis in Lung Cancer Development.** *Cancer Discov* 2016, **6**(2):188-201.
131. Donnarumma E, Fiore D, Nappa M, Roscigno G, Adamo A, Iaboni M, Russo V, Affinito A, Puoti I, Quintavalle C *et al*: **Cancer-associated fibroblasts release exosomal microRNAs that dictate an aggressive phenotype in breast cancer.** *Oncotarget* 2017, **8**(12):19592-19608.
132. Wang Q, Cai J, Wang J, Xiong C, Zhao J: **MiR-143 inhibits EGFR-signaling-dependent osteosarcoma invasion.** *Tumour Biol* 2014, **35**(12):12743-12748.
133. Xia H, Sun S, Wang B, Wang T, Liang C, Li G, Huang C, Qi D, Chu X: **miR-143 inhibits NSCLC cell growth and metastasis by targeting Limk1.** *Int J Mol Sci* 2014, **15**(7):11973-11983.
134. Wu J, Yin L, Jiang N, Guo WJ, Gu JJ, Chen M, Xia YY, Wu JZ, Chen D, Wu JF *et al*: **MiR-145, a microRNA targeting ADAM17, inhibits the invasion and migration of nasopharyngeal carcinoma cells.** *Exp Cell Res* 2015, **338**(2):232-238.
135. Zhang Y, Yang X, Wu H, Zhou W, Liu Z: **MicroRNA-145 inhibits migration and invasion via inhibition of fascin 1 protein expression in non-small-cell lung cancer cells.** *Mol Med Rep* 2015, **12**(4):6193-6198.
136. Qin J, Wang F, Jiang H, Xu J, Jiang Y, Wang Z: **MicroRNA-145 suppresses cell migration and invasion by targeting paxillin in human colorectal cancer cells.** *Int J Clin Exp Pathol* 2015, **8**(2):1328-1340.
137. Larne O, Hagman Z, Lilja H, Bjartell A, Edsjo A, Ceder Y: **miR-145 suppress the androgen receptor in prostate cancer cells and correlates to prostate cancer prognosis.** *Carcinogenesis* 2015, **36**(8):858-866.
138. Cui SY, Wang R, Chen LB: **MicroRNA-145: a potent tumour suppressor that regulates multiple cellular pathways.** *J Cell Mol Med* 2014, **18**(10):1913-1926.

139. Sachdeva M, Mo YY: **MicroRNA-145 suppresses cell invasion and metastasis by directly targeting mucin 1**. *Cancer Res* 2010, **70**(1):378-387.
140. Su J, Liang H, Yao W, Wang N, Zhang S, Yan X, Feng H, Pang W, Wang Y, Wang X *et al*: **MiR-143 and MiR-145 regulate IGF1R to suppress cell proliferation in colorectal cancer**. *PLoS One* 2014, **9**(12):e114420.
141. Yan X, Chen X, Liang H, Deng T, Chen W, Zhang S, Liu M, Gao X, Liu Y, Zhao C *et al*: **miR-143 and miR-145 synergistically regulate ERBB3 to suppress cell proliferation and invasion in breast cancer**. *Mol Cancer* 2014, **13**:220.
142. Yoshino H, Enokida H, Itesako T, Kojima S, Kinoshita T, Tatarano S, Chiyomaru T, Nakagawa M, Seki N: **Tumor-suppressive microRNA-143/145 cluster targets hexokinase-2 in renal cell carcinoma**. *Cancer Sci* 2013, **104**(12):1567-1574.
143. Liu H, Lei C, He Q, Pan Z, Xiao D, Tao Y: **Nuclear functions of mammalian MicroRNAs in gene regulation, immunity and cancer**. *Mol Cancer* 2018, **17**(1):64.
144. Huang V, Place RF, Portnoy V, Wang J, Qi Z, Jia Z, Yu A, Shuman M, Yu J, Li LC: **Upregulation of Cyclin B1 by miRNA and its implications in cancer**. *Nucleic Acids Res* 2012, **40**(4):1695-1707.
145. Xiao M, Li J, Li W, Wang Y, Wu F, Xi Y, Zhang L, Ding C, Luo H, Li Y *et al*: **MicroRNAs activate gene transcription epigenetically as an enhancer trigger**. *RNA Biol* 2017, **14**(10):1326-1334.
146. Tavazoie SF, Alarcon C, Oskarsson T, Padua D, Wang Q, Bos PD, Gerald WL, Massague J: **Endogenous human microRNAs that suppress breast cancer metastasis**. *Nature* 2008, **451**(7175):147-152.
147. Tahiri A, Leivonen SK, Luders T, Steinfeld I, Ragle Aure M, Geisler J, Makela R, Nord S, Riis ML, Yakhini Z *et al*: **Deregulation of cancer-related miRNAs is a common event in both benign and malignant human breast tumors**. *Carcinogenesis* 2014, **35**(1):76-85.
148. Luo P, Fei J, Zhou J, Zhang W: **microRNA-126 suppresses PAK4 expression in ovarian cancer SKOV3 cells**. *Oncol Lett* 2015, **9**(5):2225-2229.
149. Yang Z, Wang R, Zhang T, Dong X: **MicroRNA-126 regulates migration and invasion of gastric cancer by targeting CADM1**. *Int J Clin Exp Pathol* 2015, **8**(8):8869-8880.
150. Zhao C, Li Y, Zhang M, Yang Y, Chang L: **miR-126 inhibits cell proliferation and induces cell apoptosis of hepatocellular carcinoma cells partially by targeting Sox2**. *Hum Cell* 2015, **28**(2):91-99.
151. Zhang Y, Yang P, Sun T, Li D, Xu X, Rui Y, Li C, Chong M, Ibrahim T, Mercatali L *et al*: **miR-126 and miR-126* repress recruitment of mesenchymal stem cells and inflammatory monocytes to inhibit breast cancer metastasis**. *Nat Cell Biol* 2013, **15**(3):284-294.
152. Ren G, Kang Y: **A one-two punch of miR-126/126* against metastasis**. *Nat Cell Biol* 2013, **15**(3):231-233.
153. Shibayama Y, Kondo T, Ohya H, Fujisawa S, Teshima T, Iseki K: **Upregulation of microRNA-126-5p is associated with drug resistance to cytarabine and poor prognosis in AML patients**. *Oncol Rep* 2015, **33**(5):2176-2182.
154. Schober A, Nazari-Jahantigh M, Wei Y, Bidzhekov K, Gremse F, Grommes J, Megens RT, Heyll K, Noels H, Hristov M *et al*: **MicroRNA-126-5p promotes endothelial proliferation and limits atherosclerosis by suppressing Dlk1**. *Nat Med* 2014, **20**(4):368-376.

155. Gaelle V, Loic P, Baraa N, Gaelle B, Carlos RJ, Sylvain C, Fabrice S, Virginie M: **miR-126-5p promotes retinal endothelial cell survival through SetD5 regulation in neurons.** *Development* 2017.
156. Tao SC, Guo SC, Li M, Ke QF, Guo YP, Zhang CQ: **Chitosan Wound Dressings Incorporating Exosomes Derived from MicroRNA-126-Overexpressing Synovium Mesenchymal Stem Cells Provide Sustained Release of Exosomes and Heal Full-Thickness Skin Defects in a Diabetic Rat Model.** *Stem Cells Transl Med* 2017, **6**(3):736-747.
157. Nueda ML, Naranjo AI, Baladron V, Laborda J: **Different expression levels of DLK1 inversely modulate the oncogenic potential of human MDA-MB-231 breast cancer cells through inhibition of NOTCH1 signaling.** *FASEB journal : official publication of the Federation of American Societies for Experimental Biology* 2017, **31**(8):3484-3496.
158. Shibayama Y, Kondo T, Ohya H, Fujisawa S-I, Teshima T, Iseki KEN: **Upregulation of microRNA-126-5p is associated with drug resistance to cytarabine and poor prognosis in AML patients.** *Oncology Reports* 2015, **33**(5):2176-2182.
159. Wolf I, Levanon-Cohen S, Bose S, Ligumsky H, Sredni B, Kanety H, Kuro-o M, Karlan B, Kaufman B, Koeffler HP *et al*: **Klotho: a tumor suppressor and a modulator of the IGF-1 and FGF pathways in human breast cancer.** *Oncogene* 2008, **27**(56):7094-7105.
160. Png KJ, Halberg N, Yoshida M, Tavazoie SF: **A microRNA regulon that mediates endothelial recruitment and metastasis by cancer cells.** *Nature* 2011, **481**(7380):190-194.
161. Macfarlane LA, Murphy PR: **MicroRNA: Biogenesis, Function and Role in Cancer.** *Curr Genomics* 2010, **11**(7):537-561.
162. Valadi H, Ekstrom K, Bossios A, Sjostrand M, Lee JJ, Lotvall JO: **Exosome-mediated transfer of mRNAs and microRNAs is a novel mechanism of genetic exchange between cells.** *Nat Cell Biol* 2007, **9**(6):654-659.
163. Kogure T, Lin WL, Yan IK, Braconi C, Patel T: **Intercellular nanovesicle-mediated microRNA transfer: a mechanism of environmental modulation of hepatocellular cancer cell growth.** *Hepatology* 2011, **54**(4):1237-1248.
164. Chiba M, Kimura M, Asari S: **Exosomes secreted from human colorectal cancer cell lines contain mRNAs, microRNAs and natural antisense RNAs, that can transfer into the human hepatoma HepG2 and lung cancer A549 cell lines.** *Oncol Rep* 2012, **28**(5):1551-1558.
165. Avgeris M, Stravodimos K, Fragoulis EG, Scorilas A: **The loss of the tumour-suppressor miR-145 results in the shorter disease-free survival of prostate cancer patients.** *Br J Cancer* 2013, **108**(12):2573-2581.
166. Campayo M, Navarro A, Vinolas N, Diaz T, Tejero R, Gimferrer JM, Molins L, Cabanas ML, Ramirez J, Monzo M *et al*: **Low miR-145 and high miR-367 are associated with unfavourable prognosis in resected nonsmall cell lung cancer.** *Eur Respir J* 2013, **41**(5):1172-1178.
167. Feber A, Xi L, Pennathur A, Gooding WE, Bandla S, Wu M, Luketich JD, Godfrey TE, Litle VR: **MicroRNA prognostic signature for nodal metastases and survival in esophageal adenocarcinoma.** *Ann Thorac Surg* 2011, **91**(5):1523-1530.
168. Avgeris M, Mavridis K, Tokas T, Stravodimos K, Fragoulis EG, Scorilas A: **Uncovering the clinical utility of miR-143, miR-145 and miR-224 for predicting the survival of bladder cancer patients following treatment.** *Carcinogenesis* 2015, **36**(5):528-537.

169. Duttagupta R, Jiang R, Gollub J, Getts RC, Jones KW: **Impact of cellular miRNAs on circulating miRNA biomarker signatures.** *PLoS One* 2011, **6**(6):e20769.
170. Dragomir MP, Knutsen E, Calin GA: **SnapShot: Unconventional miRNA Functions.** *Cell* 2018, **174**(4):1038-1038 e1031.
171. Cortez MA, Valdecanas D, Zhang X, Zhan Y, Bhardwaj V, Calin GA, Komaki R, Giri DK, Quini CC, Wolfe T *et al*: **Therapeutic delivery of miR-200c enhances radiosensitivity in lung cancer.** *Mol Ther* 2014, **22**(8):1494-1503.
172. Zhao J, Kelnar K, Bader AG: **In-depth analysis shows synergy between erlotinib and miR-34a.** *PLoS One* 2014, **9**(2):e89105.
173. Reid G, Kao SC, Pavlakis N, Brahmabhatt H, MacDiarmid J, Clarke S, Boyer M, van Zandwijk N: **Clinical development of TargomiRs, a miRNA mimic-based treatment for patients with recurrent thoracic cancer.** *Epigenomics* 2016, **8**(8):1079-1085.

Paper I

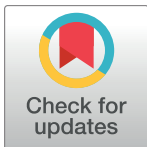
RESEARCH ARTICLE

Expression and function of the miR-143/145 cluster *in vitro* and *in vivo* in human breast cancer

Charles Johannessen^{1*}, Line Moi^{1,2}, Yury Kiselev³, Mona Irene Pedersen⁴, Stig Manfred Dalen², Tonje Braaten⁵, Lill-Tove Busund^{1,2}

1 Department of Medical Biology, UiT—The Arctic University of Norway, Tromsø, Norway, **2** Department of Clinical Pathology, University Hospital of North Norway, Tromsø, Norway, **3** Department of Life Sciences and Health, Oslo and Akershus University College of Applied Sciences, Oslo, Norway, **4** Department of Clinical Medicine, UiT—The Arctic University of Norway, Tromsø, Norway, **5** Department of Community Medicine, UiT—The Arctic University of Norway, Tromsø, Norway

* charles.johannessen@uit.no



OPEN ACCESS

Citation: Johannessen C, Moi L, Kiselev Y, Pedersen MI, Dalen SM, Braaten T, et al. (2017) Expression and function of the miR-143/145 cluster *in vitro* and *in vivo* in human breast cancer. PLoS ONE 12(10): e0186658. <https://doi.org/10.1371/journal.pone.0186658>

Editor: Aamir Ahmad, University of South Alabama Mitchell Cancer Institute, UNITED STATES

Received: June 6, 2017

Accepted: October 1, 2017

Published: October 26, 2017

Copyright: © 2017 Johannessen et al. This is an open access article distributed under the terms of the [Creative Commons Attribution License](https://creativecommons.org/licenses/by/4.0/), which permits unrestricted use, distribution, and reproduction in any medium, provided the original author and source are credited.

Data Availability Statement: The microarray data are available from the European Genome-phenome Archive (Dataset ID: EGAD00010001406).

Funding: This study was solely funded by the Northern Norway Regional Health Authority (Helse Nord RHF), responsible for the public hospitals in northern Norway. The funder had no role in study design, data collection and analysis, decision to publish, or preparation of the manuscript.

Competing interests: The authors have declared that no competing interests exist.

Abstract

MicroRNAs (miRNAs) are small non-coding RNAs that function as post-transcriptional regulators of gene expression and are dysregulated in cancer. Studies of miRNAs to explore their potential as diagnostic and prognostic markers are of great scientific interest. Here, we investigate the functional properties and expression of the miR-143/145 cluster in breast cancer (BC) *in vitro* and *in vivo*. The ER positive MCF7, the HER2 positive SK-BR-3, and the triple negative cell line MDA-MB-231 were used to assess cell proliferation and cell invasion. Expression of miRNA in 108 breast cancers in the Norwegian Women and Cancer Study and 44 benign tissue controls were analyzed by microarray and validated by RT-PCR. Further, *in situ* hybridization (ISH) was used to study the cellular and subcellular distribution of the miRNAs. *In vitro*, miR-143 promoted proliferation of MCF7 and MDA-MB-231 cells, whereas miR-145 and the cotransfection of both miRNAs inhibited proliferation in all three cell lines. The cells' invasive capacity was reduced after transfection and cotransfection of the miRNAs. In line with the tumor suppressive functions *in vitro*, the expression of miR-143 and miR-145 was lower in malignant compared to benign breast tissue, and lower in the more aggressive tumors with higher tumor grade, loss of ER and the basal-like phenotype. ISH revealed miR-143 to be cytoplasmatic and predominantly expressed in luminal cells in benign tissue, whilst miR-145 was nuclear and with strong staining in myoepithelial cells. Both miRNAs were present in malignant epithelial cells and stromal fibroblasts in BC. This study demonstrates that miR-143 and -145 have functional properties and expression patterns typical for tumor suppressors, but the function is influenced by cellular factors such as cell type and miRNA cotransfection. Further, the nuclear functions of miR-145 should be explored for a more complete understanding of the complexity of miRNA regulation and function in BC.

Introduction

Breast cancer (BC) is the most common cancer diagnosed in women [1]. Clinical classification of BC is done by assessing histological type, grade, stage and receptor status where tumors can be categorized as estrogen receptor positive (ER+), and/or human epidermal growth factor receptor 2 positive (HER2+), or triple negative (TN) [2]. The ER+ BCs constitute nearly 70% of all cases [3], and this group has extended therapeutic options, compared to the HER2+ and TN BCs.

Based on gene expression profiles, the ER+ tumors can be divided into the molecular subtypes luminal A and luminal B, where the luminal B subtype has a worse prognosis due to a higher proliferation rate and/or HER2 positivity [4, 5]. The HER2+ BCs are commonly associated with ductal carcinoma *in situ* (DCIS) and in general have a moderate to poor prognosis [4, 5]. The TN BCs constitute a heterogeneous group of tumors, where the majority of cases are presented as basal-like BCs [6]. The TN BCs typically include the most aggressive breast carcinomas, where the majority of cancer related death occur within five years from time of diagnosis [5, 6]. Molecular profiles are used to guide treatment. However, when comparing individual cases, BCs have highly heterogeneous gene expression contributing to the challenges of treating BC patients [7]. Further, BC is still one of the leading causes of cancer deaths in women [1], underlining the need for improved prognostic and predictive biomarkers for early detection, identification and stratification of the most aggressive tumors, and more targeted treatment.

MicroRNAs (miRNAs) constitute a group of small non-coding endogenous RNAs with a typical length of 18–22 nucleotides. Mature miRNAs bind to the complementary or semi complementary 3' untranslated region (3'-UTR) of mRNAs, resulting in negative regulation of protein translation [8]. The downregulation of protein synthesis can be a result of miRNA induced mRNA degradation, mRNA destabilization, or mRNA silencing [9]. The nature of the negative regulation is dependent upon the degree of complementarity between the mature miRNA and the 3'-UTR target [9]. Due to the highly pleiotropic nature of miRNAs, it is predicted that more than 60% of all human protein coding genes are influenced by miRNAs, and their dysregulation is a universal event for virtually all types of malignancies, as they have a profound influence on most cellular processes [10–12]. Expression profiles of miRNA have been shown to categorize various cancers more accurately than mRNA [13], and miRNAs can be considered novel regulators in the hallmarks of human cancers [14]. Combined with miRNAs' biochemical properties that make them suitable as biomarkers, it is of great scientific interest to investigate and characterize individual miRNAs, their expression, and their functional roles in BC and BC subtypes.

MiR-143 and miR-145 constitute a miRNA cluster and appear to have tumor suppressor functions in a variety of organ systems, both as individual miRNAs and as a cluster [15–24]. This study evaluates the miR-143 and miR-145 expression profile in an unselected cohort of BC within the Norwegian Women and Cancer Study (NOWAC) postgenome cohort [25]. Samples were stratified in subgroups based on molecular subtype, receptor status, tumor grade and lymph node status. In addition, through a series of *in vitro* experiments, including assays for cell proliferation and cell invasion, the functionality of miR-143 and miR-145 was studied in BC cell lines analogous to the major subtypes of breast cancer; ER+, HER2+ and TN BC.

Materials and methods

Ethics statement

The study of miRNA expression in BC samples from the NOWAC postgenome cohort and benign breast tissue has been approved by the regional ethical committee of North Norway

(REKnord 2010/1931, 2013/2271). The Data Inspectorate has also approved the storing of relevant, not identifiable data and the linkage to national registries. In addition, ethical aspects have been considered within the project to ensure the most efficient and accurate use of the material collected and data generated, in accordance with national and international guidelines and laws.

Functional studies

The potential function of miR-143 and miR-145 in tumorigenesis was investigated by a series of *in vitro* experiments. The experiments were performed by introducing miR-143 mimic or miR-145 mimic, alone or in combination, alongside a miRNA negative control into various BC cell lines. In this study, cell proliferation and cell invasion were assessed.

Cell cultures. The functions of miR-143 and miR-145 were evaluated in three different BC cell lines. These included the ER+ MCF7 (ATCC® HTB-22™), the HER2+ SK-BR-3 (ATCC® HTB-30™), and the TN BC cell line MDA-MB-231 (ATCC® CRM-HTB-26™). All cell lines, except MCF7, were cultured in RPMI-1640 media (cat.# R8758, Sigma-Aldrich, St. Louis, USA) supplemented with 10% fetal bovine serum (cat.# S0415, Biochrom, Berlin, Germany). MCF7 were cultured in DMEM (cat.# D5796, Sigma-Aldrich, St. Louis, USA) with the same supplements as the previously described cell lines. All cell lines were incubated at 37°C in humidified atmosphere with 5% CO₂. Total RNA from the non-cancerous breast cell line MCF-10A was a kind gift from the research group of professor E. Mortensen, RNA and molecular pathology (RAMP) research group, UiT—The Arctic University of Norway, Tromsø, Norway.

Cell transfection. All cell lines were transiently transfected with 100 nM hsa-miR-143-3p Pre-miR™ miRNA Precursor (cat.# PM10883, Thermo Fisher Scientific, USA) and/or 100 nM hsa-miR-145-5p Pre-miR™ miRNA Precursor (cat.# PM11480, Thermo Fisher Scientific, USA), alongside the Cy3™ Dye-Labeled Pre-miR Negative Control #1 (cat.# AM17120, Thermo Fisher Scientific, USA). The transfection was performed by using 6 µl/mL of the Lipofectamine® RNAiMAX transfection reagent (cat.# 13778075, Thermo Fisher Scientific, USA). Transfected Cy3™ Dye-Labeled Pre-miR Negative Control emits fluorescent light when exposed to UV-light, and the transfection efficiency was determined using a fluorescence microscope. The transfection efficiency was typically as high as 80–95%.

Total RNA isolation. Total RNA was isolated from cell lines using the miRNeasy Mini Kit (cat.# 217004, Qiagen, Hilden, Germany) according to the manufacturer's protocol. In short, cells were lysed in 700 µl QIAzol Lysis Reagent before homogenization and 5 minutes incubation at room temperature. 140 µl chloroform were added, and the samples were shaken before incubation at room temperature for 3 minutes. Samples were centrifuged for 15 minutes at 12000 g at 4°C, and the upper aqueous phase was transferred and mixed thoroughly with 100% ethanol. The samples were transferred into the RNeasy® Mini column and washed in several steps before elution with 50 µl ddH₂O. Isolated total RNA samples were stored at -70°C.

cDNA synthesis. First strand cDNA synthesis was performed using the miScript II RT Kit (cat.# 218160, Qiagen, Hilden, Germany) according to the manufacturer's protocol. Briefly, 100 ng of total RNA was mixed with 4 µl 5x miScript HiSpec Buffer, 2 µl 10x Nucleics Mix, 2 µl miScript Reverse Transcriptase Mix, and RNase-free water to a total volume of 20 µl. Samples were incubated for 60 minutes at 37°C, and subsequently incubated for 5 minutes at 95°C to inactivate enzymes. Finally, samples were diluted up to a total volume of 200 µl in RNase-free water and stored at -20°C.

RT-PCR. Endogenous levels of miR-143 and miR-145 in the selected cell lines were quantified relative to the stably expressed reference snRNA RNU6 using real-time PCR and the

miScript SYBR® Green PCR Kit (cat.# 218073, Qiagen, Hilden, Germany). Primers used were miScript Primer Assays Hs_miR-143_1 miScript Primer Assay (cat.# MS00003514, Qiagen, Hilden, Germany), Hs_miR-145_1 miScript Primer Assay (cat.# MS00003528, Qiagen, Hilden, Germany) and Hs_RNU6-2_11 miScript Primer Assay (cat.# MS00033740, Qiagen, Hilden, Germany), according to the manufacturer's protocol. Briefly, a total volume of 25 µl/well in a 96-well plate included 1 µl cDNA mixed with 12.5 µl 2x QuantiTect SYBR Green PCR Master Mix, 2.5 µl 10x miScript Universal Primer, 2.5 µl 10x miScript Primer Assay, and 6.5 µl RNase-free Water. The plate was sealed and centrifuged for 1 minute at 1000 g before it was placed in a 7300 Real-Time PCR System (Thermo Fisher Scientific, Waltham, Massachusetts, USA). Each sample was analyzed in quadruplicates, and three independent experiments were performed.

Proliferation assay. The BC cell lines' ability to proliferate after transfection was evaluated using the real-time cell analyzer system xCelligence, RTCA DP (cat#05469759001, ACEA Biosciences, San Diego, USA) fitted with the E-plate 16 (cat#05469830001, ACEA Biosciences, San Diego, USA). Prior to analysis on the xCelligence platform, cell lines were trypsinized until detached, resuspended in complete growth media, and counted. Initial titration experiments estimated approximately 8000 cells per well to be optimal. In accordance with the manufacturer's protocol, cells were seeded in quadruplicates into an E-plate after baseline measurements. The E-plate containing cells was incubated for 30 minutes at room temperature before positioned in the RTCA DP instrument, which was located in an incubator preserving the same conditions as used for routine cultivation of cell lines. The instrument denotes the cellular growth rate as 'Cell Index', which is an arbitrary unit reflecting the cell-sensor impedance. The cell index was recorded by the instrument every 30 minutes. Growth curves were calculated with the RTCA software version 1.2.1 (ACEA Biosciences, San Diego, USA). A minimum of three independent experiments were performed for each cell line.

Invasion assay. The cell lines invasiveness after transfection was tested using the CytoSelect™ 96-well Cell Invasion Assay, Basement membrane (cat.# CBA-112, Cell Biolabs, San Diego, USA) according to the manufacturer's protocol. Briefly, 50000 pretransfected and serum starved cells were seeded in the upper chamber of a modified Boyden chamber. The chamber was coated with a basement membrane consisting of a protein matrix isolated from Engelbreth-Holm-Swarm tumor cells, and the cells were allowed to invade for 24 h towards the bottom chamber containing media+10% FBS. Cancer cells able to invade the basement membrane and pass through the porous membrane to the bottom side of the membrane were lysed, stained, and fluorescence was measured at 480/520 nm using the CLARIOstar® microplate reader (BMG LABTECH, Ortenberg, Germany). All experiments were performed in quadruplicates, and a minimum of three independent experiments were performed for each cell line.

Patient material and tumor classification

The patient samples were collected from the NOWAC postgenome cohort [25]. The NOWAC participants included in this study were diagnosed with breast cancer at the Department of Pathology at the University Hospital of North Norway in Tromsø, or the Nordland Hospital in Bodø in the years 2004–2010. Archived formalin-fixed paraffin-embedded (FFPE) tissue blocks, and hematoxylin and eosin stained slides were collected. Histological grading of tumors was based on the criteria modified by Elston and Ellis [26] and immunohistochemical (IHC) analyses of ER, progesterone receptor (PR) and HER2 were done on needle biopsies as part of routine diagnostics. The cut-off value for ER positivity was $\geq 1\%$, for PR $\geq 10\%$ and a HER2 score of 3+ was considered positive, a score of 0–1+ negative whereas a score of 2+ lead

to silver in situ hybridization (SISH) where HER2 was considered negative if HER2/chromosome 17-ratio was < 2 . IHC staining for the proliferation marker Ki67 was done on slides from the primary surgery, and the expression evaluated in at least 500 tumor cells in the most proliferative areas of the tumor and the result reported as a percentage of positive tumor cells. Subtyping of the tumors according to molecular profile were based on the surrogate markers ER, PR, HER2 and Ki67 according to recommendations by the St Gallen International Expert Consensus and previous publications [27, 28]. The subtyping was performed as follows: luminal A (ER+ and/or PR+, HER2- and Ki67 $\leq 30\%$), luminal B (ER+ and/or PR+, HER2- and Ki67 $> 30\%$ or ER+ and/or PR+ and HER2+), HER2 positive (ER- and PR- and HER2+) and basal-like (ER-, PR- and HER2-). Histopathological data were collected from the original pathology reports, and reevaluated and completed according to updated criteria by a breast pathologist (L.M.). As benign tissue controls, FFPE tissue cores from 44 breast reduction surgery specimens were included in the study.

miRNA microarray

Total RNA was extracted from FFPE tissue cores from both malignant and benign breast tissue using the RecoverAll Total Nucleic Acid Isolation kit (Life Technologies, Grand Island, NY, USA) following the manufacturer's instructions. RNA quality and quantity was assessed using the NanoDrop 1000 spectrophotometer (Thermo Fisher Scientific, Wilmington, DE). Microarray hybridization and analyses were performed as a bought service by Exiqon (Vedbaek, Denmark). In short, the miRCURY LNATM microRNA Hi-Power Labeling Kit (Exiqon) was used to label 250 ng total RNA from samples and reference with Hy3TM and Hy5TM, respectively. The Hy5TM-labeled reference RNA contained an equal aliquot of all RNA species included in the study. Labeled samples and reference RNA were mixed before hybridization to the 7th generation miRCURY LNA microRNA array (Exiqon), using a Tecan HS4800 hybridization station (Tecan, Austria). The microarray contained capture probes for miRNAs in human, mouse and rat as annotated in miRBASE version 19.0. The slides were scanned on the Agilent G2565BA Microarray Scanner System (Agilent technologies Inc., USA) and the ImageGene 9.0 software (BioDiscovery Inc., USA) was used for image analysis. The quantified signals were background corrected and normalized using quantile normalization method and detection threshold set as 1.2 times the 25th percentile of the overall signal intensity of the individual slides.

Validation of microarray and quantification of miRNAs by RT-qPCR

Microarray miRNA analyses were validated using RT-qPCR. 40 tumor samples representing the four major molecular subtypes of cancer included in the study, and 20 of the benign breast tissue controls were included in the PCR validation done by Exiqon. In short, RNA was extracted from FFPE tissue cores using the Qiagen miRNeasy FFPE kit according to the manufacturer's instructions (Qiagen, Hilden, Germany). 10 ng RNA was reverse transcribed using the miRCURY LNA Universal RT microRNA PCR, Polyadenylation and cDNA synthesis kit (Exiqon) and PCR-reactions performed on 100 x diluted cDNA using ExiLENT SYBR Green master mix. The amplification was done in a Light Cycler 480 Real-Time PCR System (Roche) in 384 well plates. All reverse transcription reactions were done in duplicates. Based on stable expression across the data set, the most suitable reference miRNAs were evaluated by Exiqon using the Normfinder software. Of the suitable reference miRNAs, miR-664a-3p was detected in all samples and was used for normalization. Normalized expression values for each miRNA in each sample were calculated using the quantification cycle (Cq) from PCR analyses and the formula: average Cq (all samples)–assay Cq (sample).

In situ hybridization

In order to study the cellular and subcellular location of miR-143 and miR-145 in benign and malignant breast tissue, we analyzed the miRNA *in situ* hybridization (ISH) staining in full histological slides of 16 tumors with adjacent normal tissue. Buffers and detection reagents were purchased from Roche (Basel, Switzerland) and labelled locked nucleic acid (LNA) modified probes purchased from Exiqon (Vedbaek, Denmark). The chromogen ISH was performed in the Ventana Discovery Ultra instrument for IHC and ISH (Ventana Medical Systems Inc, Arizona, USA) with deparaffinization, pretreatment, hybridization, chromogen staining and counterstaining automatized in the instrument. In short, 4 μ m tissue sections were incubated overnight at 60°C to attach tissue to Super Frost Plus slides. To ensure good distribution of reagents and protect sections from drying, liquid coverslip oil (Roche) was added during incubation. Sections were deparaffinized in EZ Prep buffer (Roche) at 68°C (3 x 12 min), followed by heat-mediated retrieval pretreatment at 95°C with CC1 buffer (Roche) for 40 minutes and rinsing with Reaction Buffer (Roche) followed by RiboWash SSPE buffer (Roche). In this study, we used 5 nM miR-145-5p target probe, 10 nM miR-143-3p target probe, 10 nM scramble miR negative control probe and 0.5 nM U6 positive control probe. Positive and negative tissue controls for both miRNAs were included by using a TMA multi-organ slide.

All slides were denaturated for 8 min at 90°C, hybridization with probes took place for 60 min at 50°C for miR-145, 55°C for miR-143, 57°C for scramble miR and 55°C for U6. Stringent washes were done 2 x 8 minutes with 2.0X RiboWash SSPE, followed by rinsing with Reaction Buffer and blocking against unspecific binding with blocking solution (Roche) for 16 minutes at 37°C. Immunological detection was done with prediluted alkaline phosphatase (AP)-conjugated anti-DIG (Roche) at 37°C for 20 minutes. The sections were rinsed with Reaction Buffer and EZ Prep before the substrate enzymatic reactions were carried out with NBT/BCIP (CromoMap Blue kit, Roche) for 60 minutes at 37°C. Sections were rinsed with Reaction Buffer and counterstained for 4 minutes with Red Stain II (Roche). Dehydration of the sections was performed by increasing gradients of ethanol and finally the tissue sections were mounted with glass cover slips.

Scoring of ISH staining intensity. ISH stained full slides of selected tumors were used to collect information on staining intensity and density in tumor cells, stromal fibroblast and adjacent normal breast tissue. The tumors were randomly selected from histological slides of good quality with well preserved invasive carcinoma present. For each slide, three areas of tumor tissue and tumor-associated stromal tissue were evaluated using a microscope at 200x magnification. By morphologic criteria, the tumor cells and stromal fibroblasts were scored for staining intensity with the dominant staining intensity scored as: 0 = negative, 1 = weak, 2 = moderate, 3 = strong. From the observed ISH staining pattern, both tumor cells and stromal fibroblasts stained diffusely and homogenously and hence staining density was not scored since it did not give any additional information. All samples were independently scored by two experienced pathologists (L.M. and S.M.D.).

Statistics

The miRNA microarray and PCR expression data from the breast cancer samples in the NOWAC study were analyzed using the Limma package in R (Linear Models for Microarray and RNA-Seq Data). Moderated F-statistics were applied, with p-values corrected for multiple testing by controlling the false discovery rate using the method of Benjamini & Hochberg. Descriptive statistics, non-parametric tests and correlation analysis were performed using Stata, version 14.

For the qPCR results from the *in vitro* experiments, the standard error was calculated using all four technical replicates from a representative biological experiment. For the proliferation study, each proliferation curve was tested against the miRNA control using one-way ANOVA with p-values corrected for multiple testing by controlling the false discovery rate using the method of Benjamini & Hochberg. For the invasion study, the standard error was calculated using all four technical replicates from a representative biological experiment.

Results

Relative expression of miR-143 and miR-145 in breast cancer

The endogenous expression of miR-143 and miR-145 in the studied BC cell lines was quantified relative to the non-cancerous cell line MCF-10A (Fig 1). Relative to MCF-10A, endogenous expression levels of miR-143 and miR-145 were downregulated in all BC cell lines. This pattern was also evident in the NOWAC patient material, as described later.

Functional studies on miR-143 and miR-145 *in vitro*

The potential functional role of miR-143 and miR-145 in breast cancer tumorigenesis was explored by a series of *in vitro* experiments. Proliferation and invasion were assessed after

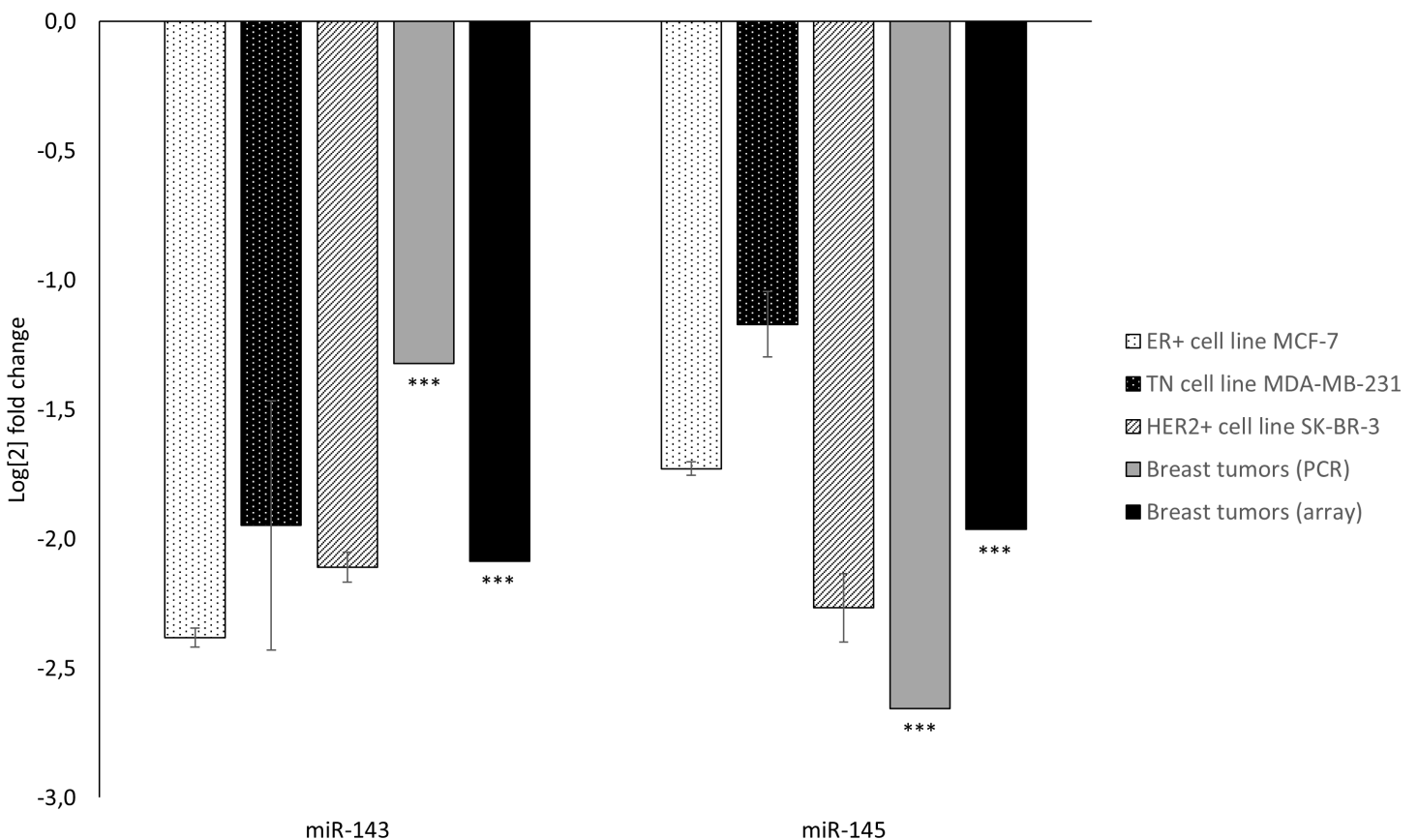


Fig 1. MiRNA expression in breast cancer cell lines and tumor tissue relative to non-cancerous control. Endogenous expression of miR-143 and miR-145 in breast cancer cell lines compared to the non-cancerous breast cell line MCF-10A and in breast cancer tumors compared to benign breast tissue, analyzed using PCR or microarray technology. Data from cell lines are presented as mean log fold change \pm SE from a representative biological replicate using all four technical replicates. *** signifies $P < 0.001$ using moderated F-statistics and the Benjamini & Hochberg correction.

<https://doi.org/10.1371/journal.pone.0186658.g001>

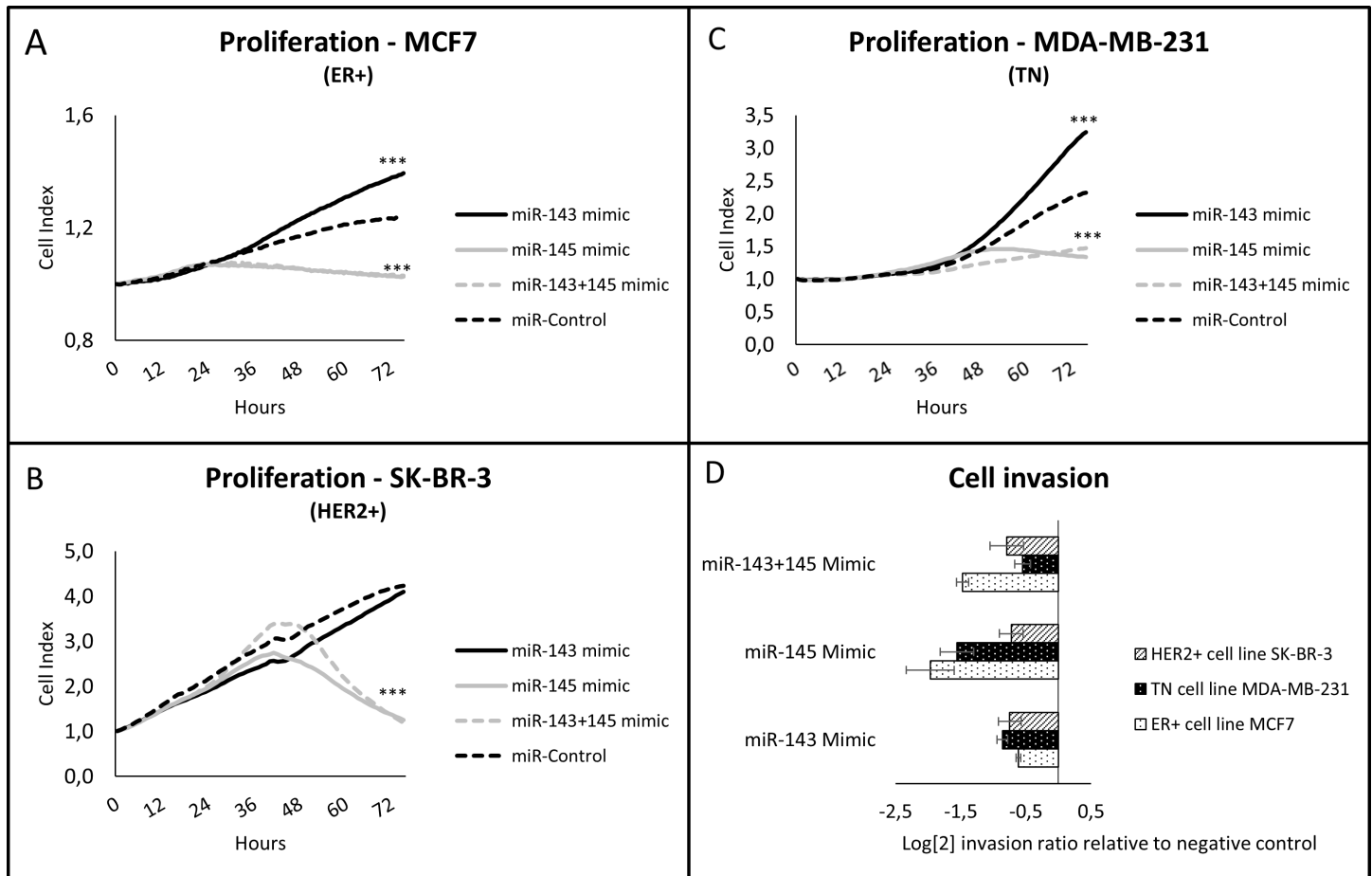


Fig 2. Functional studies on BC cell lines after transfection with miR-143 and/or miR-145. ER+ MCF7 cells (panel A), HER2+ SK-BR-3 cells (panel B) and triple negative MDA-MB-231 cells (panel C) were transfected with miR-143 mimic, miR-145 mimic, either alone or in combination, or with control mimic, and cell proliferation monitored in real time using xCelligence. Data presented are representative for all three biological replicates, and include four technical replicates for each transfection. *** signifies $P < 0.001$ using one-way ANOVA and the Benjamini & Hochberg correction comparing miR-143 and/or miR-145 transfected cells to controls. The invasion capacity (panel D) of all BC cell lines transfected with either miR-143, miR-145, or miR-143 and miR-145, was studied using the CytoSelect Cell Invasion Assay with chambers separated by a basement membrane. Results are presented as mean log fold change \pm SE of transfected cells relative to negative controls from a representative biological experiment with four technical replicates for each cell line.

<https://doi.org/10.1371/journal.pone.0186658.g002>

transfecting BC cell lines with either miR-143, miR-145, or miR-143 and miR-145 in combination.

miR-143 promotes proliferation *in vitro*. The proliferation rate of the BC cell lines was assessed using the real-time monitoring system xCelligence, fitted with a proliferation plate. Interestingly, transfection of miR-143 led to increased proliferation in the ER+ cell line MCF7 and the TN cell line MDA-MB-231 (Fig 2A and 2C). The HER2+ cell line, however, did not demonstrate any significant change in proliferation when transfected with miR-143 (Fig 2B).

miR-145 inhibits proliferation *in vitro*. All three studied BC cell lines demonstrated a dramatic drop in proliferation when transfected with miR-145 (Fig 2A–2C). The shift in proliferation capacity occurred between 24–48 hours after transfection, depending on the cell line.

miR-143 and miR-145 inhibits invasion *in vitro*. The cells' invasive abilities were studied using a Boyden chamber assay. Pretransfected cells were seeded in serum-free media in the upper chambers, and allowed to invade through a basement membrane extract towards the bottom chamber containing media with 10% serum. Invading cells were quantified 20–24

hours after being seeded to the upper chamber. Both miR-143 and miR-145 had a profound effect on cell invasion (Fig 2D). All cell lines demonstrated reduced invasive capacity 24 hours after transfection.

Cotransfection of miR-143 and miR-145 results in a tumor suppressor phenotype. In addition to investigating the functional effects of each individual miRNA, we also wanted to study the effects of cotransfecting miR-143 and miR-145. The BC cell lines were simultaneously transfected with 50 nM of both miR-143 and miR-145. The proliferation of cells cotransfected with miR-143 and miR-145 was dramatically reduced in all three cell lines and was similar to the proliferation pattern of cells transfected with miR-145 alone (Fig 2A–2C). The proliferation promoting effects observed for miR-143 in the ER+ cell line and the TN cell line were cancelled by the simultaneous transfection of miR-145 (Fig 2A and 2C). Cotransfection of miR-143 and miR-145 had an inhibitory effect on invasion, in line with the observations made for each individual miRNA (Fig 2D). The cumulative effect of cotransfection using both miRNAs was not significantly different from experiments where only one miRNA was used.

Patient material

A total of 108 NOWAC postgenome cohort participants were diagnosed with BC at the pathology departments in Northern Norway in the years 2004–2010 and included in the study. Of these, one case had no FFPE tissue block with enough tumor tissue for further analyses. Five cases and six of the benign tissue controls had poor RNA quality, leaving 102 BC surgery specimens and 38 of the 44 benign breast specimens to be included in the miRNA microarray. After microarray miRNA analyses, an additional case and two of the controls were identified as outliers and excluded from further statistical analyses. The histopathological variables for the study cohort are presented in Table 1.

Expression of miR-143 and miR-145 in benign and malignant breast tissue and according to histopathological parameters: microarray and PCR-results

Microarray miRNA analyses demonstrated that miR-143 and miR-145 were significantly downregulated in BC tissue compared to benign breast tissue ($p < 0.001$ for both comparisons) and the downregulation was validated and confirmed by PCR ($p < 0.001$) (Fig 1). Of note, microarray- and PCR-based expression levels were significantly correlated for both miR-143 ($r = 0.60$, $p < 0.001$) and miR-145 ($r = 0.72$, $p < 0.001$). Additionally, the expression levels of miR-143 and miR-145 were highly correlated ($R = 0.88$, $p < 0.001$, Fig 3).

Based on PCR measurements, both miR-143 and miR-145 demonstrated significantly higher expression in tumors that typically have a better prognosis compared to the rest. There was higher expression of both miR-143 and miR-145 in low and intermediate grade tumors compared to the high grade tumors, as shown in Tables 2 and 3 and Fig 4, and in ER-positive compared to ER-negative tumors (Table 4). MiR-145 displayed higher expression in luminal A tumors compared to the other molecular subtypes, and the expression of both miRNAs was lower in basal-like tumors compared to the other major subtypes (Table 5 and Fig 5). The means plot for miR-143 and miR-145 in Fig 6A and 6B, respectively, illustrates the distribution of expression across molecular subtypes. The same trends were observed in the microarray results, but the differences were not statistically significant. There were no significant differences in miR-143 and miR-145 expression between tumor groups stratified according to tumor size or lymph node metastases.

Table 1. Histopathological variables for the breast cancer cases included in the study.

NOWAC study		
Variables		N (%)
Study subjects	All	108 (100)
Tumor size	≤10 mm	23 (21.3)
	11–20 mm	50 (46.3)
	>20 mm	34 (31.5)
	Unknown	1 (0.9)
Histological grade	1	34 (31.5)
	2	42 (38.9)
	3	28 (25.9)
	Unknown	4 (3.7)
Receptor status	HR+/HER2-	70 (64.8)
	HR+/HER2+	11 (10.2)
	HR-/HER2+	9 (8.3)
	HR-/HER2-	16 (14.8)
	Unknown	2 (1.9)
Lymph node met	No	73 (67.6)
	Yes	34 (31.5)
	Unknown	1 (0.9)
Molecular subtype	Luminal A	58 (53.7)
	Luminal B	22 (20.4)
	HER2+	9 (8.3)
	Basal-like	16 (14.8)
	Unknown	3 (2.8)

<https://doi.org/10.1371/journal.pone.0186658.t001>

ISH expression of miR-143 and miR-145 in benign and malignant breast tissue

The cellular and subcellular expression of miR-143 and miR-145 in benign and malignant breast tissue was evaluated in full histological slides of 16 tumors with adjacent benign breast tissue. MiR-143 ISH staining was mainly cytoplasmatic and found predominantly in luminal cells in benign breast tissue. Noteworthy, the staining intensity in benign breast ducts and lobuli was strong and homogenous, and appeared stronger in benign tissue compared to adjacent tumor tissue, also in the tumors with moderate to strong staining intensity (Fig 7). As in benign tissue, miR-143 was expressed in the cytoplasm of tumor cells and stromal fibroblasts. However, in the tumors with high staining intensity in stromal cells, the staining was both cytoplasmatic and nuclear.

In contrast to the cytoplasmatic staining pattern for miR-143, miR-145 was expressed in the nuclei and with the strongest staining intensity in the myoepithelial cells in benign breast tissue (Fig 7). MiR-145 staining intensity was strong in benign breast tissue and tended to be stronger in benign compared to malignant breast tissue, but the difference was not as clear as for miR-143 (Fig 7). Also in tumor cells and stromal fibroblasts, miR-145 staining was predominantly nuclear.

Tumor cells and stromal fibroblasts were scored for staining intensity as illustrated in Fig 8. Noteworthy, all 16 tumors had positive staining for both miR-143 and miR-145 in both tumor cells and fibroblasts. The mean staining intensity for miR-143 in tumor cells was 2.17 and in stromal fibroblasts 2.06 whereas mean miR-145 staining intensity was 2.10 in tumor cells and 1.69 in stromal fibroblasts. Using Spearman’s rho, the staining intensity in tumor cells and

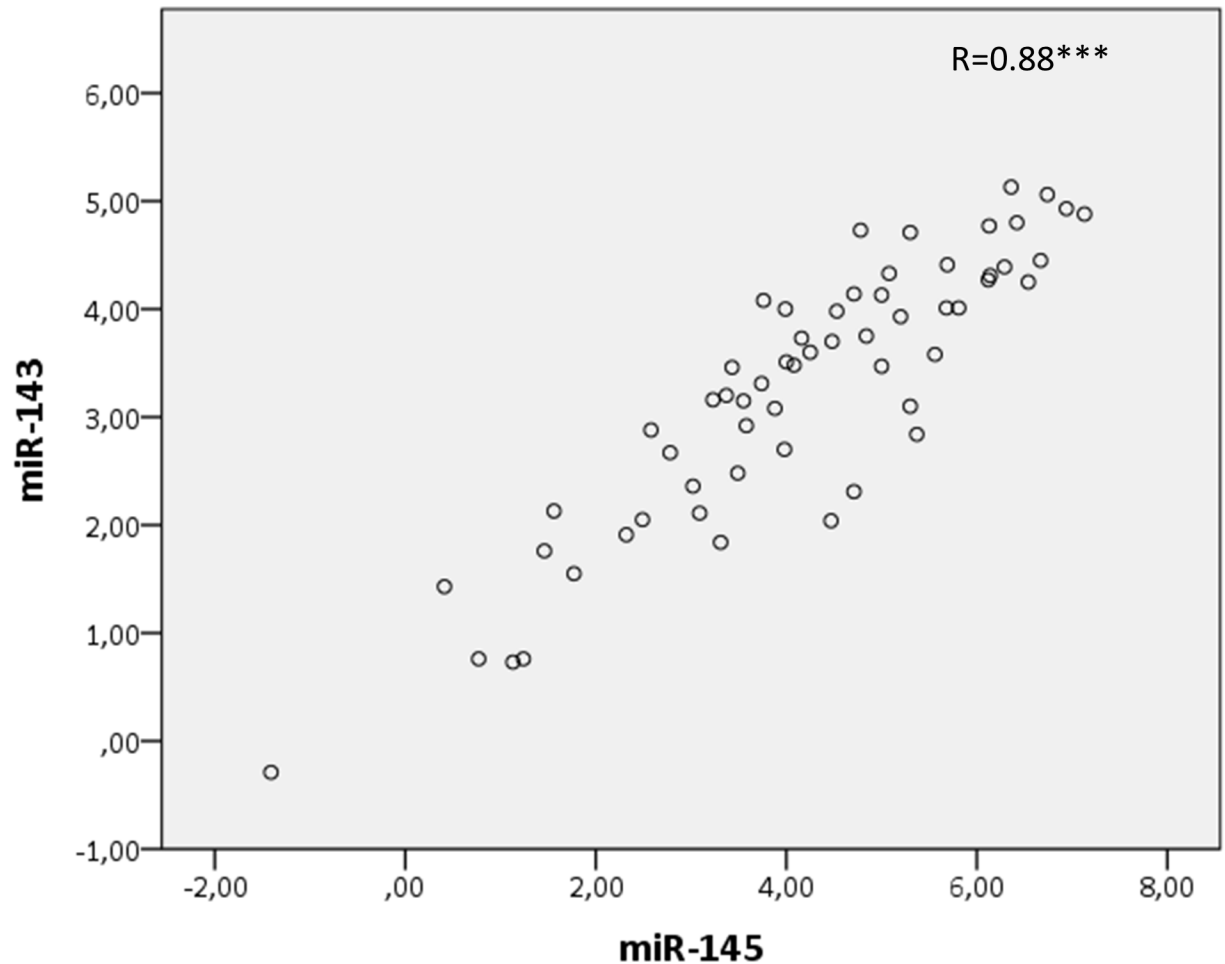


Fig 3. Scatterplot of miR-143 and miR-145 expression in breast tumor tissue. Scatterplot of miR-143 and miR-145 expression in tumor tissue, measured by PCR. Spearman's rho (R) is presented in the figure (***) $P < 0.001$.

<https://doi.org/10.1371/journal.pone.0186658.g003>

stromal fibroblasts was found to be positively correlated for both miR-143 ($p = 0.006$) and miR-145 ($p = 0.006$). Stromal ISH expression of miR-143 and miR-145 was also correlated ($p = 0.049$) (Table 6).

Discussion

This study characterizes the functional properties and expression pattern of the miRNA cluster miR-143 and miR-145 in BC.

Using microarray and PCR, we found a significant downregulation of miR-143 and miR-145 in malignant tumors compared to normal tissue, which is in line with previously published studies in breast cancer [29–31] and other tissues, especially colorectal carcinomas [32]. However, in our study the results were also verified by ISH, which added interesting data on the cellular and subcellular location of these miRNAs in benign and malignant breast tissue. Using ISH, we found the highest expression of miR-145 in myoepithelial cells in benign breast tissue. This is in line with other smaller studies using FISH or laser microdissection and PCR-analyses of miRNA expression [33, 34]. Further, we observed a distinct nuclear enrichment of mature miR-145, as has been previously reported in both breast and other tissues [34–36]. This is interesting, as the general dogma of miRNA biosynthesis and function involves post-

Table 2. Descriptive data for miR-143 and miR-145 PCR measurements in breast tumors according to histological grade.

Tumor grade		miR-143	miR-145
Control	Mean	4.18	5.98
	SD	0.81	0.69
	N (%)	19 (100)	19 (100)
All cancers	Mean	2.82	3.32
	SD	1.16	1.53
	N (%)	40 (100)	40 (100)
Tumor grade 1	Mean	2.77	3.40
	SD	1.07	1.21
	N (%)	7 (17.5)	7 (17.5)
Tumor grade 2	Mean	3.21	3.92
	SD	0.85	1.05
	N (%)	17 (42.5)	17 (42.5)
Tumor grade 3	Mean	2.47	2.62
	SD	1.41	1.84
	N (%)	16 (40)	16 (40)

<https://doi.org/10.1371/journal.pone.0186658.t002>

transcriptional regulation of mRNA in the cytoplasm [37]. Although the nuclear functions of mature miRNAs remain elusive, there is growing evidence of specific miRNAs localized to the nucleus [38–40]. Park et al. suggest that nuclear miRNAs could uncover an entirely new role for this family of non-coding RNAs [40] where transportation across the nuclear membrane could regulate miRNA storage and function. Further, it is suggested that nuclear miRNA could be involved in post-transcriptional gene silencing via the nuclear RNA induced silencing complex (nRISC), transcriptional gene activation via recruitment of transcriptional activators, and influence splicing decisions at specific exons (alternative splicing) [41].

Using microarray and PCR, we found miR-145 to be significantly higher in ER+ tumors, which is in line with a previous study on lymph-node negative tumors where ER status was based on gene expression using microarray [42]. In our study, the expression of both miR-143 and miR-145 was elevated in the least aggressive tumor types, which is in line with the tumor suppressor functions described for these miRNAs in previous publications [15–19, 43]. Further, the expression of the two miRNAs seems to correlate in benign and malignant breast tissue and between tumor types, an observation that could partly be contributed to their

Table 3. Contrast tests of miR-143 and miR-145 PCR measurements in breast tumors according to histological grade.

miRNA	Test	Mean difference	P*
miR-143	Control vs cancer	1.36	<0.001
	Grade 1 vs 2 and 3	-0.07	0.88
	Grade 1 and 2 vs 3	0.52	0.17
	Grade 1 vs 3	0.30	0.56
miR-145	Control vs cancer	2.66	<0.001
	Grade 1 vs 2 and 3	0.13	0.82
	Grade 1 and 2 vs 3	1.04	0.03
	Grade 1 vs 3	0.78	0.23

*False discovery rate (FDR) adjusted P-value

<https://doi.org/10.1371/journal.pone.0186658.t003>

Tumor grade comparison

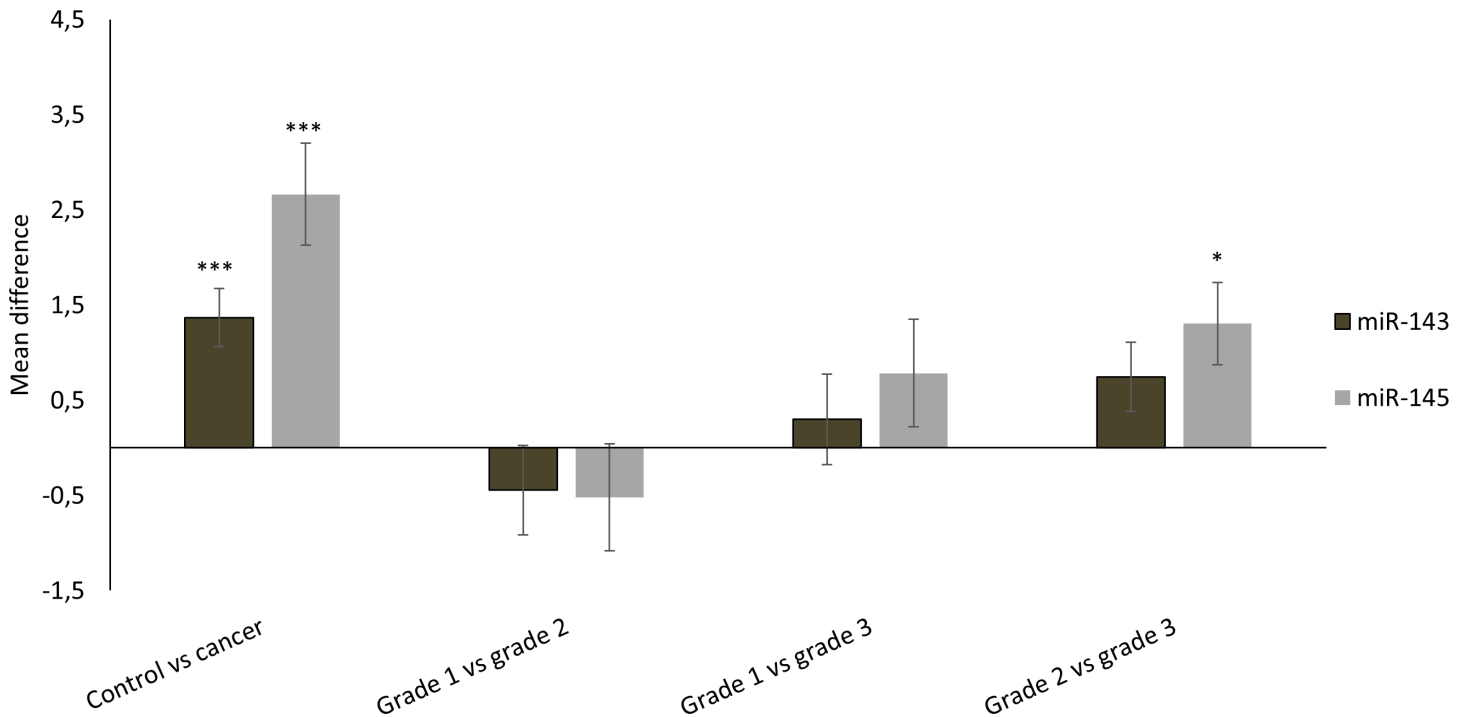


Fig 4. MiRNA expression in tumor tissue, stratified according to histological grade. Mean differences \pm SD in miRNA expression in tumor versus benign breast tissue and between tumors stratified according to histological grade, are presented. Statistics are calculated using one-way ANOVA with p-values corrected for multiple testing (* $P < 0.05$, *** $P < 0.001$).

<https://doi.org/10.1371/journal.pone.0186658.g004>

transcriptional regulation, where the two miRNAs are located within the same chromosomal region and are transcribed as a cluster.

However, miRNA functions are complex. In our *in vitro* experiments, miR-143 was revealed to increase the proliferative capacity of the ER+ cell line MCF7 and the TN cell line MDA-MB-231, whilst having no significant effect on proliferation in the HER2+ cell line SK-BR-3. The effect was pronounced (Fig 2A and 2C), and reproduced in three biological replicates. This finding is in contrast to the majority of studies regarding the effect of miR-143 on proliferation [15–19]. Interestingly, we found that miR-143 had a significant inhibitory effect on cell invasion in all cell lines. The overexpression of miR-145 led to inhibition of both proliferation and invasion, which is in accordance with the general consensus [19, 20, 22–24, 44–51]. Noteworthy, the coexpression of miR-143 and miR-145 led to inhibition of proliferation and invasion, which is also described in previous publications [52–55]. At present, we do not have enough information to offer any explanatory model for the effects demonstrated by miR-

Table 4. Contrast tests of miR-143 and miR-145 PCR measurements in breast tumors according to ER-status.

miRNA	ER-positive (n = 23)	ER-negative (n = 17)	Mean difference	P*
miR-143	3.18	2.37	0.81	0.02
miR-145	3.89	2.52	1.37	<0.001

*FDR adjusted P-value

<https://doi.org/10.1371/journal.pone.0186658.t004>

Table 5. Contrast tests of miR-143 and miR-145 PCR measurements in breast tumors according to molecular subtype.

miRNA	Test	Mean difference	P*
miR-143	Control vs cancer	1.36	<0.001
	Luminal A vs others	0.61	0.13
	Luminal B vs others	0.37	0.36
	HER2+ vs others	0.08	0.88
	Basal-like vs others	-1.06	0.01
miR-145	Control vs cancer	2.66	<0.001
	Luminal A vs others	1.02	0.02
	Luminal B vs others	0.66	0.11
	HER2+ vs others	-0.03	0.96
	Basal-like vs others	-1.65	<0.001

*FDR adjusted P-value

<https://doi.org/10.1371/journal.pone.0186658.t005>

143 in our proliferation studies. However, Dimitrova et al. describe stromal expression of the miR-143/145 cluster as a stimulator of neoangiogenesis, and a supporter of tumor expansion in lung [56]. Recently, Donnarumma et al. reported that the levels of miR-143 are increased in exosomes from cancer associated fibroblasts, and could promote breast cancer progression

Molecular subtype comparison

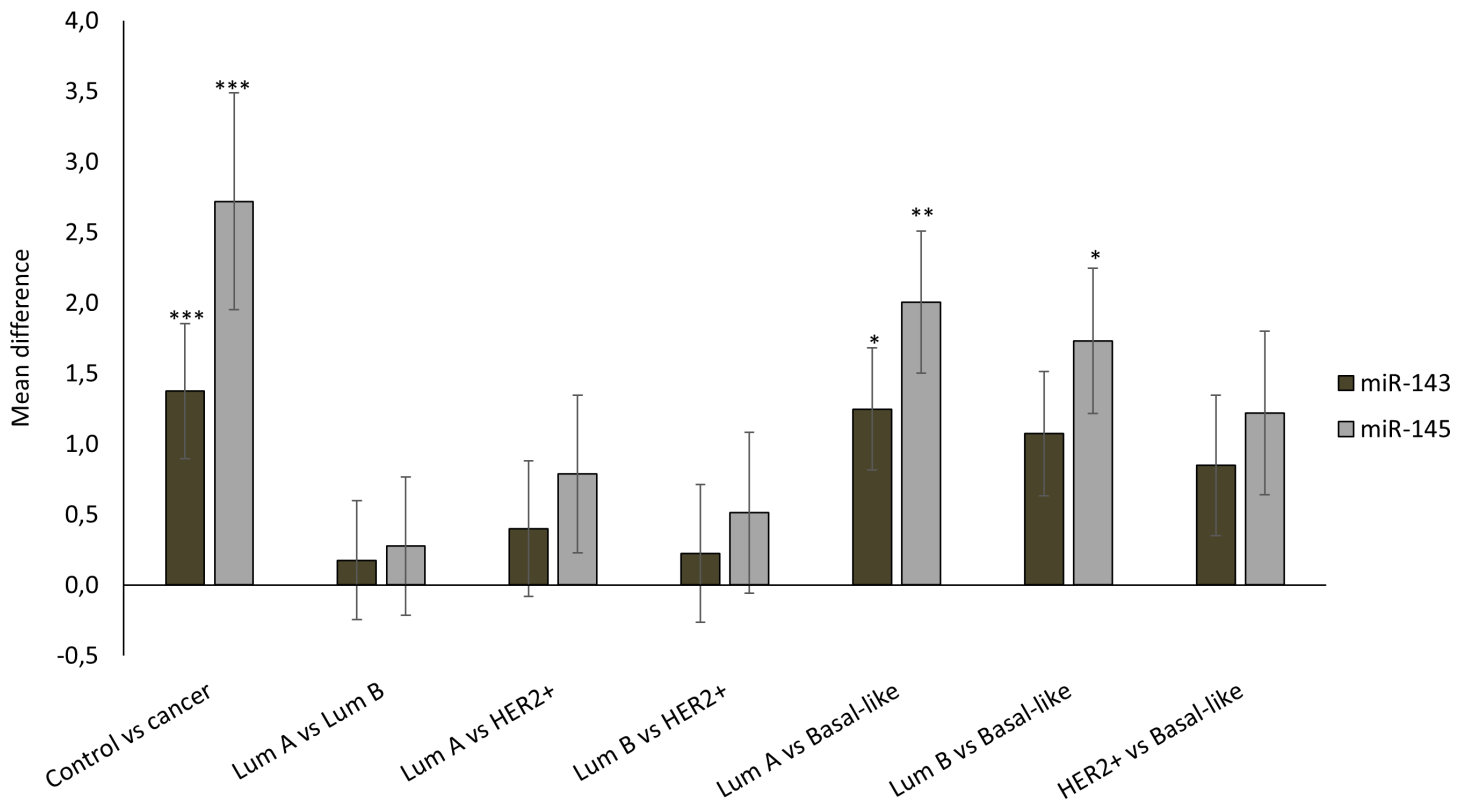


Fig 5. MiRNA expression in tumor tissue, stratified according to molecular subtype. Mean differences ±SD in miRNA expression between tumors stratified according to molecular subtype are presented. Statistics are calculated using one-way ANOVA with p-values corrected for multiple testing. (*P<0.05, **P<0.01, ***P<0.001).

<https://doi.org/10.1371/journal.pone.0186658.g005>

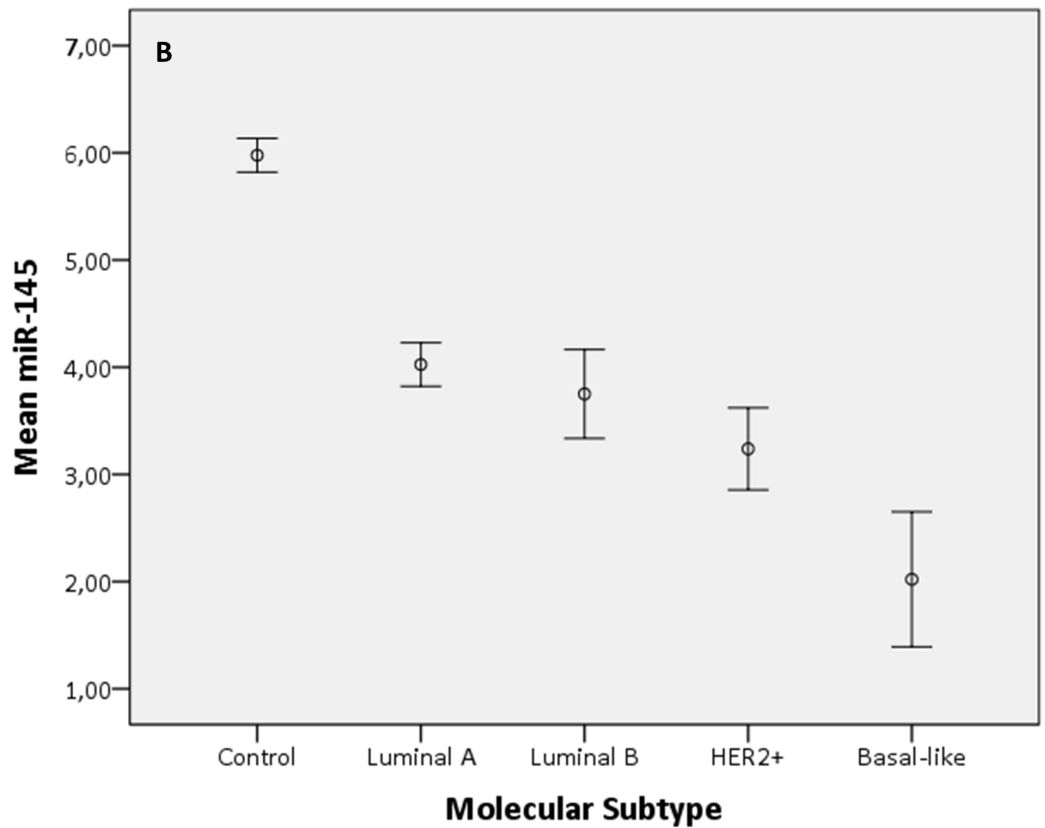
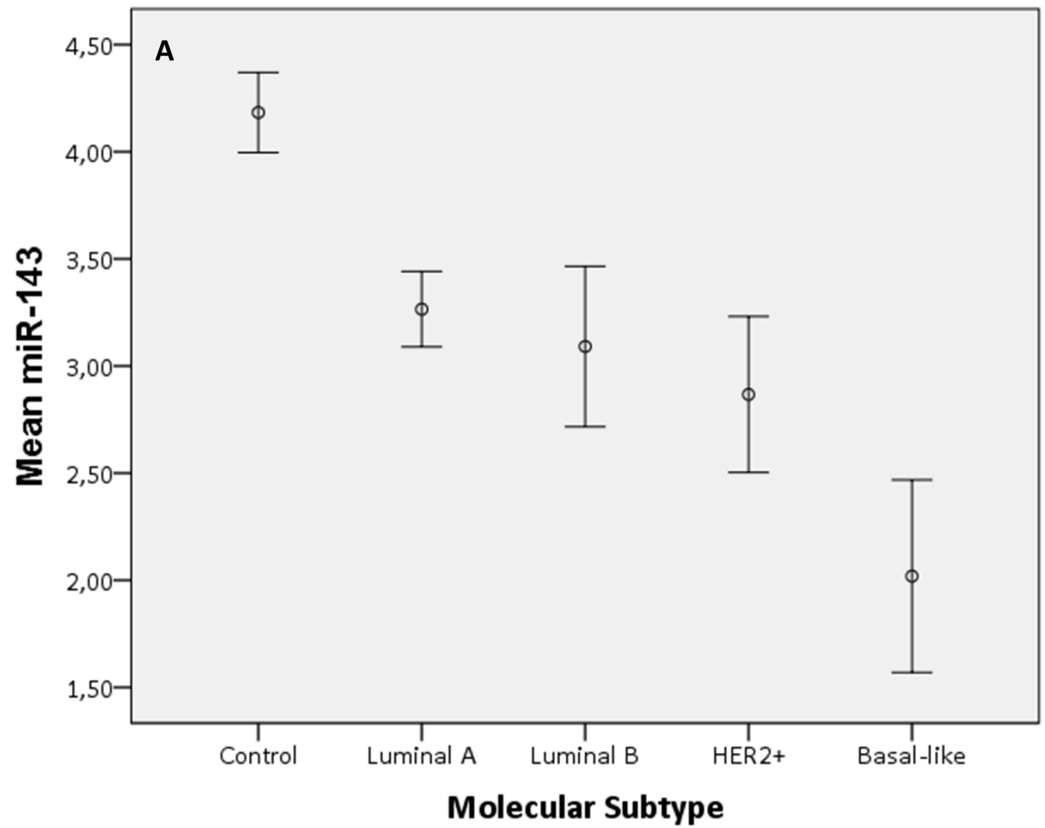


Fig 6. Means plot of miR-143 and miR-145 in breast tumors according to molecular subtype. Means plot for the expression of miR-143 (panel A) and miR-145 (panel B) according to molecular subgroup, using PCR. Error bars describe the standard error in each subgroup.

<https://doi.org/10.1371/journal.pone.0186658.g006>

through exosome-mediated delivery of miRNA to breast cancer cells [57]. Estradiol has been published to downregulate expression of miR-143 in an ER-dependent manner in the ER+ cell line MCF7, whilst having no effect on miRNA levels in the TN cell line MDA-MB-231 [43]. Downregulation of miR-143 appears to contribute to the estradiol-mediated upregulation of bcl-2 and survivin. These observations underline that effects of signaling molecules, where miRNAs could be included, are highly dependent on the cellular context. Further, the stimulation of proliferation and, at the same time, inhibition of invasion, argue for several regulated target genes which could have opposing effects in tumorigenesis, as indeed demonstrated by the target genes for miR-143 listed in S1 Table.

Spizzo et al. verified miR-145 to directly target ER, and at the same time activate TP53, and in turn apoptosis [51]. These results may in part explain some of the inhibitory effects we

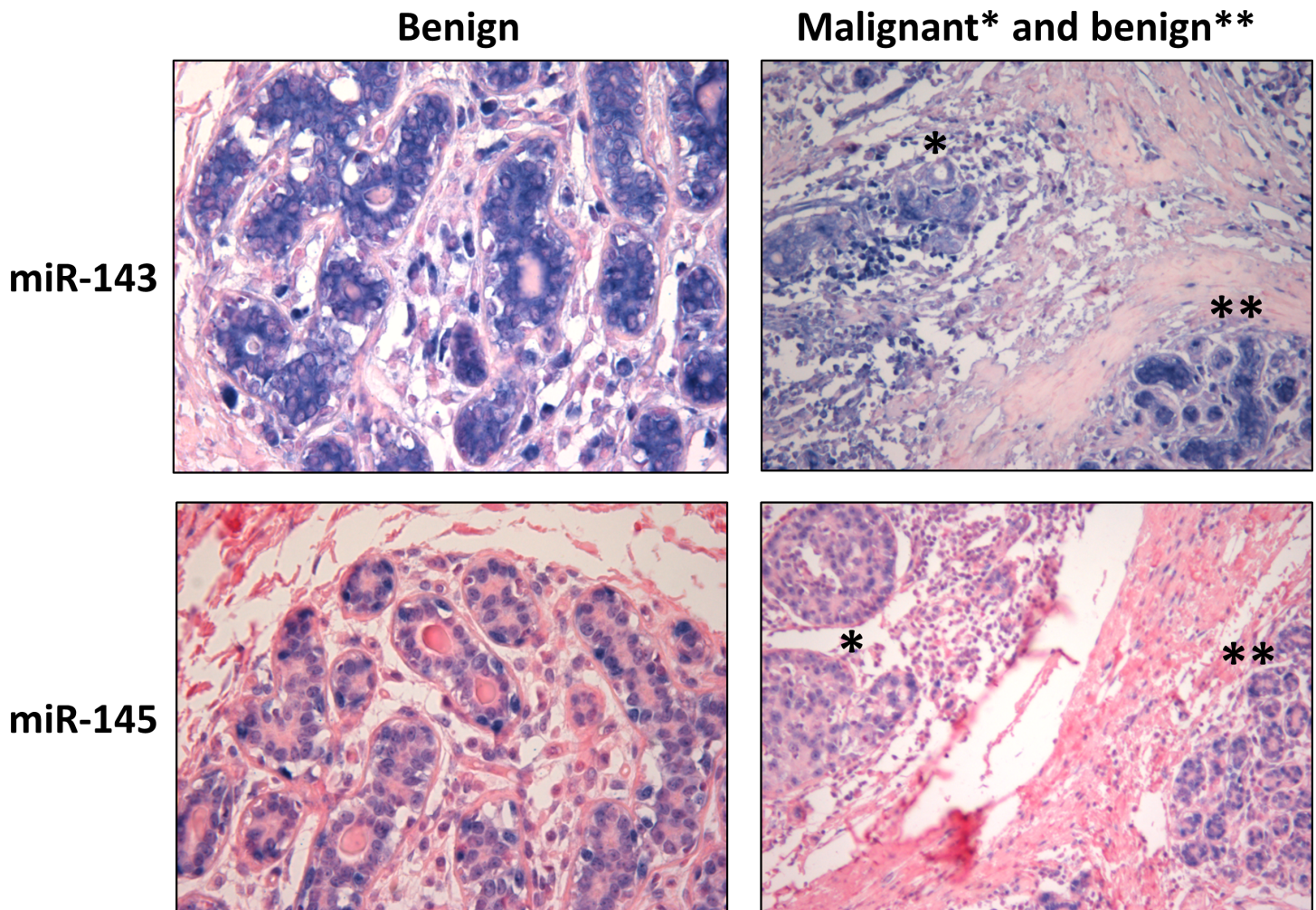


Fig 7. MiR-143 and miR-145 *in situ* hybridization staining pattern in breast tissue. Illustrative examples of miR-143 and miR-145 *in situ* hybridization staining pattern in benign breast tissue (x400 magnification) and adjacent benign and malignant breast tissue (x200 magnification).

<https://doi.org/10.1371/journal.pone.0186658.g007>

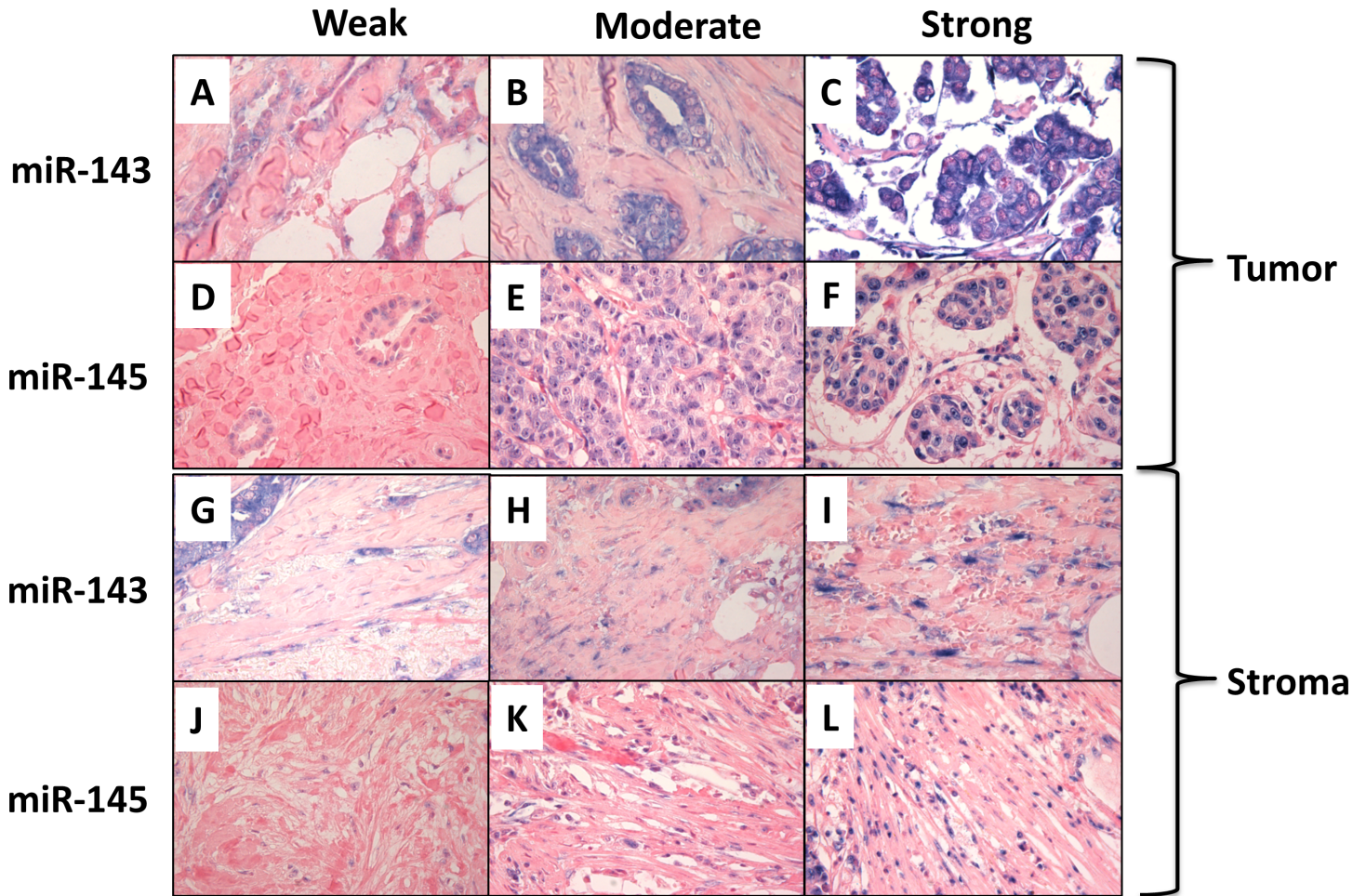


Fig 8. MiR-143 and miR-145 *in situ* hybridization staining intensities in tumor and stromal cells. *In situ* hybridization staining of miR-143 and miR-145 in tumor cells (panel A-C and panel D-F, respectively) and stromal fibroblasts (panel G-I and panel J-L, respectively) with examples of staining intensities corresponding to score weak, moderate and strong. Light microscope images, x400 magnification.

<https://doi.org/10.1371/journal.pone.0186658.g008>

observed in cell lines transfected with miR-145, but our experiments also demonstrated inhibition of proliferation and invasion in the TN *p53* mutant MDA-MB-231 and the ER- *p53* mutant SK-BR-3. These results argue for a different tumor suppressive pathway than described by Spizzo et al. However, the list of verified miR-145 target genes involved in tumor

Table 6. Correlations of miR-143 and miR-145 *in situ* hybridization staining intensities in tumor and stromal cells.

	N = 16		miR-143		miR-145	
			Tumor	Stroma	Tumor	Stroma
miR-143	Tumor	r		0.657**	0.335	0.411
	Stroma	r	0.657**		0.275	0.499*
miR-145	Tumor	r	0.335	0.275		0.651**
	Stroma	r	0.411	0.499*	0.651**	

Spearman's correlation, Spearman's rho (r) presented in the table.

*P<0.05

**P<0.01.

<https://doi.org/10.1371/journal.pone.0186658.t006>

progression is wide-ranging (S2 Table), and the dominant active pathway(s) at any given time would be challenging to predict. S1 and S2 Tables present the validated mRNA targets for miR-143 and miR-145, based on searches using the online database miRTarBase [58].

Synergistic effects of miR-143 and miR-145 on BC cell proliferation have been demonstrated in MCF7 and MBA-MD-231 cells and in a mouse model using MCF7 xenografts [53]. Interestingly, both miRNAs, although not sharing sequence homology, were demonstrated to bind to the 3'-UTR region of HER3, the most potent effects were demonstrated by miR-145. Further, high HER3 expression could rescue the cells from the inhibitory effects of miR-143 and miR-145, underlining the importance of the cellular context and active signaling pathways on the net effect of miRNA up- or downregulation. Different results in different cell lines may be explained by miRNAs effects on target genes that are operating or driving the oncogenic phenotype in specific cell types where ER would be the classical example in ER+ BC. Noteworthy, miRNA-profiling of BC cells has demonstrated that miRNA-based clusters follow ER-based dichotomization of cell lines, indicating that a significant number of miRNAs may directly, or indirectly, be regulated by ER-signaling [59].

The results in this study, including the differential effects *in vitro* of miR-143 in BC cell lines, the effects of cotransfecting miR-143 and miR-145, and the nuclear enrichment of miR-145 in breast tissue, underline the complexity of miRNA regulation and function. Studies of miRNA expression in tissues and cancer types should be supplied by functional research of individual miRNAs where non-canonical effects of miRNAs are being explored in greater detail.

Supporting information

S1 Table. List of miR-143 target genes verified by reporter assay and western blot.
(PDF)

S2 Table. List of miR-145 target genes verified by reporter assay and western blot.
(PDF)

Acknowledgments

We would like to thank engineer Magnus Persson (Department of Clinical Pathology, University Hospital of Northern Norway) and Kristin Sorensen (UiT The Arctic University of Norway) for assistance in the laboratory.

Author Contributions

Data curation: Tonje Braaten.

Formal analysis: Charles Johannessen, Mona Irene Pedersen.

Supervision: Lill-Tove Busund.

Visualization: Charles Johannessen.

Writing – original draft: Charles Johannessen, Line Moi.

Writing – review & editing: Line Moi, Yury Kiselev, Mona Irene Pedersen, Stig Manfred Dalen, Tonje Braaten, Lill-Tove Busund.

References

1. DeSantis CE, Lin CC, Mariotto AB, Siegel RL, Stein KD, Kramer JL, et al. Cancer treatment and survivorship statistics, 2014. *CA Cancer J Clin.* 2014; 64(4):252–71. <https://doi.org/10.3322/caac.21235> PMID: 24890451.

2. Vuong D, Simpson PT, Green B, Cummings MC, Lakhani SR. Molecular classification of breast cancer. *Virchows Arch*. 2014; 465(1):1–14. <https://doi.org/10.1007/s00428-014-1593-7> PMID: 24878755.
3. Goldhirsch A, Wood WC, Coates AS, Gelber RD, Thurlimann B, Senn HJ, et al. Strategies for subtypes—dealing with the diversity of breast cancer: highlights of the St. Gallen International Expert Consensus on the Primary Therapy of Early Breast Cancer 2011. *Ann Oncol*. 2011; 22(8):1736–47. <https://doi.org/10.1093/annonc/mdr304> PMID: 21709140; PubMed Central PMCID: PMC3144634.
4. Perou CM, Sorlie T, Eisen MB, van de Rijn M, Jeffrey SS, Rees CA, et al. Molecular portraits of human breast tumours. *Nature*. 2000; 406(6797):747–52. <https://doi.org/10.1038/35021093> PMID: 10963602.
5. Masood S. Breast cancer subtypes: morphologic and biologic characterization. *Womens Health (Lond)*. 2016; 12(1):103–19. <https://doi.org/10.2217/whe.15.99> PMID: 26756229.
6. Yadav BS, Sharma SC, Chanana P, Jhamb S. Systemic treatment strategies for triple-negative breast cancer. *World J Clin Oncol*. 2014; 5(2):125–33. <https://doi.org/10.5306/wjco.v5.i2.125> PMID: 24829859; PubMed Central PMCID: PMC4014784.
7. Sotiriou C, Neo SY, McShane LM, Korn EL, Long PM, Jazaeri A, et al. Breast cancer classification and prognosis based on gene expression profiles from a population-based study. *Proc Natl Acad Sci U S A*. 2003; 100(18):10393–8. <https://doi.org/10.1073/pnas.1732912100> PMID: 12917485; PubMed Central PMCID: PMC193572.
8. Jonas S, Izaurralde E. Towards a molecular understanding of microRNA-mediated gene silencing. *Nat Rev Genet*. 2015; 16(7):421–33. <https://doi.org/10.1038/nrg3965> PMID: 26077373.
9. Winter J, Jung S, Keller S, Gregory RI, Diederichs S. Many roads to maturity: microRNA biogenesis pathways and their regulation. *Nat Cell Biol*. 2009; 11(3):228–34. <https://doi.org/10.1038/ncb0309-228> PMID: 19255566.
10. Calin GA, Croce CM. MicroRNA signatures in human cancers. *Nat Rev Cancer*. 2006; 6(11):857–66. <https://doi.org/10.1038/nrc1997> PMID: 17060945.
11. Naeini MM, Ardekani AM. Noncoding RNAs and Cancer. *Avicenna J Med Biotechnol*. 2009; 1(2):55–70. PMID: 23407615; PubMed Central PMCID: PMC3558126.
12. Zhang C. MicroRNAs: role in cardiovascular biology and disease. *Clin Sci (Lond)*. 2008; 114(12):699–706. <https://doi.org/10.1042/CS20070211> PMID: 18474027.
13. Lu J, Getz G, Miska EA, Alvarez-Saavedra E, Lamb J, Peck D, et al. MicroRNA expression profiles classify human cancers. *Nature*. 2005; 435(7043):834–8. <https://doi.org/10.1038/nature03702> PMID: 15944708.
14. Ruan K, Fang X, Ouyang G. MicroRNAs: novel regulators in the hallmarks of human cancer. *Cancer Lett*. 2009; 285(2):116–26. <https://doi.org/10.1016/j.canlet.2009.04.031> PMID: 19464788.
15. Liu J, Mao Y, Zhang D, Hao S, Zhang Z, Li Z, et al. MiR-143 inhibits tumor cell proliferation and invasion by targeting STAT3 in esophageal squamous cell carcinoma. *Cancer letters*. 2016; 373(1):97–108. <https://doi.org/10.1016/j.canlet.2016.01.023> PMID: 26806810.
16. Xu YF, Li YQ, Guo R, He QM, Ren XY, Tang XR, et al. Identification of miR-143 as a tumour suppressor in nasopharyngeal carcinoma based on microRNA expression profiling. *Int J Biochem Cell Biol*. 2015; 61:120–8. <https://doi.org/10.1016/j.biocel.2015.02.006> PMID: 25701793.
17. Wang Q, Cai J, Wang J, Xiong C, Zhao J. MiR-143 inhibits EGFR-signaling-dependent osteosarcoma invasion. *Tumour Biol*. 2014; 35(12):12743–8. <https://doi.org/10.1007/s13277-014-2600-y> PMID: 25227664.
18. Xia H, Sun S, Wang B, Wang T, Liang C, Li G, et al. miR-143 inhibits NSCLC cell growth and metastasis by targeting Limk1. *Int J Mol Sci*. 2014; 15(7):11973–83. <https://doi.org/10.3390/ijms150711973> PMID: 25003638; PubMed Central PMCID: PMC4139824.
19. Zhang W, Wang Q, Yu M, Wu N, Wang H. MicroRNA-145 function as a cell growth repressor by directly targeting c-Myc in human ovarian cancer. *Technology in cancer research & treatment*. 2014; 13(2):161–8. Epub 2013/08/08. <https://doi.org/10.7785/tcrt.2012.500367> PMID: 23919393.
20. Wu J, Yin L, Jiang N, Guo WJ, Gu JJ, Chen M, et al. MiR-145, a microRNA targeting ADAM17, inhibits the invasion and migration of nasopharyngeal carcinoma cells. *Exp Cell Res*. 2015; 338(2):232–8. <https://doi.org/10.1016/j.yexcr.2015.08.006> PMID: 26297956.
21. Chen JJ, Cai WY, Liu XW, Luo QC, Chen G, Huang WF, et al. Reverse Correlation between MicroRNA-145 and FSCN1 Affecting Gastric Cancer Migration and Invasion. *PLoS One*. 2015; 10(5):e0126890. <https://doi.org/10.1371/journal.pone.0126890> PMID: 26010149; PubMed Central PMCID: PMC4444015.
22. Qin J, Wang F, Jiang H, Xu J, Jiang Y, Wang Z. MicroRNA-145 suppresses cell migration and invasion by targeting paxillin in human colorectal cancer cells. *Int J Clin Exp Pathol*. 2015; 8(2):1328–40. PMID: 25973017; PubMed Central PMCID: PMC4396207.

23. Larne O, Hagman Z, Lilja H, Bjartell A, Edsjo A, Ceder Y. miR-145 suppress the androgen receptor in prostate cancer cells and correlates to prostate cancer prognosis. *Carcinogenesis*. 2015; 36(8):858–66. <https://doi.org/10.1093/carcin/bgv063> PMID: 25969144.
24. Zhang Y, Yang X, Wu H, Zhou W, Liu Z. MicroRNA-145 inhibits migration and invasion via inhibition of fascin 1 protein expression in non-small-cell lung cancer cells. *Mol Med Rep*. 2015; 12(4):6193–8. <https://doi.org/10.3892/mmr.2015.4163> PMID: 26238532.
25. Dumeaux V, Borresen-Dale AL, Frantzen JO, Kumle M, Kristensen VN, Lund E. Gene expression analyses in breast cancer epidemiology: the Norwegian Women and Cancer postgenome cohort study. *Breast cancer research*. 2008; 10(1):R13. Epub 2008/02/15. <https://doi.org/10.1186/bcr1859> PMID: 18271962; PubMed Central PMCID: PMCPMC2374969.
26. Elston CW, Ellis IO. Pathological prognostic factors in breast cancer. I. The value of histological grade in breast cancer: experience from a large study with long-term follow-up. *Histopathology*. 1991; 19(5):403–10. Epub 1991/11/01. PMID: 1757079.
27. Coates AS, Winer EP, Goldhirsch A, Gelber RD, Gnani M, Piccart-Gebhart M, et al. Tailoring therapies—improving the management of early breast cancer: St Gallen International Expert Consensus on the Primary Therapy of Early Breast Cancer 2015. *Ann Oncol*. 2015; 26(8):1533–46. Epub 2015/05/06. <https://doi.org/10.1093/annonc/mdv221> PMID: 25939896; PubMed Central PMCID: PMCPMC4511219.
28. Vasconcelos I, Hussainzada A, Berger S, Fietze E, Linke J, Siedentopf F, et al. The St. Gallen surrogate classification for breast cancer subtypes successfully predicts tumor presenting features, nodal involvement, recurrence patterns and disease free survival. *Breast*. 2016; 29:181–5. Epub 2016/08/22. <https://doi.org/10.1016/j.breast.2016.07.016> PMID: 27544822.
29. Zheng T, Zhang X, Wang Y, Yu X. Predicting associations between microRNAs and target genes in breast cancer by bioinformatics analyses. *Oncology letters*. 2016; 12(2):1067–73. Epub 2016/07/23. <https://doi.org/10.3892/ol.2016.4731> PMID: 27446395; PubMed Central PMCID: PMCPMC4950656.
30. Iorio MV, Ferracin M, Liu C-G, Veronese A, Spizzo R, Sabbioni S, et al. MicroRNA Gene Expression Deregulation in Human Breast Cancer. *Cancer Research*. 2005; 65(16):7065–70. <https://doi.org/10.1158/0008-5472.CAN-05-1783> PMID: 16103053
31. Navon R, Wang H, Steinfeld I, Tsalenko A, Ben-Dor A, Yakhini Z. Novel Rank-Based Statistical Methods Reveal MicroRNAs with Differential Expression in Multiple Cancer Types. *PLOS ONE*. 2009; 4(11):e8003. <https://doi.org/10.1371/journal.pone.0008003> PMID: 19946373
32. Michael MZ, O' Connor SM, van Holst Pellekaan NG, Young GP, James RJ. Reduced Accumulation of Specific MicroRNAs in Colorectal Neoplasia. *Molecular Cancer Research*. 2003; 1(12):882–91. PMID: 14573789
33. Bockmeyer CL, Christgen M, Muller M, Fischer S, Ahrens P, Langer F, et al. MicroRNA profiles of healthy basal and luminal mammary epithelial cells are distinct and reflected in different breast cancer subtypes. *Breast cancer research and treatment*. 2011; 130(3):735–45. Epub 2011/03/17. <https://doi.org/10.1007/s10549-010-1303-3> PMID: 21409395.
34. Sempere LF, Christensen M, Silahtaroglu A, Bak M, Heath CV, Schwartz G, et al. Altered MicroRNA expression confined to specific epithelial cell subpopulations in breast cancer. *Cancer Res*. 2007; 67(24):11612–20. Epub 2007/12/20. <https://doi.org/10.1158/0008-5472.CAN-07-5019> PMID: 18089790.
35. Sangiao-Alvarellos S, Manfredi-Lozano M, Ruiz-Pino F, León S, Morales C, Cordido F, et al. Testicular expression of the Lin28/let-7 system: Hormonal regulation and changes during postnatal maturation and after manipulations of puberty. *Scientific Reports*. 2015; 5:15683. doi: 10.1038/srep15683. <http://www.nature.com/articles/srep15683#supplementary-information>. PMID: 26494358
36. Liu Y, Wu C, Wang Y, Wen S, Wang J, Chen Z, et al. Expression of miR-224, miR-145, and their putative target ADAM17 in hepatocellular carcinoma. *Acta Biochimica et Biophysica Sinica*. 2014; 46(8):720–2. <https://doi.org/10.1093/abbs/gmu052> PMID: 24969373
37. Ha M, Kim VN. Regulation of microRNA biogenesis. *Nat Rev Mol Cell Biol*. 2014; 15(8):509–24. <https://doi.org/10.1038/nrm3838> PMID: 25027649.
38. Li ZF, Liang YM, Lau PN, Shen W, Wang DK, Cheung WT, et al. Dynamic localisation of mature microRNAs in Human nucleoli is influenced by exogenous genetic materials. *PLoS One*. 2013; 8(8):e70869. <https://doi.org/10.1371/journal.pone.0070869> PMID: 23940654; PubMed Central PMCID: PMCPMC3735495.
39. Wei Y, Li L, Wang D, Zhang CY, Zen K. Importin 8 regulates the transport of mature microRNAs into the cell nucleus. *J Biol Chem*. 2014; 289(15):10270–5. <https://doi.org/10.1074/jbc.C113.541417> PMID: 24596094; PubMed Central PMCID: PMCPMC4036152.
40. Park CW, Zeng Y, Zhang X, Subramanian S, Steer CJ. Mature microRNAs identified in highly purified nuclei from HCT116 colon cancer cells. *RNA Biol*. 2010; 7(5):606–14. <https://doi.org/10.4161/rna.7.5.13215> PMID: 20864815; PubMed Central PMCID: PMCPMC3073257.

41. Roberts TC. The MicroRNA Biology of the Mammalian Nucleus. *Molecular therapy Nucleic acids*. 2014; 3:e188. Epub 2014/08/20. <https://doi.org/10.1038/mtna.2014.40> PMID: 25137140; PubMed Central PMCID: PMC4221600.
42. Foekens JA, Sieuwerts AM, Smid M, Look MP, de Weerd V, Boersma AW, et al. Four miRNAs associated with aggressiveness of lymph node-negative, estrogen receptor-positive human breast cancer. *Proc Natl Acad Sci U S A*. 2008; 105(35):13021–6. Epub 2008/08/30. <https://doi.org/10.1073/pnas.0803304105> PMID: 18755890; PubMed Central PMCID: PMC2529088.
43. Yu X, Zhang X, Dhakal IB, Beggs M, Kadlubar S, Luo D. Induction of cell proliferation and survival genes by estradiol-repressed microRNAs in breast cancer cells. *BMC cancer*. 2012; 12:29. Epub 2012/01/21. <https://doi.org/10.1186/1471-2407-12-29> PMID: 22260523; PubMed Central PMCID: PMC3274428.
44. Liu Y, Wu C, Wang Y, Wen S, Wang J, Chen Z, et al. MicroRNA-145 inhibits cell proliferation by directly targeting ADAM17 in hepatocellular carcinoma. *Oncol Rep*. 2014; 32(5):1923–30. <https://doi.org/10.3892/or.2014.3424> PMID: 25174729.
45. Sachdeva M, Mo Y-Y. MicroRNA-145 Suppresses Cell Invasion and Metastasis by Directly Targeting Mucin 1. *Cancer Research*. 2010; 70(1):378–87. <https://doi.org/10.1158/0008-5472.CAN-09-2021> PMID: 19996288
46. Sachdeva M, Mo YY. MicroRNA-145 suppresses cell invasion and metastasis by directly targeting mucin 1. *Cancer Res*. 2010; 70(1):378–87. <https://doi.org/10.1158/0008-5472.CAN-09-2021> PMID: 19996288; PubMed Central PMCID: PMC2805032.
47. Fan L, Wu Q, Xing X, Wei Y, Shao Z. MicroRNA-145 targets vascular endothelial growth factor and inhibits invasion and metastasis of osteosarcoma cells. *Acta Biochim Biophys Sin (Shanghai)*. 2012; 44(5):407–14. <https://doi.org/10.1093/abbs/gms019> PMID: 22472569.
48. Cui SY, Wang R, Chen LB. MicroRNA-145: a potent tumour suppressor that regulates multiple cellular pathways. *Journal of cellular and molecular medicine*. 2014; 18(10):1913–26. Epub 2014/08/16. <https://doi.org/10.1111/jcmm.12358> PMID: 25124875; PubMed Central PMCID: PMC4244007.
49. Wang S, Bian C, Yang Z, Bo Y, Li J, Zeng L, et al. miR-145 inhibits breast cancer cell growth through RTKN. *International journal of oncology*. 2009; 34(5):1461–6. Epub 2009/04/11. PMID: 19360360.
50. Cho WC, Chow AS, Au JS. MiR-145 inhibits cell proliferation of human lung adenocarcinoma by targeting EGFR and NUDT1. *RNA Biol*. 2011; 8(1):125–31. PMID: 21289483.
51. Spizzo R, Nicoloso MS, Lupini L, Lu Y, Fogarty J, Rossi S, et al. miR-145 participates with TP53 in a death-promoting regulatory loop and targets estrogen receptor-alpha in human breast cancer cells. *Cell death and differentiation*. 2010; 17(2):246–54. Epub 2009/09/05. <https://doi.org/10.1038/cdd.2009.117> PMID: 19730444; PubMed Central PMCID: PMC3648637.
52. Su J, Liang H, Yao W, Wang N, Zhang S, Yan X, et al. MiR-143 and MiR-145 regulate IGF1R to suppress cell proliferation in colorectal cancer. *PLoS One*. 2014; 9(12):e114420. <https://doi.org/10.1371/journal.pone.0114420> PMID: 25474488; PubMed Central PMCID: PMC4256231.
53. Yan X, Chen X, Liang H, Deng T, Chen W, Zhang S, et al. miR-143 and miR-145 synergistically regulate ERBB3 to suppress cell proliferation and invasion in breast cancer. *Molecular cancer*. 2014; 13:220. Epub 2014/09/25. <https://doi.org/10.1186/1476-4598-13-220> PMID: 25248370; PubMed Central PMCID: PMC4181414.
54. Yoshino H, Enokida H, Itesako T, Kojima S, Kinoshita T, Tatarano S, et al. Tumor-suppressive micro-RNA-143/145 cluster targets hexokinase-2 in renal cell carcinoma. *Cancer Sci*. 2013; 104(12):1567–74. <https://doi.org/10.1111/cas.12280> PMID: 24033605.
55. Zhang X, Dong Y, Ti H, Zhao J, Wang Y, Li T, et al. Down-regulation of miR-145 and miR-143 might be associated with DNA methyltransferase 3B overexpression and worse prognosis in endometrioid carcinomas. *Hum Pathol*. 2013; 44(11):2571–80. <https://doi.org/10.1016/j.humpath.2013.07.002> PMID: 24071015.
56. Dimitrova N, Gocheva V, Bhutkar A, Resnick R, Jong RM, Miller KM, et al. Stromal Expression of miR-143/145 Promotes Neoangiogenesis in Lung Cancer Development. *Cancer Discov*. 2016; 6(2):188–201. <https://doi.org/10.1158/2159-8290.CD-15-0854> PMID: 26586766; PubMed Central PMCID: PMC4744583.
57. Donnarumma E, Fiore D, Nappa M, Roscigno G, Adamo A, Iaboni M, et al. Cancer-associated fibroblasts release exosomal microRNAs that dictate an aggressive phenotype in breast cancer. *Oncotarget*. 2017; 8(12):19592–608. <https://doi.org/10.18632/oncotarget.14752> PMID: 28121625; PubMed Central PMCID: PMC5386708.
58. Chou CH, Chang NW, Shrestha S, Hsu SD, Lin YL, Lee WH, et al. miRTarBase 2016: updates to the experimentally validated miRNA-target interactions database. *Nucleic Acids Res*. 2016; 44(D1):D239–47. <https://doi.org/10.1093/nar/gkv1258> PMID: 26590260; PubMed Central PMCID: PMC4702890.

59. Riaz M, van Jaarsveld MT, Hollestelle A, Prager-van der Smissen WJ, Heine AA, Boersma AW, et al. miRNA expression profiling of 51 human breast cancer cell lines reveals subtype and driver mutation-specific miRNAs. *Breast cancer research*. 2013; 15(2):R33. Epub 2013/04/23. <https://doi.org/10.1186/bcr3415> PMID: [23601657](https://pubmed.ncbi.nlm.nih.gov/23601657/); PubMed Central PMCID: [PMCPmc3672661](https://pubmed.ncbi.nlm.nih.gov/PMC3672661/).

Paper II

1 *Manuscript*

2 **Different functional roles and expression of miR-126-3p and**
3 **miR-126-5p in breast cancer cell lines and tissues**

4 Charles Johannessen^{1*}, Yury Kiselev², Mona Irene Pedersen³, Stig Manfred Dalen⁴, Lill-Tove
5 Rasmussen Busund^{1, 4}, Eiliv Lund⁵, Karina Standahl Olsen⁵, Line Moi^{1, 4}

6

7 ¹ Department of Medical Biology, UiT - The Arctic University of Norway, Tromsø, Norway

8 ² Department of Life Sciences and Health, OsloMet – Oslo Metropolitan University, Oslo,
9 Norway

10 ³ Department of Clinical Medicine, UiT - The Arctic University of Norway, Tromsø, Norway

11 ⁴ Department of Clinical Pathology, University Hospital of North Norway, Tromsø, Norway

12 ⁵ Department of Community Medicine, UiT - The Arctic University of Norway, Tromsø, Norway

13

14 * E-mail: charles.johannessen@uit.no

15

16

17 **Abstract**

18 **Background**

19 MiRNAs are regulators of gene expression and are involved in carcinogenesis through regulation
20 of oncogenes, tumor suppressors and cellular oncogenic properties such as invasion and
21 metastasis. MiR-126 has tumor suppressor function in various cancers, and seems to regulate the
22 metastatic process in BC both *in vitro* and *in vivo*.

23 **Methods**

24 Functions of miR-126-3p and the passenger strand miR-126-5p were explored in the ER+ breast
25 cancer cell line MCF7, HER2+ SK-BR-3 cells and triple negative MDA-MB-231 cells using the
26 proliferation platform xCelligence and invasion assay CytoSelect Cell Invasion. MiRNA
27 expression in malignant and benign breast tissue were analyzed by microarray and RT-PCR, and
28 cell specific in-tumor fibroblasts and epithelium using ISH and tissue microarrays.

29 **Results**

30 MiR-126-3p transfection led to decreased proliferation and invasion in all cell lines, whereas
31 miR-126-5p had the opposite effect in MDA-MB-231 cells where miR-126-5p was the dominant
32 strand determined by RT-PCR analysis. Both miR-126 strands were downregulated in cancer
33 compared to benign tissue, and in lymph node positive breast cancers compared to tumors
34 without nodal involvement. MiR-126-5p ISH stromal staining was significantly higher in high
35 grade tumors and in stroma and tumor cells of luminal B, HER2 positive and triple negative
36 tumors compared to luminal A.

37 **Conclusions**

38 MiR-126-3p has tumor suppressor functions in breast cancer cell lines. MiR-126-5p, however,
39 promotes proliferation and invasion in triple negative cancer cells and demonstrates higher
40 expression in tumors of high grade and aggressive molecular subtypes. Different functions and
41 expression of the miR-126 strands in breast cancer subtypes add to the complexity of miRNAs'
42 regulatory network in malignant disease.

43

44 **Introduction**

45 Breast cancer (BC) in women accounts for 30% of all new cancer cases, and is the most common
46 cancer diagnosed worldwide in the female population [1, 2]. BC is a highly heterogeneous
47 malignancy, contributing to the challenges of determining the most effective treatment regimens
48 [3, 4]. There are different approaches to subgrouping of BC, where tumor grade, TNM-stage
49 (tumor, node, metastasis), molecular subtype and/or receptor status are the principal categories
50 [5-9]. Despite extensive efforts to improve prognosis in BC patients, it remains the second largest
51 cause of cancer related deaths in women [1, 2, 4]. More than 90% of BC mortality is due to local
52 recurrence and distant metastases [10, 11]. Cells from the primary tumor are known to
53 metastasize and disseminate in the bone marrow at a presymptomatic stage in the tumorigenesis,
54 and may persevere in a dormant state for years, even decades, before becoming clinically evident,
55 contributing to the challenges in accurate diagnosis, treatment and follow-up [4, 12]. Improving
56 the prognostic and predictive biomarkers for early detection of primary and metastatic disease,
57 alongside with the identification and stratification of the most aggressive tumors with focus on
58 targeted treatments, still needs to be a priority in BC research.

59 MicroRNAs (miRNAs) constitute a conserved class of endogenous small non-coding RNAs first
60 discovered in *Caenorhabditis elegans* [13]. They function as post-transcriptional gene expression
61 regulators and, depending on the degree of base complementarity to the 3' untranslated region
62 (3'-UTR) of target mRNAs, they suppress gene expression by either complete mRNA
63 degradation, mRNA destabilization, or mRNA silencing [14-16]. According to the miRBase
64 database of published miRNA sequences and annotations, there are currently described more than
65 2500 unique mature miRNAs [17].

66 In BC, various miRNAs have been studied, where some contribute to the upregulation of
67 oncogenes, while others activate tumor suppressor genes [18, 19]. Moreover, studies have shown
68 that miRNA expression profiles vary between different subcategories of BC [20, 21]. Some of the
69 best described miRNAs differentially expressed in BC, are the miR-200 family and the miR-21
70 [22, 23]. The miR-200 family consists of five individual miRNAs, and they are suppressed during
71 epithelial to mesenchymal transition (EMT), a central step in metastasis and cancer progression
72 [24, 25]. MiR-21 is highly expressed in BC, and has been shown to inhibit several tumor
73 suppressors in BC. High expression of miR-21 is associated with overall tumor progression and
74 poor prognosis [23, 26]. It is of great interest to investigate and characterize individual miRNAs,
75 their expression and functional roles in BC and their subtypes.

76 MiR-126 was initially described as a regulator of megakaryocytopoiesis and leukemia [27], but
77 has since been designated a tumor suppressor role in various cancers [28-31]. Reduced
78 expression of miR-126 has been linked to invasion and metastasis, especially through the
79 regulation of ADAM9 [32-34], and miR-126 has been described as predicting response to
80 chemotherapy and bevacizumab treatment [35]. Noteworthy, miR-126 has been shown to be a
81 negative regulator of metastatic progression, mainly through downregulation of key functions
82 such as cell proliferation, migration, and survival of BC cells [36].

83 Through a series of *in vitro* experiments, we sought to study the functional effects of both miR-
84 126-3p, and its passenger strand miR-126-5p, in BC cell lines reflecting different subtypes of
85 breast cancer: Estrogen receptor positive (ER+), human epithelial growth factor receptor positive
86 (HER2+), and triple negative (TN) BCs. Using an unselected cohort of BC patients participating
87 in the Norwegian Woman and Cancer Study (NOWAC) [37], we further wanted to evaluate the

88 tissue- and cell specific expression of miR-126-3p and miR-126-5p using *in situ* hybridization
89 methods.

90 **Methods**

91 **Functional studies**

92 To investigate the functional properties of miR-126-3p and miR-126-5p in tumorigenesis, we
93 performed a series of *in vitro* experiments. A miR-126-3p and a miR-126-5p mimic were
94 introduced into different BC cell lines. The miRNAs were introduced alone or in combination,
95 alongside a miRNA negative control, to study cell proliferation and cell invasion.

96 **Cell cultures**

97 The functional properties of miR-126-3p and miR-126-5p were evaluated in three different BC
98 cell lines: the ER+ cell line MCF7 (ATCC ® HTB-22™), the HER2+ cell line SK-BR-3
99 (ATCC® HTB-30™), and the triple negative (TN) cell line MDA-MB-231. SK-BR-3 and MDA-
100 MB-231 were cultured in RPMI-1640 media (cat.# R8758, Sigma-Aldrich, St. Louis, USA)
101 supplemented with 10% fetal bovine serum (cat.# S0415, Biochrom, Berlin, Germany). MCF7
102 cells were cultured in DMEM (cat.# D5796, Sigma-Aldrich, St. Louis, USA) with the same
103 supplements as the other two cell lines. All cell lines were incubated at 37°C in a humidified
104 atmosphere with 5% CO₂. Additionally, total RNA from the non-cancerous breast cell line MCF-
105 10A was used in qPCR experiments. This was as a kind gift from the RNA and molecular
106 pathology (RAMP) research group, UiT - The Arctic University of Norway, Tromsø, Norway.

107 **Cell transfection**

108 BC cell lines were transiently transfected with 100 nM hsa-miR-126-3p Pre-miR™ miRNA
109 Precursor (cat.# PM12841, Thermo Fisher Scientific, USA) and/or 100 nM hsa-miR-126-5p Pre-

110 miRTM miRNA Precursor (cat.# PM10401, Thermo Fisher Scientific, USA), alongside the Cy3TM
111 Dye-Labeled Pre-miR Negative Control #1 (cat.# AM17120, Thermo Fisher Scientific, USA).
112 The transfection was performed using 8 µl/mL of the Lipofectamine® RNAiMAX transfection
113 reagent (cat.# 13778075, Thermo Fisher Scientific, USA). Transfected Cy3TM Dye-Labeled Pre-
114 miR Negative Control emits fluorescent light when exposed to UV-light to allow detection of
115 transfected cells, and the transfection efficiency was determined using a fluorescence microscope.
116 The transfection efficiency was typically as high as 80% - 95%.

117 **Total RNA isolation**

118 Total RNA was isolated from cells using the miRNeasy Mini Kit (cat.# 217004, Qiagen, Hilden,
119 Germany) according to the manufacturer's protocol. Briefly, cells were lysed using 700 µl
120 QiAzol Lysis Reagent before homogenization and incubation for 5 minutes at room temperature.
121 Next, 140 µl chloroform were added, and the samples were shaken before incubation at room
122 temperature for 3 minutes. Samples were then centrifuged for 15 minutes at 12000 g at 4°C, and
123 the upper aqueous phase was transferred and mixed thoroughly with 100% ethanol. Finally,
124 samples were transferred into the RNeasy® Mini column and washed in several steps before
125 elution with 50 µl ddH₂O. Isolated total RNA samples were stored at -70°C.

126 **cDNA synthesis**

127 Synthesis of first strand cDNA was performed using the miScript II RT Kit (cat.# 218160,
128 Qiagen, Hilden, Germany) according to the manufacturer's protocol. In short, 100 ng of total
129 RNA was mixed with 4 µl 5x miScript HiSpec Buffer, 2 µl 10x Nucleics Mix, 2 µl miScript
130 Reverse Transcriptase Mix, and RNase-free water to a total volume of 20 µl. Next, samples were
131 incubated for 60 minutes at 37°C, and subsequently incubated for 5 minutes at 95°C to inactivate
132 enzymes. Finally, samples were diluted with 200 µl RNase-free water and stored at -20°C.

133 **RT-PCR**

134 Endogenous levels of miR-126-3p and miR-126-5p in the BC cell lines were quantified relative
135 to the reference snRNA RNU6 using the miScript SYBR® Green PCR Kit (cat.# 218073,
136 Qiagen, Hilden, Germany) and real-time PCR. The primers used in this study were miScript
137 Primer Assays Hs_miR-126_1 miScript Primer Assay (cat.# MS00003430, Qiagen, Hilden,
138 Germany), Hs_miR-126*_1 miScript Primer Assay (cat.# MS00006636, Qiagen, Hilden,
139 Germany), and Hs_RNU6-2_11 miScript Primer Assay (cat.# MS00033740, Qiagen, Hilden,
140 Germany), and all primers were used according to the manufacturer's protocol. Briefly, a total
141 volume of 25 µl/well in a 96-well plate included 1 µl cDNA mixed with 12.5 µl 2x QuantiTect
142 SYBR Green PCR Master Mix, 2.5 µl 10x miScript Universal Primer, 2.5 µl 10x miScript Primer
143 Assay, and 6.5 µl RNase-free Water. The plate was sealed and centrifuged for 1 minute at 1000 g
144 before it was placed in a 7300 Real-Time PCR System (Thermo Fisher Scientific, Waltham,
145 Massachusetts, USA). Each sample was analyzed in quadruplicates, and three independent
146 experiments were performed.

147 **Proliferation assay**

148 The real-time cell analyzer system xCelligence, RTCA DP (cat#05469759001, ACEA
149 Biosciences, San Diego, USA) fitted with the E-plate 16 (cat#05469830001, ACEA Biosciences,
150 San Diego, USA) was used to study the proliferation of the BC cell lines. Cells were trypsinized
151 until detached, resuspended in complete growth media and counted before analysis on the
152 xCelligence platform. Approximately 8000 cells per well were estimated to be optimal through
153 initial titration experiments. In line with the manufacturer's protocol, cells were seeded in
154 quadruplicates into an E-plate after baseline measurements, and the E-plate incubated for 30
155 minutes at room temperature before being positioned in the RTCA DP instrument. The

156 instrument was located in an incubator preserving the same conditions as used for routine
157 cultivation of cell lines. The cellular growth rate is denoted as 'Cell Index' and recorded by the
158 instrument every 30 minutes, where the index is an arbitrary unit reflecting the cell-sensor
159 impedance. The RTCA software version 1.2.1 was used to calculate growth curves. Three
160 independent experiments were performed as a minimum for each cell line.

161 **Invasion assay**

162 The invasiveness of the BC cell lines was tested using the CytoSelect™ 96-well Cell Invasion
163 Assay, Basement membrane (cat.# CBA-112, Cell Biolabs, San Diego, USA) according to the
164 manufacturer's protocol. In short, a modified Boyden chamber was used, and 50000
165 pretransfected and serum starved cells were seeded in the upper chamber precoated with a
166 basement membrane (a protein matrix isolated from Engelbreth-Holm-Swarm tumor cells). The
167 cells were allowed to invade for 24 h towards the bottom chamber containing media +10% FBS.
168 Cancer cells that were able to invade and pass through the porous membrane to the bottom side of
169 the membrane were lysed and stained before fluorescence was measured at 480/520 nm using the
170 CLARIOstar® microplate reader (BMG LABTECH, Ortenberg, Germany). All experiments were
171 performed in quadruplicates. Three independent experiments were performed as a minimum for
172 each cell line.

173 **Classification of human breast cancer samples**

174 The patient samples included in the study were retrieved from the archives at the Department of
175 Pathology at the University Hospital of North Norway in Tromsø and the Nordland Hospital in
176 Bodø. The BC cases were NOWAC participants diagnosed with breast cancer in the years 2004 –
177 2010. FFPE tissue cores from breast reduction surgery specimens were included in the study as
178 benign tissue controls. Histological grading and immunohistochemical (IHC) analyses of ER,

179 progesterone receptor (PR) and HER2 were done as part of routine diagnostics, but validated by a
 180 breast pathologist (L.M.). Cut-off values for ER positivity was $\geq 1\%$, for PR $\geq 10\%$ and for
 181 HER2 score 3+. Silver in situ hybridization (SISH) was done when HER2 IHC was inconclusive
 182 (score 2+). The proliferation marker Ki67 was evaluated in at least 500 tumor cells in the most
 183 proliferative areas of the tumor on slides from the primary surgery and reported as percentage of
 184 positive tumor cells. Molecular subtyping of tumors was based on the surrogate markers ER, PR,
 185 HER2 and Ki67 according to recommendations by the St Gallen International Expert Consensus
 186 and previous publications [38, 39] as presented in table 1:

187 **Table 1: Molecular subtyping of tumors based on surrogate markers.**

	ER/PR	HER2	Ki67
Luminal A	ER+ and/or PR+	–	$\leq 30\%$
Luminal B	ER+ and/or PR+	Any	$>30\%$ if HER2–
HER2 positive	–	+	Any
Basal like	–	–	Any

188

189 **MiRNA microarray and validation by PCR**

190 Tissue cores from formalin-fixed paraffin-embedded (FFPE) tissue blocks were collected. Total
 191 RNA was extracted from the tissue cores using the RecoverAll Total Nucleic Acid Isolation kit
 192 (Life Technologies, Grand Island, NY, USA) according to the manufacturer's instructions, and
 193 RNA quality and quantity assessed using the NanoDrop 1000 spectrophotometer (Thermo Fisher
 194 Scientific, Wilmington, DE). Exiqon (Vedbaek, Denmark) performed the microarray
 195 hybridization and analyses as a paid service. In summary, 250 ng total RNA from samples and
 196 reference were labeled with Hy3TM and Hy5TM, using the miRCURY LNATM microRNA Hi-
 197 Power Labeling Kit (Exiqon). An aliquot of all RNA species included in the study was used as

198 the Hy5TM-labeled reference RNA. Samples and reference RNA were mixed before
199 hybridization on a Tecan HS4800 hybridization station (Tecan, Austria) to the 7th generation
200 miRCURY LNA microRNA array containing probes for miRNAs in human, mouse and rat as
201 annotated in miRBASE version 19.0. Slides were scanned on the Agilent G2565BA Microarray
202 Scanner System (Agilent technologies Inc., USA) before image analysis using the ImaGene 9.0
203 software (BioDiscovery Inc., USA). The detection threshold was set as 1.2 times the 25th
204 percentile of the overall signal intensity of individual slides.

205 Forty tumor samples and 20 of the benign breast tissue controls were included in PCR validation,
206 also performed by Exiqon. RNA was extracted from FFPE tissue cores according to the
207 manufacturer's instruction using the Qiagen miRNeasy FFPE kit (Qiagen, Hilden, Germany), and
208 10 ng RNA was reverse transcribed using the miRCURY LNA Universal RT microRNA PCR,
209 Polyadenylation and cDNA synthesis kit (Exiqon). 100 x diluted cDNA went into PCR-reactions
210 using ExiLENT SYBR Green master mix in 384 well plates on a Light Cycler 480 Real-Time
211 PCR System (Roche). Suitable reference miRNAs were evaluated by Exiqon using the
212 Normfinder software. Based on stable expression across the data set, miR-664a-3p was used for
213 normalization. The expression values were calculated using the quantification cycle (Cq) from
214 PCR analyses and the formula: average Cq (all samples) – assay Cq (sample).

215 **Tissue microarray**

216 Full histological slides of tumor tissue from resection specimens were evaluated by two
217 pathologists (L.M. and L.T.B) and representative areas of tumor tissue carefully selected and
218 marked. The tissue microarray (TMA) was constructed using a tissue-arraying instrument
219 (Beecher Instruments, Silver Spring, MD) as previously published [40]. In short, a 0.6 mm-
220 diameter stylet was used to collect a total of four replicate tissue cores from each donor block and

221 transferred to the recipient block. 4 μm sections were cut with a Microm microtome HM355S
222 (Microm, Walldorf, Germany) and used for hematoxylin and eosin staining and later *in situ*
223 hybridization.

224 ***In situ* hybridization**

225 The miRNA *in situ* hybridization (ISH) was performed in Ventana Discovery Ultra instrument
226 (Ventana Medical Systems Inc, Arizona, USA). Reagents were supplied by Roche (Bacel,
227 Switzerland). Labelled locked nucleic acid (LNA) modified probes and controls were delivered
228 by Exiqon (Vedbaek, Denmark). For this study, the hsa-miR-126-3p (619866-360), hsa-miR-126-
229 5p (612156-360), U6 snRNA positive control probe and Scramble-miR negative control probe
230 were used. Exiqon analyzed the LNATM oligonucleotides by CE or HPLC, and confirmed the
231 identity of compound by MS.

232 First, 4 μm breast TMA sections were cut with a Micron microtome (HM355S) and placed on
233 SuperFrost Plus glass slides. Second, sections were incubated at 60°C overnight to melt the
234 paraffin and increase attachment to the slides. During the process of sectioning and staining,
235 cautions were taken to prevent RNase contamination of reagents and degradation of the RNA
236 samples.

237 As positive and negative tissue controls, sections from a TMA multi-organ tissue block were
238 used. It included benign and malign tissue from 12 different human organs.

239 Hybridization conditions were optimized for temperature and concentration for each LNA probe.
240 For breast TMA FFPE, a hybridization temperature of 51°C gave specific staining for both miR-
241 126-3p and miR-126-5p. The best staining intensity for miR-126-3p was achieved at a
242 concentration of 2 nM, while for the miR-126-5p the optimal concentration was 10 nM.

243 Sensitivity level of the ISH protocol was consolidated by clean and strong staining with 0.5 nM
244 U6 snRNA. Concentrations between 0.1-2.0 nM were required for optimal sensitivity. Scramble
245 miR negative control probe gave negative staining at standard conditions. For deparaffinization,
246 pretreatments and chromogen staining, the well-established standard ISH protocols in the
247 Discovery Ultra instrument were used. This methodology is described in more detail in our
248 previous publication on miRNAs [41].

249 **Scoring of ISH staining intensity**

250 For semiquantitative evaluation of ISH staining intensities for miR-126-3p and -5p, TMA tissue
251 slides were used. For each sample, a minimum of two tissue cores of tumor tissue and tumor-
252 associated stromal tissue were evaluated using a microscope at 200x magnification. By
253 morphologic criteria, tumor cells and stromal fibroblasts were scored for staining intensity with
254 the dominant staining intensity scored as: 0 = negative, 1 = weak, 2 = moderate, 3 = strong. From
255 the observed ISH staining pattern, both tumor cells and stromal fibroblasts stained diffusely and
256 homogenously and hence staining density was not scored since it did not give any additional
257 information. All cores were independently scored by two pathologists (L.M. and S.M.D.) who
258 were blinded to each other's score and histopathological parameters. In case of disagreement
259 (score discrepancy > 1), the slides were re-examined and a consensus was reached by the
260 observers. Mean score for each case was calculated from both cores and both examiners.

261 **Statistics**

262 The descriptive statistics, the non-parametric tests, and the correlation analysis were performed
263 using IBM SPSS Statistics, version 25. Standard error for the qPCR quantification and the
264 invasion study was calculated using four technical replicates from a representative experiment.
265 Statistics in the proliferation experiments were calculated using one-way ANOVA with p-values

266 corrected for multiple testing by controlling the false discovery rate implementing the method of
267 Benjamini & Hochberg.

268 **Results**

269 **Relative expression of miR-126-3p and miR-126-5p in breast cancer cell lines**

270 To evaluate the endogenous expression of miR-126-3p and miR-126-5p, miRNA levels in BC
271 cell lines were quantified relative to the levels in the non-cancerous breast cell line MCF-10A.
272 RT-qPCR revealed downregulated levels of both miR-126-3p and miR-126-5p in all three BC
273 cell lines (Fig. 1A). Noteworthy, the highest relative levels of the lead strand, miR-126-3p,
274 compared to the passenger strand, miR-126-5p, were observed in the non-cancerous breast cell
275 line MCF-10A, whilst the lowest relative levels were observed in the TN BC cell line MDA-MB-
276 231 (Fig. 2). Interestingly, in contrast to the other cell lines, miR-126-5p appears to be more
277 abundant than miR-126-3p in the TN BC cell line (Fig. 2).

278

279

280 **Functional studies of miR-126-3p and miR-126-5p *in vitro***

281 The potential functional roles of miR-126-3p and miR-126-5p in the three BC cell lines were
282 explored by *in vitro* experiments. Effects on proliferation and invasion were evaluated after
283 transfecting the BC cell lines with either miR-126-3p mimic, miR-126-5p mimic or both in
284 combination and in equal concentrations.

285 **Transfection of miR-126-3p inhibits proliferation and invasion *in vitro***

286 All three BC cell lines demonstrated a significant drop in proliferation when transfected with
287 miR-126-3p (Fig. 3). Depending on the cell line, the shift in proliferation occurred 12-48 hours
288 after transfection.

289 Further, the invasive potential of all three cell lines were significantly reduced when transfected
290 with miR-126-3p (Fig. 4). The degree of inhibition seemed to be uniform across cell lines,
291 independent of receptor status.

292 **Transfection of miR-126-5p increases proliferation and promotes invasion in the TN**

293 **BC cell line MDA-MB-231**

294 The proliferation rate, as denoted by cell index, of the TN cell line MDA-MB-231 was
295 significantly increased when transfected with miR-126-5p mimic. The effect was highly
296 significant, reproducible, and was observed almost immediately after transfection (Fig. 3C). In
297 contrast, the proliferation rates of the ER+ and HER2+ BC cell lines were reduced compared to
298 negative control, although not to the same extent as for cells transfected with miR-126-3p (Fig.
299 3A-B).

300 In the invasion experiment, where cells were allowed to invade and migrate through a basement
301 membrane matrix, the TN cell line MDA-MB-231 displayed an increase in invasive ratio after

302 transfection with miR-126-5p (Fig. 4). In contrast, the invasion ratios of the ER+ and HER2+ cell
303 lines were not significantly different in cells transfected with miR-126-5p compared to negative
304 control (Fig. 4).

305 **Cotransfection of miR-126-3p and miR-126-5p inhibits proliferation and invasion *in*** 306 ***vitro***

307 Cotransfecting miR-126-3p and miR-126-5p in equal concentrations resulted in a tumor
308 suppressor phenotype in all BC cell lines (Fig. 4). In the cell lines MCF-7 and SK-BR-3, where
309 both miR-126-3p and miR-126-5p alone demonstrated inhibition of proliferation and invasion,
310 the combination of the two demonstrated a similar effect, and the magnitude of this inhibition
311 was comparable to that of miR-126-3p alone (Figs. 3A-B, 4). Transfecting miR-126-5p into the
312 TN cell line resulted in an increase in both proliferation and invasion, but the cotransfection of
313 both miRNAs in equal concentration resulted in inhibition of proliferation and invasion (Figs. 3C,
314 4). Again, the magnitude of this inhibition was equivalent to that of miR-126-3p transfection
315 alone.

316 **Expression of miR-126-3p and miR-126-5p in the BC patient cohort using** 317 **microarray and PCR**

318 A total of 108 NOWAC BC cases from the postgenome cohort and 44 benign tissue controls
319 were included in the study. One case had to be excluded because of insufficient amount of tumor
320 tissue and five cases and six controls were excluded due to poor RNA quality, leaving 102 BC
321 cases and 38 benign tissue controls to be analyzed using miRNA microarray. An additional case
322 and two of the controls were identified as outliers after microarray and excluded from further
323 statistical analyses. 40 tumor samples and 20 of the controls were included in PCR validation.

324 Table 1 presents the expression levels of miR-126-3p and -5p in the BC tumors and benign tissue
325 controls.

326 Microarray miRNA analysis revealed a significant downregulation of both miR-126-3p and miR-
327 126-5p in BC tissue compared to benign breast tissue ($p<0.001$). This result was validated and
328 confirmed by PCR analyses ($p<0.001$) (Fig. 1B and Table 2). Microarray- and PCR-based
329 expression levels were significantly correlated for both miR-126-3p ($r=0.47$, $p<0.001$) and miR-
330 126-5p ($r=0.46$, $p<0.001$). Noteworthy, we found lower expression of miR-126-3p and -5p in
331 tumors with lymph node metastases compared to breast cancer cases without nodal involvement
332 (Table 2 and Fig. 5). Further subgroup analyses did not demonstrate any significant differences in
333 the expression of any of the miR-126 strands between tumors of different histological grade or
334 molecular subtype.

335

336
337

Table 2: Histopathological variables and descriptive data for breast cancer cases and controls with miR-126-3p and miR-126-5p expression data.

		PCR		Array	
		miR-126-3p	miR-126-5p	miR-126-3p	miR-126-5p
Control	Mean	4,24	-0,86	9,28	7,16
	SD	0,79	0,8	1,13	0,52
	N (%)	20 (100)	20 (100)	38 (100)	38 (100)
All tumors	Mean	3,02	-2,01	7,38	6,13
	SD	0,33	0,32	0,49	0,19
	N (%)	40 (100)	40 (100)	102 (100)	102 (100)
	P*	<0.001	<0.001	<0.001	<0.001
Tumor grade 1	Mean	3,21	-1,81	7,44	6,17
	SD	1,1	1,03	0,42	0,20
	N (%)	7 (17.5)	7 (17.5)	31 (32)	31 (32)
Tumor grade 2	Mean	3,29	-1,75	7,30	6,10
	SD	0,8	0,72	0,49	0,18
	N (%)	17 (42.5)	17 (42.5)	41 (41)	41 (41)
Tumor grade 3	Mean	2,55	-2,46	7,43	6,10
	SD	1,15	1,14	0,53	0,17
	N (%)	16 (40)	16 (40)	26 (27)	26 (27)
	P*	0.269	0.356	0.536	0.328
Luminal A	Mean	3,13	-1,91	7,38	6,14
	SD	0,8	0,64	0,49	0,19
	N (%)	12 (30)	12 (30)	54 (54.5)	54 (54.5)
Luminal B	Mean	3,14	-1,84	7,41	6,13
	SD	1,41	1,37	0,37	0,16
	N (%)	11 (27.5)	11 (27.5)	20 (21.5)	20 (21.5)
HER2+	Mean	3,11	-1,99	7,56	6,18
	SD	0,88	0,78	0,54	0,16
	N (%)	7 (17.5)	7 (17.5)	9 (8)	9 (8)
Basal-like	Mean	2,52	-2,48	7,26	6,06
	SD	0,94	1,01	0,54	0,20
	N (%)	10 (25)	10 (25)	16 (16)	17 (16)
	P*	0.866	0.917	0.716	0.514
Lymph node pos	Mean	2,44	-2,63	7,22	6,06
	SD	0,76	0,65	0,45	0,16
	N (%)	11 (27)	11 (27)	31	31
Lymph node neg	Mean	3,18	-1,82	7,48	6,17
	SD	1,04	0,98	0,47	0,19
	N (%)	29 (73)	29 (73)	69	69
	P*	0.049*	0.010*	0.021*	0.025*

338 **Stromal ISH expression of miR-126-5p increases with both histological grade and**
339 **molecular subtype**

340 The cellular and subcellular expression of miR-126-3p and miR-126-5p in BC tissue was
341 evaluated by ISH in TMA slides, and staining intensity in tumor cells and fibroblasts scored as a
342 semiquantitative measure of miRNA expression (Fig. 6). ISH staining for both strands of miR-
343 126 was cytoplasmic and observed in malignant epithelial cells and cancer-associated stromal
344 fibroblasts. Further, it was noted positive staining for miR-126-3p and -5p in endothelial cells and
345 inflammatory cells within the tumor.

346 In TMA, 90 of the BC tumors had representative tissue cores with tumor and stromal cells
347 represented, from which ISH staining intensity could be analyzed. Noteworthy, positive ISH
348 staining for miR-126-3p and -5p was observed in all tumors. The mean score for miR-126-3p in
349 tumor and stroma was 2.22 and 2.60, respectively, compared to 1.35 in tumor and 1.09 in stroma
350 for miR-126-5p. Mean miR-126-5p staining intensity in tumor cells was significantly different in
351 tumors grouped according to molecular subtype ($p=0.006$) where subgroup analyses revealed a
352 significantly lower miR-126-5p expression in tumor cells of luminal A tumors compared to
353 luminal B ($p=0.035$), HER2+ ($p=0.011$) and basal-like cancers ($p=0.012$) (Fig. 7A).

354 Interestingly, the main differences in expression of miR-126 between tumor groups were found
355 when exploring the staining of miR-126-5p in the stromal compartment. The stromal expression
356 of miR-126-5p was significantly different between tumors of different histological grade with
357 lower expression in grade 1 tumors compared to grade 3 ($p=0.006$) (Fig. 7B), and in luminal A
358 tumors compared to luminal B ($p=0.022$), HER2 positive ($p=0.002$) and the basal-like subgroup
359 ($p<0.001$) (Fig. 6A). Both miR-126-3p and -5p staining in tumor cells and stroma was higher in
360 ER- compared to ER+ tumors, whereas HER2+ tumors had higher miR-126-5p staining in tumor

361 cells and stroma compared to HER2- tumors. There were no significant differences in miR-126-
 362 3p and -5p mean staining intensity in tumor or stromal cells between tumors according to lymph
 363 node status, although the lowest levels were found in tumors with nodal metastases. ISH scores
 364 according to histopathological variables are presented in Table 3.

365 **Table 3: In situ hybridization scores for miR-126-3p and miR-126-5p.** Data presented as
 366 mean score in tumor cells and stroma of breast cancer tumors according to histopathological
 367 variables.

		miR-126-3p		miR-126-5p	
		Tumor	Stroma	Tumor	Stroma
Histological grade	Grade 1	2.14	2.59	1.19	0.80
	Grade 2	2.22	2.64	1.35	1.11
	Grade 3	2.31	2.57	1.52	1.38
	P	0.67	0.83	0.094	0.023*
Molecular subtype	Luminal A	2.13	2.56	1.17	0.76
	Luminal B	2.21	2.60	1.52	1.21
	HER2+	2.39	2.50	1.72	1.78
	Basal-like	2.39	2.80	1.48	1.63
	P	0.35	0.11	0.006*	<0.001**
ER status	Positive	2.14	2.56	1.27	0.84
	Negative	2.42	2.71	1.56	1.67
	P	0.042*	0.017*	0.008*	<0.001**
HER2 status	Positive	2.22	2.58	1.62	1.53
	Negative	2.22	2.61	1.30	1.00
	P	0.97	0.98	0.029*	0.027*
Lymph node status	Positive	2.12	2.52	1.28	0.94
	Negative	2.27	2.64	1.39	1.16
	P	0.32	0.20	0.20	0.16

368

369

370 There was a positive correlation between the ISH staining intensity in tumor cells and stromal
 371 fibroblasts for both miR-126-3p and miR-126-5p (Table 4). Interestingly, the proliferative marker
 372 Ki67 displayed a positive correlation with the stromal expression of miR-126-5p which was
 373 borderline significant at the $p \leq 0.05$ level ($r=0.24$, $p=0.055$).

374 **Table 4: Correlation of miR-126-3p and miR-126-5p from *in situ* hybridization staining.**

			miR-126-3p		miR-126-5p		Ki67
			N=90				N=63
	Tumor	r	Tumor	Stroma	Tumor	Stroma	
miR-126-3p	Tumor	r		0.47**	0.42**	0.29**	0.09
	Stroma	r			0.24*	0.39**	0.11
miR-126-5p	Tumor	r				0.70**	0.18
	Stroma	r					0.24(*)

375

376 Discussion

377 Herein, we describe the miR-126-3p and its passenger strand, miR-126-5p, in BC using both
 378 functional studies of BC cell lines and studies of the miRNAs' expression patterns in samples
 379 from BC patients.

380 Endogenous expression of miR-126-3p and miR-126-5p was found to be downregulated both in
 381 malignant tumors from women participating in the NOWAC study, and in the three different cell
 382 lines representing the BC subtypes ER+, HER2+, and TN tumors. This is in line with other
 383 studies where expression of miR-126 has been reported to be downregulated in malignant
 384 compared to benign breast tissue [42]. Promoter regulation of the host gene of miR-126, *EGFL7*,
 385 has been reported as a possible underlying mechanism [30, 43].

386 Expression of miR-126-3p is considered tumor suppressive [30, 44-46], and the functional
 387 experiments presented in this study support this perception, as all three studied BC cell lines

388 displayed inhibition of both proliferation and invasion when transfected with miR-126-3p.
389 Interestingly, the passenger strand, miR-126-5p, appears to be a potent driver of tumorigenesis in
390 the TN cell line MDA-MB-231, whilst having tumor suppressive effects in the ER+ MCF7 and
391 the HER2+ SK-BR-3 cell line. Proliferation and invasion significantly increased in the TN cell
392 line when transfected with miR-126-5p. The effect was profound, especially in the proliferation
393 assays, and this was reproduced in a minimum of three independent experiments. Other studies of
394 miR-126 in BC have reported the passenger strand miR-126-5p to be a tumor suppressor working
395 in synergy with the lead strand, miR-126-3p [30, 47]. However, there are reports of miR-126-5p
396 being associated with tumor promoting properties, such as drug resistance and poor prognosis in
397 acute myeloid leukemia (AML) patients [48], promotion and protection of endothelial
398 proliferation by inhibition of Dlk1 and SetD5 [49, 50], and induction of proliferation and
399 angiogenesis in non-tumorigenic cells via the PI3K/AKT and MAPK/ERK pathways [51].
400 Interestingly, the epidermal growth factor-like protein Delta-like homolog 1 (Dlk1) is suppressed
401 by miR-126-5p, but not miR-126-3p, in endothelial cells [49]. Dlk1 is an inhibitor of NOTCH-
402 receptors, which, depending on cellular context, have oncogenic or tumor suppressor properties.
403 Low levels of Dlk1 and thereby higher levels of NOTCH-signaling have been reported to
404 increase cell proliferation and cell invasion of MDA-MB-231 cells [52], the TN BC cell line used
405 in our study. Further, transfection of miR-126-5p in other cell types has been shown to inhibit the
406 expression of the *klotho* gene, and increase the phosphorylation of Akt [53]. Klotho exerts
407 inhibitory effects on the IGF-1 signaling pathway and has tumor suppressive effects in BC cells
408 [54]. Downregulation of *klotho* and Dlk1 represents possible underlying mechanisms for the
409 observed tumor promoting effects of miR-126-5p in the TN BC cell line in our study.

410 For the ER+ and the HER2+ cell lines, transfection with miR-126-5p led to a tumor suppressive
411 response in the proliferation experiments, although the effect was less pronounced when
412 compared to the experiments with the lead strand, miR-126-3p. Notably, when transfecting the
413 ER+ and HER2+ BC cell lines using miR-126-5p, their invasion potential did not significantly
414 differ to that of the control transfection.

415 The passenger strands of miRNAs are typically degraded after processing, and are consequently
416 less abundant compared to their lead strand [15]. This is also evident for mature miR-126 in our
417 study, where expression of miR-126-3p in the patient cohort and the BC cell lines MCF7 and SK-
418 BR-3 is greater compared to expression of miR-126-5p. Interestingly, when comparing
419 endogenous levels of miR-126-3p with endogenous levels of miR-126-5p in the non-cancerous
420 cell line MCF-10A, the ER+ BC cell line MCF-7, the HER2+ BC cell line SK-BR-3, and the TN
421 BC cell line MDA-MB-231, we found an incremental shift in the miR-126-3p/miR-126-5p
422 expression pattern. The non-cancerous cell line MCF-10A appears to harbor the largest relative
423 amount of miR-126-3p, followed by ER+ MCF-7 and HER2+ SK-BR-3, whilst the TN MDA-
424 MB-231 has the opposite expression pattern, with miR-126-5p presenting as the more abundant
425 strand. It is possible that mechanisms responsible for targeting the passenger strand miR-126-5p
426 for degradation are either corrupted or in some way modified to allow miR-126-5p to accumulate.
427 As a consequence, a larger part of the mature passenger strand, miR-126-5p, is eligible to interact
428 with the RISC-complex to exhibit a more potent biological response in the TN BC cell line which
429 represents the most aggressive BC subtype (Fig. 8).

430 Studies of miRNA biogenesis, expression and functions have reported that different miRNA
431 strands can be selected in a tissue specific manner and during cancer progression [55, 56].
432 Further, high abundance of target mRNAs may block miRNA release from their targets and

433 protect miRNA strands from degradation by exoribonucleases [56]. Hence, regulation of miRNA
434 strand selection and stability could add to the complexity of miRNA expression and function in
435 different BC subtypes, as illustrated by the different functions of miR-126-3p and miR-126-5p in
436 different BC cell lines in the present study.

437 In the clinical tumor samples, the expression of miR-126-3p and -5p, analyzed by microarray and
438 PCR, was lower in lymph node positive breast cancers compared to tumors without nodal
439 metastases. Interestingly, miR-126 has been shown to be a negative regulator of the metastatic
440 process in BC in part by suppressing tumor growth *in vitro* using highly metastatic breast cancer
441 cell lines [36]. In a murine model of breast cancer, miR-126 knockdown cells were shown to
442 form metastases with high blood vessel density due to increased recruitment of endothelial cells
443 to the metastatic cells [57]. The target genes demonstrated to mediate the suppressive effects of
444 miR-126 on metastasis formation were *IGFBP2*, the receptor kinase *MERTK* and the
445 phosphatidylinositol transfer protein *PITPNC1*, which in sum mediate a positive migratory and
446 chemotactic signal to endothelial cells.

447 The expression of miR-126-3p and -5p was not significantly different between tumors of
448 different histological grade or molecular subtype when analyzed using microarray and PCR
449 technology. The homogenized tissue used for RNA extraction and later microarray and PCR
450 contains RNA contributions not only from epithelial cells, but also from other cellular
451 components in benign and malignant tissue such as fibroblast, endothelial cells, adipocytes and
452 lymphocytes. However, in this study, ISH analysis of both miRNA strands was included,
453 allowing us to explore the *in situ* expression of miR-126 in both tumor and stromal BC cells.
454 Interestingly, stromal levels of miR-126-5p were significantly associated with both molecular
455 subtype and histological grade, with the highest levels of miR-126-5p observed in the tumors

456 belonging to the BC subtypes with the worst prognosis. Although not statistically significant
457 ($p=0.055$), the positive correlation between miR-126-5p and the proliferation marker Ki67 is
458 noteworthy in this context. These findings are especially interesting when considering the *in vitro*
459 experiments where the introduction of miR-126-5p produced a more aggressive phenotype in the
460 TN BC cell line MDA-MB-231. The linkage between miR-126-5p expression and BC subtype
461 and grade was highly significant in BC stroma, i.e. in fibroblasts within the tumor. Fibroblasts are
462 involved in tumorigenesis and constitute the majority of stromal cells in breast tumors [58].
463 Several studies have described considerable crosstalk between tumor and stroma via exosomal
464 transfer of miRNAs [59-61] where microvesicles containing miRNAs derived from cancer cells
465 convert fibroblast into cancer associated fibroblasts (CAFs) with tumor-promoting properties.
466 Further, exosomes from fibroblast can also affect cancer cell functions, e.g. miRNAs from CAFs
467 have been shown to be directly involved in ER repression in breast cancer through secreted
468 exosomes [62]. Hence, the increased stromal miR-126-5p expression and its association with
469 more advanced breast cancers is an interesting finding, given the diversity of miR-126-5p effects
470 in functional studies.

471 This study has increased our understanding and awareness of miRNAs duplexity in regulation
472 and function. Through *in vitro* studies we have described the mature miR-126 as having both
473 potent tumor suppressor and tumor driver functions with opposite effects of the two different
474 miR-126 strands in TN BC. Functional studies on individual miRNAs are an important tool in
475 detecting and understanding these two-faced properties which are recurrently emerging for
476 several miRNAs.

477

478

- 480 1. Miller KD, Siegel RL, Lin CC, Mariotto AB, Kramer JL, Rowland JH, et al. Cancer treatment and
481 survivorship statistics, 2016. *CA Cancer J Clin.* 2016;66(4):271-89. doi: 10.3322/caac.21349. PubMed
482 PMID: 27253694.
- 483 2. Cancer Facts & Figures 2017. American Cancer Society. 2017.
- 484 3. Yadav BS, Sharma SC, Chanana P, Jhamb S. Systemic treatment strategies for triple-negative
485 breast cancer. *World J Clin Oncol.* 2014;5(2):125-33. doi: 10.5306/wjco.v5.i2.125. PubMed PMID:
486 24829859; PubMed Central PMCID: PMCPMC4014784.
- 487 4. Nakamura S, Yagata H, Ohno S, Yamaguchi H, Iwata H, Tsunoda N, et al. Multi-center study
488 evaluating circulating tumor cells as a surrogate for response to treatment and overall survival in
489 metastatic breast cancer. *Breast Cancer.* 2010;17(3):199-204. doi: 10.1007/s12282-009-0139-3. PubMed
490 PMID: 19649686.
- 491 5. Perou CM, Sorlie T, Eisen MB, van de Rijn M, Jeffrey SS, Rees CA, et al. Molecular portraits of
492 human breast tumours. *Nature.* 2000;406(6797):747-52. doi: 10.1038/35021093. PubMed PMID:
493 10963602.
- 494 6. Masood S. Breast cancer subtypes: morphologic and biologic characterization. *Womens Health*
495 *(Lond).* 2016;12(1):103-19. doi: 10.2217/whe.15.99. PubMed PMID: 26756229.
- 496 7. Vuong D, Simpson PT, Green B, Cummings MC, Lakhani SR. Molecular classification of breast
497 cancer. *Virchows Arch.* 2014;465(1):1-14. doi: 10.1007/s00428-014-1593-7. PubMed PMID: 24878755.
- 498 8. Cancer Genome Atlas N. Comprehensive molecular portraits of human breast tumours. *Nature.*
499 2012;490(7418):61-70. doi: 10.1038/nature11412. PubMed PMID: 23000897; PubMed Central PMCID:
500 PMCPMC3465532.
- 501 9. Goldhirsch A, Wood WC, Coates AS, Gelber RD, Thurlimann B, Senn HJ, et al. Strategies for
502 subtypes--dealing with the diversity of breast cancer: highlights of the St. Gallen International Expert
503 Consensus on the Primary Therapy of Early Breast Cancer 2011. *Ann Oncol.* 2011;22(8):1736-47. doi:
504 10.1093/annonc/mdr304. PubMed PMID: 21709140; PubMed Central PMCID: PMCPMC3144634.
- 505 10. Zielinska HA, Bahl A, Holly JM, Perks CM. Epithelial-to-mesenchymal transition in breast cancer: a
506 role for insulin-like growth factor I and insulin-like growth factor-binding protein 3? *Breast Cancer (Dove*
507 *Med Press).* 2015;7:9-19. doi: 10.2147/BCTT.S43932. PubMed PMID: 25632238; PubMed Central PMCID:
508 PMCPMC4304531.
- 509 11. Siegel RL, Miller KD, Jemal A. Cancer statistics, 2016. *CA Cancer J Clin.* 2016;66(1):7-30. doi:
510 10.3322/caac.21332. PubMed PMID: 26742998.
- 511 12. Schwartz RS, Erban JK. Timing of Metastasis in Breast Cancer. *N Engl J Med.* 2017;376(25):2486-8.
512 doi: 10.1056/NEJMcibr1701388. PubMed PMID: 28636861.
- 513 13. Lee RC, Feinbaum RL, Ambros V. The *C. elegans* heterochronic gene *lin-4* encodes small RNAs
514 with antisense complementarity to *lin-14*. *Cell.* 1993;75(5):843-54. PubMed PMID: 8252621.
- 515 14. Winter J, Jung S, Keller S, Gregory RI, Diederichs S. Many roads to maturity: microRNA biogenesis
516 pathways and their regulation. *Nat Cell Biol.* 2009;11(3):228-34. doi: 10.1038/ncb0309-228. PubMed
517 PMID: 19255566.
- 518 15. Macfarlane LA, Murphy PR. MicroRNA: Biogenesis, Function and Role in Cancer. *Curr Genomics.*
519 2010;11(7):537-61. doi: 10.2174/138920210793175895. PubMed PMID: 21532838; PubMed Central
520 PMCID: PMCPMC3048316.
- 521 16. Ha M, Kim VN. Regulation of microRNA biogenesis. *Nat Rev Mol Cell Biol.* 2014;15(8):509-24. doi:
522 10.1038/nrm3838. PubMed PMID: 25027649.

- 523 17. Kozomara A, Griffiths-Jones S. miRBase: annotating high confidence microRNAs using deep
524 sequencing data. *Nucleic Acids Res.* 2014;42(Database issue):D68-73. doi: 10.1093/nar/gkt1181. PubMed
525 PMID: 24275495; PubMed Central PMCID: PMC3965103.
- 526 18. Takahashi RU, Miyazaki H, Ochiya T. The Roles of MicroRNAs in Breast Cancer. *Cancers (Basel).*
527 2015;7(2):598-616. doi: 10.3390/cancers7020598. PubMed PMID: 25860815; PubMed Central PMCID:
528 PMC4491673.
- 529 19. Graveel CR, Calderone HM, Westerhuis JJ, Winn ME, Sempere LF. Critical analysis of the potential
530 for microRNA biomarkers in breast cancer management. *Breast Cancer (Dove Med Press).* 2015;7:59-79.
531 doi: 10.2147/BCTT.S43799. PubMed PMID: 25759599; PubMed Central PMCID: PMC4346363.
- 532 20. Blenkinson C, Goldstein LD, Thorne NP, Spiteri I, Chin SF, Dunning MJ, et al. MicroRNA expression
533 profiling of human breast cancer identifies new markers of tumor subtype. *Genome Biol.*
534 2007;8(10):R214. doi: 10.1186/gb-2007-8-10-r214. PubMed PMID: 17922911; PubMed Central PMCID:
535 PMC2246288.
- 536 21. de Rinaldis E, Gazinska P, Mera A, Modrusan Z, Fedorowicz GM, Burford B, et al. Integrated
537 genomic analysis of triple-negative breast cancers reveals novel microRNAs associated with clinical and
538 molecular phenotypes and sheds light on the pathways they control. *BMC Genomics.* 2013;14:643. doi:
539 10.1186/1471-2164-14-643. PubMed PMID: 24059244; PubMed Central PMCID: PMC4008358.
- 540 22. Altuvia Y, Landgraf P, Lithwick G, Elefant N, Pfeffer S, Aravin A, et al. Clustering and conservation
541 patterns of human microRNAs. *Nucleic Acids Res.* 2005;33(8):2697-706. doi: 10.1093/nar/gki567.
542 PubMed PMID: 15891114; PubMed Central PMCID: PMC1110742.
- 543 23. Frankel LB, Christoffersen NR, Jacobsen A, Lindow M, Krogh A, Lund AH. Programmed cell death
544 4 (PDCD4) is an important functional target of the microRNA miR-21 in breast cancer cells. *J Biol Chem.*
545 2008;283(2):1026-33. doi: 10.1074/jbc.M707224200. PubMed PMID: 17991735.
- 546 24. Huber MA, Azoitei N, Baumann B, Grunert S, Sommer A, Pehamberger H, et al. NF-kappaB is
547 essential for epithelial-mesenchymal transition and metastasis in a model of breast cancer progression. *J*
548 *Clin Invest.* 2004;114(4):569-81. doi: 10.1172/JCI21358. PubMed PMID: 15314694; PubMed Central
549 PMCID: PMC503772.
- 550 25. Korpala M, Lee ES, Hu G, Kang Y. The miR-200 family inhibits epithelial-mesenchymal transition
551 and cancer cell migration by direct targeting of E-cadherin transcriptional repressors ZEB1 and ZEB2. *J*
552 *Biol Chem.* 2008;283(22):14910-4. doi: 10.1074/jbc.C800074200. PubMed PMID: 18411277; PubMed
553 Central PMCID: PMC3258899.
- 554 26. Yadav P, Mirza M, Nandi K, Jain SK, Kaza RC, Khurana N, et al. Serum microRNA-21 expression as
555 a prognostic and therapeutic biomarker for breast cancer patients. *Tumour Biol.* 2016;37(11):15275-82.
556 doi: 10.1007/s13277-016-5361-y. PubMed PMID: 27696295.
- 557 27. Garzon R, Pichiorri F, Palumbo T, Iuliano R, Cimmino A, Aqeilan R, et al. MicroRNA fingerprints
558 during human megakaryocytopoiesis. *Proc Natl Acad Sci U S A.* 2006;103(13):5078-83. doi:
559 10.1073/pnas.0600587103. PubMed PMID: 16549775; PubMed Central PMCID: PMC1458797.
- 560 28. Wang J, Zhou Y, Fei X, Chen X, Yan J, Liu B, et al. ADAM9 functions as a promoter of gastric cancer
561 growth which is negatively and post-transcriptionally regulated by miR-126. *Oncol Rep.* 2017;37(4):2033-
562 40. doi: 10.3892/or.2017.5460. PubMed PMID: 28260063.
- 563 29. Han IB, Kim M, Lee SH, Kim JK, Kim SH, Chang JH, et al. Down-regulation of MicroRNA-126 in
564 Glioblastoma and its Correlation with Patient Prognosis: A Pilot Study. *Anticancer Res.* 2016;36(12):6691-
565 7. doi: 10.21873/anticancer.11280. PubMed PMID: 27920004.
- 566 30. Zhang Y, Yang P, Sun T, Li D, Xu X, Rui Y, et al. miR-126 and miR-126* repress recruitment of
567 mesenchymal stem cells and inflammatory monocytes to inhibit breast cancer metastasis. *Nat Cell Biol.*
568 2013;15(3):284-94. doi: 10.1038/ncb2690. PubMed PMID: 23396050; PubMed Central PMCID:
569 PMC3672398.

- 570 31. Du C, Lv Z, Cao L, Ding C, Gyabaah OA, Xie H, et al. MiR-126-3p suppresses tumor metastasis and
571 angiogenesis of hepatocellular carcinoma by targeting LRP6 and PIK3R2. *J Transl Med.* 2014;12:259. doi:
572 10.1186/s12967-014-0259-1. PubMed PMID: 25240815; PubMed Central PMCID: PMC4189615.
- 573 32. Xiang LY, Ou HH, Liu XC, Chen ZJ, Li XH, Huang Y, et al. Loss of tumor suppressor miR-126
574 contributes to the development of hepatitis B virus-related hepatocellular carcinoma metastasis through
575 the upregulation of ADAM9. *Tumour Biol.* 2017;39(6):1010428317709128. doi:
576 10.1177/1010428317709128. PubMed PMID: 28639884.
- 577 33. Xiong Y, Kotian S, Zeiger MA, Zhang L, Kebebew E. miR-126-3p Inhibits Thyroid Cancer Cell
578 Growth and Metastasis, and Is Associated with Aggressive Thyroid Cancer. *PLoS One.*
579 2015;10(8):e0130496. doi: 10.1371/journal.pone.0130496. PubMed PMID: 26244545; PubMed Central
580 PMCID: PMC4526518.
- 581 34. Jiang L, He A, Zhang Q, Tao C. miR-126 inhibits cell growth, invasion, and migration of
582 osteosarcoma cells by downregulating ADAM-9. *Tumour Biol.* 2014;35(12):12645-54. doi:
583 10.1007/s13277-014-2588-3. PubMed PMID: 25213697.
- 584 35. Hansen TF, Carlsen AL, Heegaard NH, Sorensen FB, Jakobsen A. Changes in circulating microRNA-
585 126 during treatment with chemotherapy and bevacizumab predicts treatment response in patients with
586 metastatic colorectal cancer. *Br J Cancer.* 2015;112(4):624-9. doi: 10.1038/bjc.2014.652. PubMed PMID:
587 25584492; PubMed Central PMCID: PMC4333496.
- 588 36. Tavazoie SF, Alarcon C, Oskarsson T, Padua D, Wang Q, Bos PD, et al. Endogenous human
589 microRNAs that suppress breast cancer metastasis. *Nature.* 2008;451(7175):147-52. doi:
590 10.1038/nature06487. PubMed PMID: 18185580; PubMed Central PMCID: PMC2782491.
- 591 37. Dumeaux V, Borresen-Dale AL, Frantzen JO, Kumle M, Kristensen VN, Lund E. Gene expression
592 analyses in breast cancer epidemiology: the Norwegian Women and Cancer postgenome cohort study.
593 *Breast cancer research.* 2008;10(1):R13. Epub 2008/02/15. doi: 10.1186/bcr1859. PubMed PMID:
594 18271962; PubMed Central PMCID: PMC4374969.
- 595 38. Coates AS, Winer EP, Goldhirsch A, Gelber RD, Gnant M, Piccart-Gebhart M, et al. Tailoring
596 therapies--improving the management of early breast cancer: St Gallen International Expert Consensus
597 on the Primary Therapy of Early Breast Cancer 2015. *Ann Oncol.* 2015;26(8):1533-46. Epub 2015/05/06.
598 doi: 10.1093/annonc/mdv221. PubMed PMID: 25939896; PubMed Central PMCID: PMC4511219.
- 599 39. Vasconcelos I, Hussainzada A, Berger S, Fietze E, Linke J, Siedentopf F, et al. The St. Gallen
600 surrogate classification for breast cancer subtypes successfully predicts tumor presenting features, nodal
601 involvement, recurrence patterns and disease free survival. *Breast.* 2016;29:181-5. Epub 2016/08/22.
602 doi: 10.1016/j.breast.2016.07.016. PubMed PMID: 27544822.
- 603 40. Bremnes RM, Veve R, Gabrielson E, Hirsch FR, Baron A, Bemis L, et al. High-Throughput Tissue
604 Microarray Analysis Used to Evaluate Biology and Prognostic Significance of the E-Cadherin Pathway in
605 Non-Small-Cell Lung Cancer. *Journal of Clinical Oncology.* 2002;20(10):2417-28. doi:
606 doi:10.1200/JCO.2002.08.159. PubMed PMID: 12011119.
- 607 41. Johannessen C, Moi L, Kiselev Y, Pedersen MI, Dalen SM, Braaten T, et al. Expression and function
608 of the miR-143/145 cluster in vitro and in vivo in human breast cancer. *PLoS One.* 2017;12(10):e0186658.
609 doi: 10.1371/journal.pone.0186658. PubMed PMID: 29073169; PubMed Central PMCID:
610 PMC45657998.
- 611 42. Tahiri A, Leivonen SK, Luders T, Steinfeld I, Ragle Aure M, Geisler J, et al. Deregulation of cancer-
612 related miRNAs is a common event in both benign and malignant human breast tumors. *Carcinogenesis.*
613 2014;35(1):76-85. doi: 10.1093/carcin/bgt333. PubMed PMID: 24104550.
- 614 43. Sezer Zhmurov C, Timirci-Kahraman O, Amadou FZ, Fazliogullari O, Basaran C, Catal T, et al.
615 Expression of Egfl7 and miRNA-126-5p in Symptomatic Carotid Artery Disease. *Genet Test Mol*
616 *Biomarkers.* 2016;20(3):125-9. doi: 10.1089/gtmb.2015.0252. PubMed PMID: 26799121.

- 617 44. Luo P, Fei J, Zhou J, Zhang W. microRNA-126 suppresses PAK4 expression in ovarian cancer
618 SKOV3 cells. *Oncology letters*. 2015;9(5):2225-9. doi: 10.3892/ol.2015.3012. PubMed PMID: 26137045;
619 PubMed Central PMCID: PMC4467333.
- 620 45. Yang Z, Wang R, Zhang T, Dong X. MicroRNA-126 regulates migration and invasion of gastric
621 cancer by targeting CADM1. *Int J Clin Exp Pathol*. 2015;8(8):8869-80. PubMed PMID: 26464628; PubMed
622 Central PMCID: PMC4583860.
- 623 46. Zhao C, Li Y, Zhang M, Yang Y, Chang L. miR-126 inhibits cell proliferation and induces cell
624 apoptosis of hepatocellular carcinoma cells partially by targeting Sox2. *Hum Cell*. 2015;28(2):91-9. doi:
625 10.1007/s13577-014-0105-z. PubMed PMID: 25585946.
- 626 47. Ren G, Kang Y. A one-two punch of miR-126/126* against metastasis. *Nat Cell Biol*.
627 2013;15(3):231-3. doi: 10.1038/ncb2703. PubMed PMID: 23449143.
- 628 48. Shibayama Y, Kondo T, Ohya H, Fujisawa S, Teshima T, Iseki K. Upregulation of microRNA-126-5p
629 is associated with drug resistance to cytarabine and poor prognosis in AML patients. *Oncol Rep*.
630 2015;33(5):2176-82. doi: 10.3892/or.2015.3839. PubMed PMID: 25759982; PubMed Central PMCID:
631 PMC4391586.
- 632 49. Schober A, Nazari-Jahantigh M, Wei Y, Bidzhekov K, Gremse F, Grommes J, et al. MicroRNA-126-
633 5p promotes endothelial proliferation and limits atherosclerosis by suppressing Dlk1. *Nat Med*.
634 2014;20(4):368-76. Epub 2014/03/04. doi: 10.1038/nm.3487. PubMed PMID: 24584117; PubMed Central
635 PMCID: PMC4398028.
- 636 50. Gaelle V, Loic P, Baraa N, Gaelle B, Carlos RJ, Sylvain C, et al. miR-126-5p promotes retinal
637 endothelial cell survival through SetD5 regulatio in neurons. *Development*. 2017. doi:
638 10.1242/dev.156232. PubMed PMID: 29180574.
- 639 51. Tao SC, Guo SC, Li M, Ke QF, Guo YP, Zhang CQ. Chitosan Wound Dressings Incorporating
640 Exosomes Derived from MicroRNA-126-Overexpressing Synovium Mesenchymal Stem Cells Provide
641 Sustained Release of Exosomes and Heal Full-Thickness Skin Defects in a Diabetic Rat Model. *Stem Cells*
642 *Transl Med*. 2017;6(3):736-47. doi: 10.5966/sctm.2016-0275. PubMed PMID: 28297576; PubMed Central
643 PMCID: PMC442792.
- 644 52. Nueda ML, Naranjo AI, Baladron V, Laborda J. Different expression levels of DLK1 inversely
645 modulate the oncogenic potential of human MDA-MB-231 breast cancer cells through inhibition of
646 NOTCH1 signaling. *FASEB journal : official publication of the Federation of American Societies for*
647 *Experimental Biology*. 2017;31(8):3484-96. Epub 2017/05/04. doi: 10.1096/fj.201601341RRR. PubMed
648 PMID: 28461338.
- 649 53. Shibayama Y, Kondo T, Ohya H, Fujisawa S-I, Teshima T, Iseki KEN. Upregulation of microRNA-
650 126-5p is associated with drug resistance to cytarabine and poor prognosis in AML patients. *Oncology*
651 *reports*. 2015;33(5):2176-82. doi: 10.3892/or.2015.3839. PubMed PMID: PMC4391586.
- 652 54. Wolf I, Levanon-Cohen S, Bose S, Ligumsky H, Sredni B, Kanety H, et al. Klotho: a tumor
653 suppressor and a modulator of the IGF-1 and FGF pathways in human breast cancer. *Oncogene*.
654 2008;27(56):7094-105. Epub 2008/09/03. doi: 10.1038/onc.2008.292. PubMed PMID: 18762812.
- 655 55. Griffiths-Jones S, Hui JHL, Marco A, Ronshaugen M. MicroRNA evolution by arm switching. *EMBO*
656 *Reports*. 2011;12(2):172-7. doi: 10.1038/embor.2010.191. PubMed PMID: PMC3049427.
- 657 56. Tsai K-W, Leung C-M, Lo Y-H, Chen T-W, Chan W-C, Yu S-Y, et al. Arm Selection Preference of
658 MicroRNA-193a Varies in Breast Cancer. *Scientific Reports*. 2016;6:28176. doi: 10.1038/srep28176.
659 PubMed PMID: PMC4910092.
- 660 57. Png KJ, Halberg N, Yoshida M, Tavazoie SF. A microRNA regulon that mediates endothelial
661 recruitment and metastasis by cancer cells. *Nature*. 2011;481(7380):190-4. Epub 2011/12/16. doi:
662 10.1038/nature10661. PubMed PMID: 22170610.
- 663 58. Bussard KM, Mutkus L, Stumpf K, Gomez-Manzano C, Marini FC. Tumor-associated stromal cells
664 as key contributors to the tumor microenvironment. *Breast cancer research : BCR*. 2016;18(1):84. Epub

665 2016/08/16. doi: 10.1186/s13058-016-0740-2. PubMed PMID: 27515302; PubMed Central PMCID:
666 PMCPmc4982339.

667 59. Valadi H, Ekstrom K, Bossios A, Sjostrand M, Lee JJ, Lotvall JO. Exosome-mediated transfer of
668 mRNAs and microRNAs is a novel mechanism of genetic exchange between cells. *Nat Cell Biol.*
669 2007;9(6):654-9. doi: 10.1038/ncb1596. PubMed PMID: 17486113.

670 60. Kogure T, Lin WL, Yan IK, Braconi C, Patel T. Intercellular nanovesicle-mediated microRNA
671 transfer: a mechanism of environmental modulation of hepatocellular cancer cell growth. *Hepatology.*
672 2011;54(4):1237-48. doi: 10.1002/hep.24504. PubMed PMID: 21721029; PubMed Central PMCID:
673 PMCPMC3310362.

674 61. Chiba M, Kimura M, Asari S. Exosomes secreted from human colorectal cancer cell lines contain
675 mRNAs, microRNAs and natural antisense RNAs, that can transfer into the human hepatoma HepG2 and
676 lung cancer A549 cell lines. *Oncol Rep.* 2012;28(5):1551-8. doi: 10.3892/or.2012.1967. PubMed PMID:
677 22895844; PubMed Central PMCID: PMCPMC3583404.

678 62. Shah SH, Miller P, Garcia-Contreras M, Ao Z, Machlin L, Issa E, et al. Hierarchical paracrine
679 interaction of breast cancer associated fibroblasts with cancer cells via hMAPK-microRNAs to drive ER-
680 negative breast cancer phenotype. *Cancer Biol Ther.* 2015;16(11):1671-81. Epub 2015/07/18. doi:
681 10.1080/15384047.2015.1071742. PubMed PMID: 26186233; PubMed Central PMCID:
682 PMCPMC4846097.

683

Figures

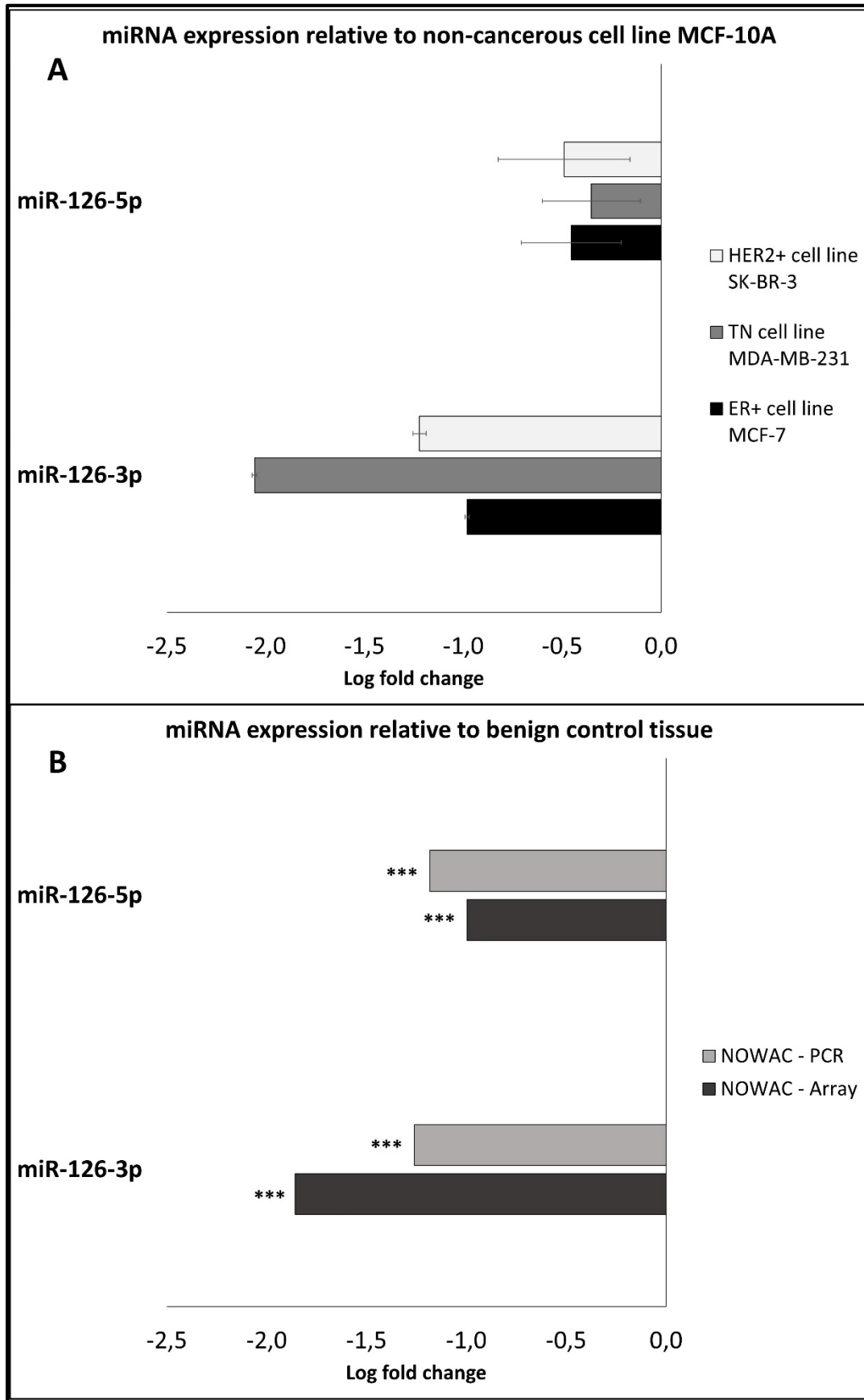


Fig. 1 – Endogenous expression. Endogenous miR-126 expression in three BC cell lines relative to the non-cancerous breast cell line MCF-10A (A), and the endogenous expression in BC tumors compared to benign breast tissue (B). Cell line data is displayed as mean log fold change \pm SE from a representative biological replicate. The annotation *** signifies $P < 0.001$ using the Mann–Whitney U test for independent samples.

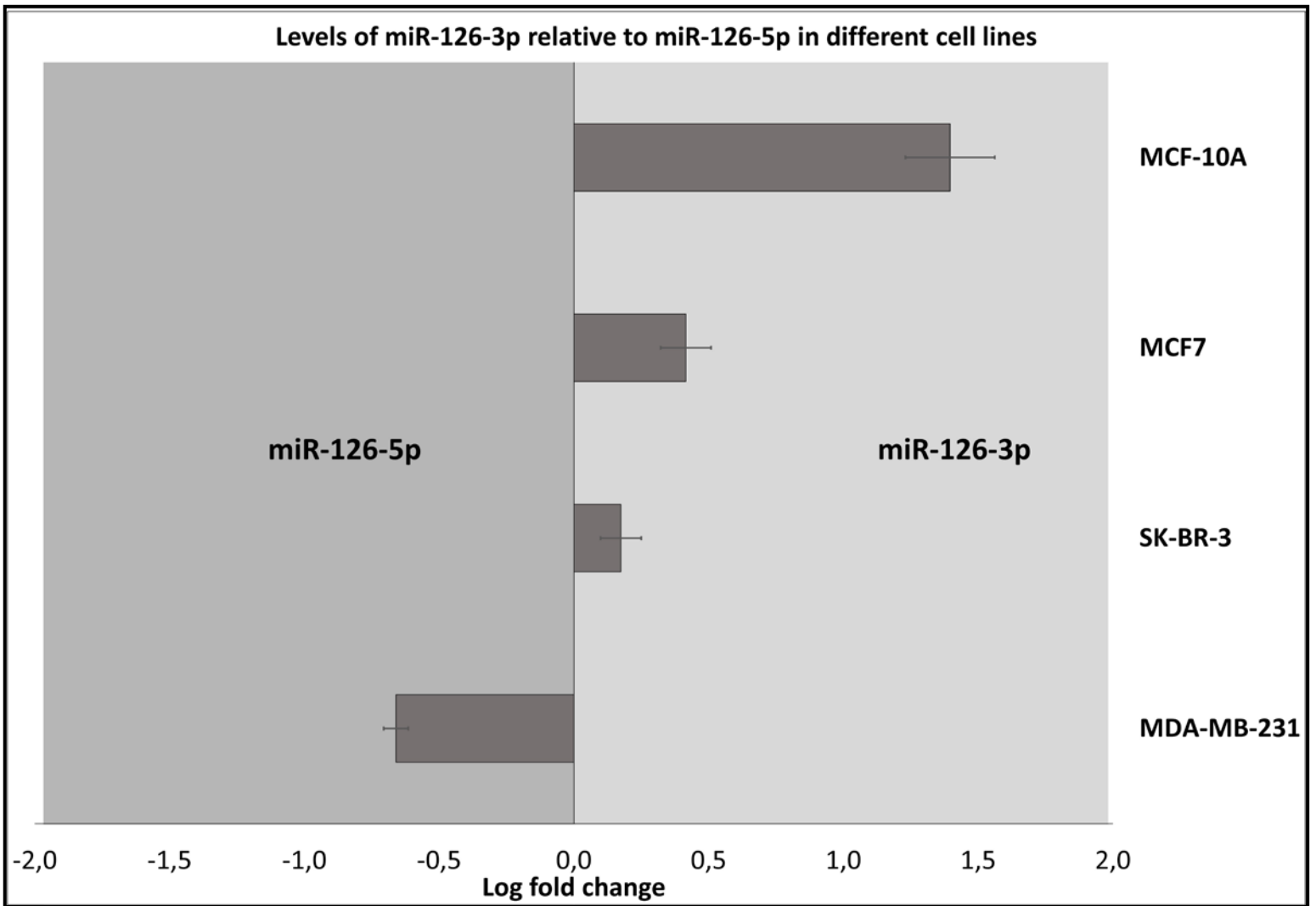


Fig. 2 – Expression pattern. The relative expression pattern between miR-126-3p and miR-126-5p in different breast cell lines. Based on RT-qPCR data, the relationship between miR-126-3p and miR-126-5p was studied in the non-cancerous breast cell line MCF-10A, the ER+ BC cell line MCF7, the HER2+ BC cell line SK-BR-3 and the TN BC cell line MDA-MB-231. Data are displayed as mean log fold change \pm SE from a representative biological replicate.

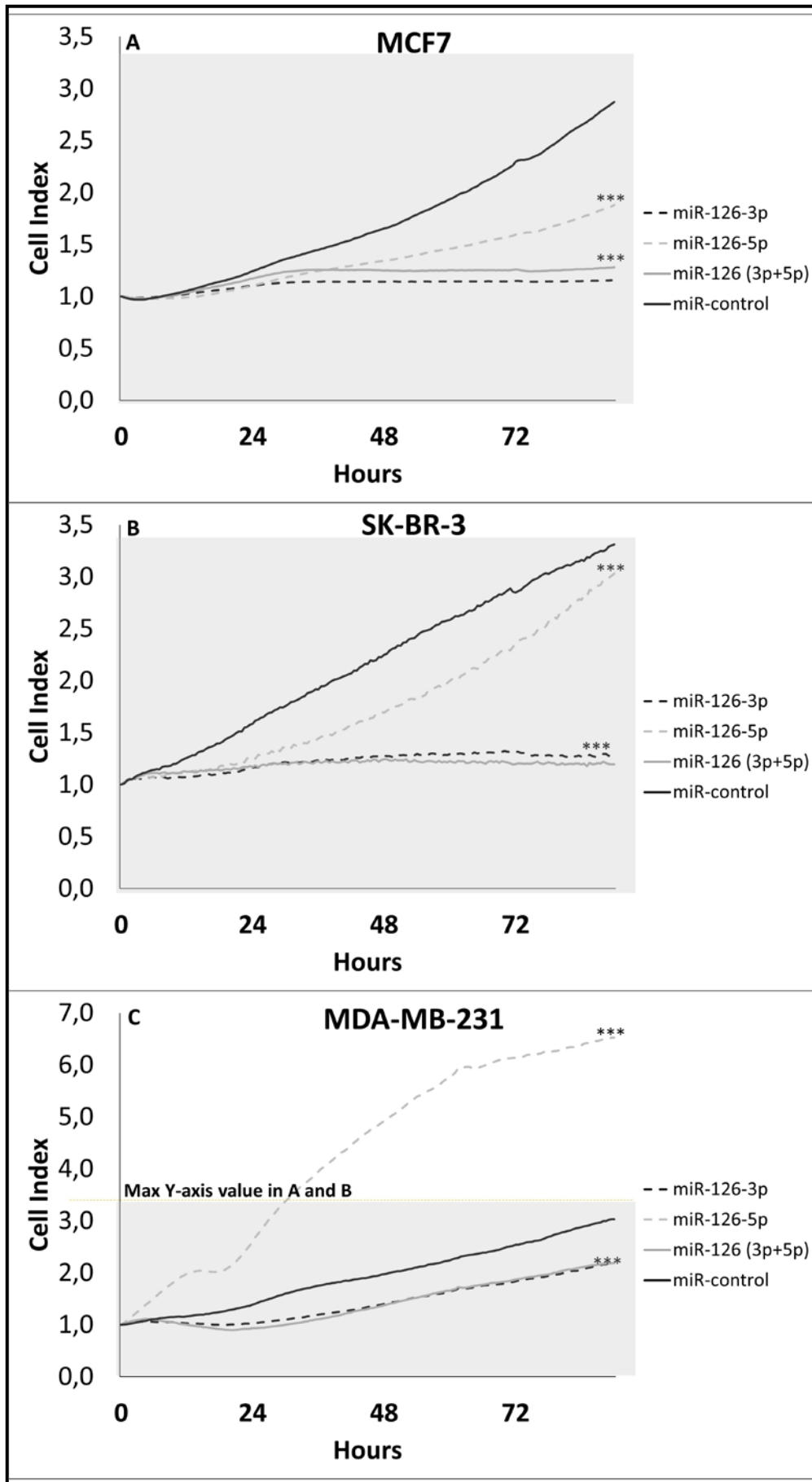


Fig. 3 - Proliferation. Experimental study on BC cell lines transfected with miR-126 performed in real-time using the xCelligence system. Proliferation in different BC cell lines after transfection with either miR-126-3p mimic, miR-126-p mimic or mimics 3p+5p in combination and equal concentration. Proliferation was assessed for the ER+ BC cell line MCF7 (A), the HER2+ BC cell line SK-BR-3 (B) and the TN BC cell line MDA-MB-231. Results are representative for all biological replicate, and each experiment includes four technical replicates. The annotation *** signifies $P < 0.001$ with one-way ANOVA and the Benjamini & Hochberg correction comparing different transfections to controls.

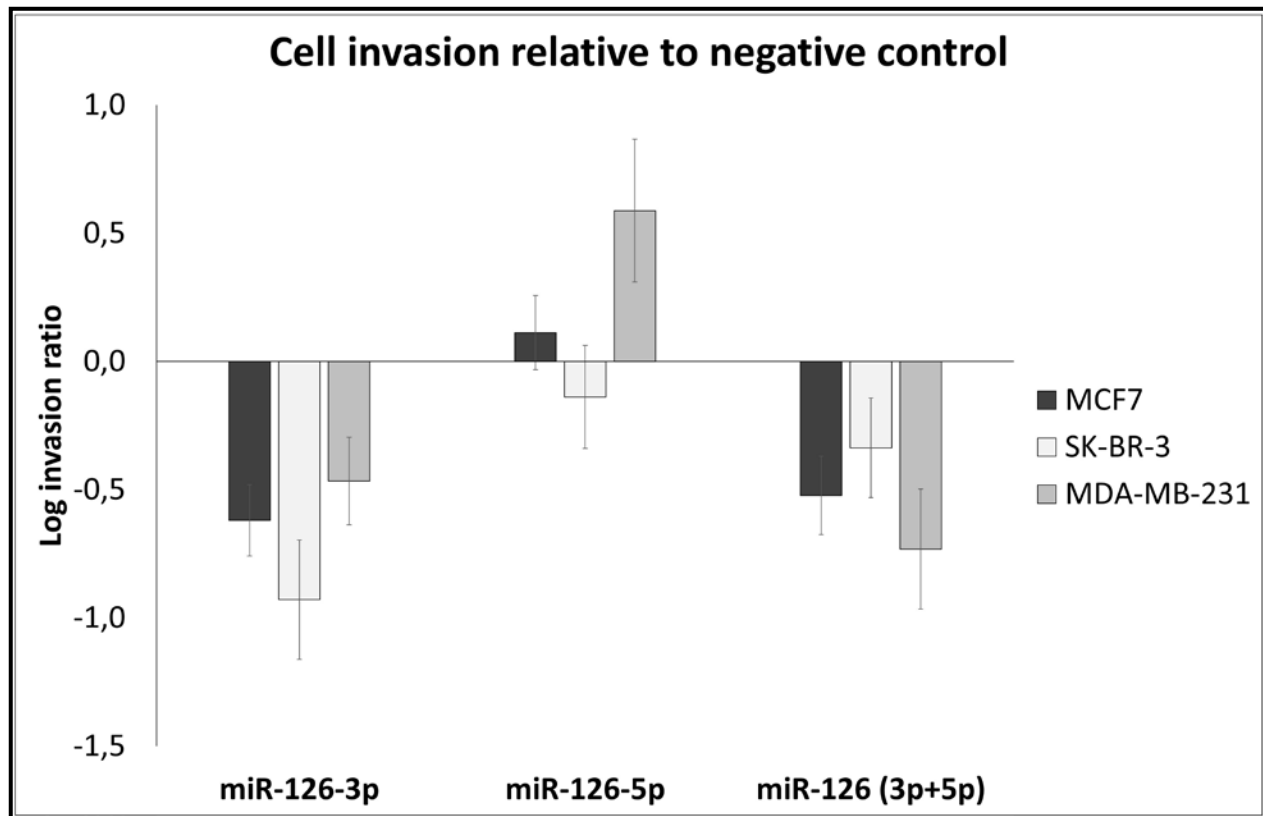


Fig. 4 – Invasion. Experimental study on invasion to assess the invasion potential in BC cell lines transfected with miR-126 performed using a Boyden chamber assay coated with a basement membrane matrix. BC cell lines transfected with either miR-126-3p, miR-126-5p or miR-126-3p + miR-126-5p in equal concentrations, were seeded in the upper wells of a modified Boyden chamber assay. Cells were allowed to invade, and migrate through, the basement membrane towards the bottom chamber containing bovine serum as a chemoattractant. Results are displayed as mean log fold change \pm SD of miR-126 transfected cells relative to miR-control transfected cells. Data presented are from a representative biological experiment, which include four technical replicates for each cell line.

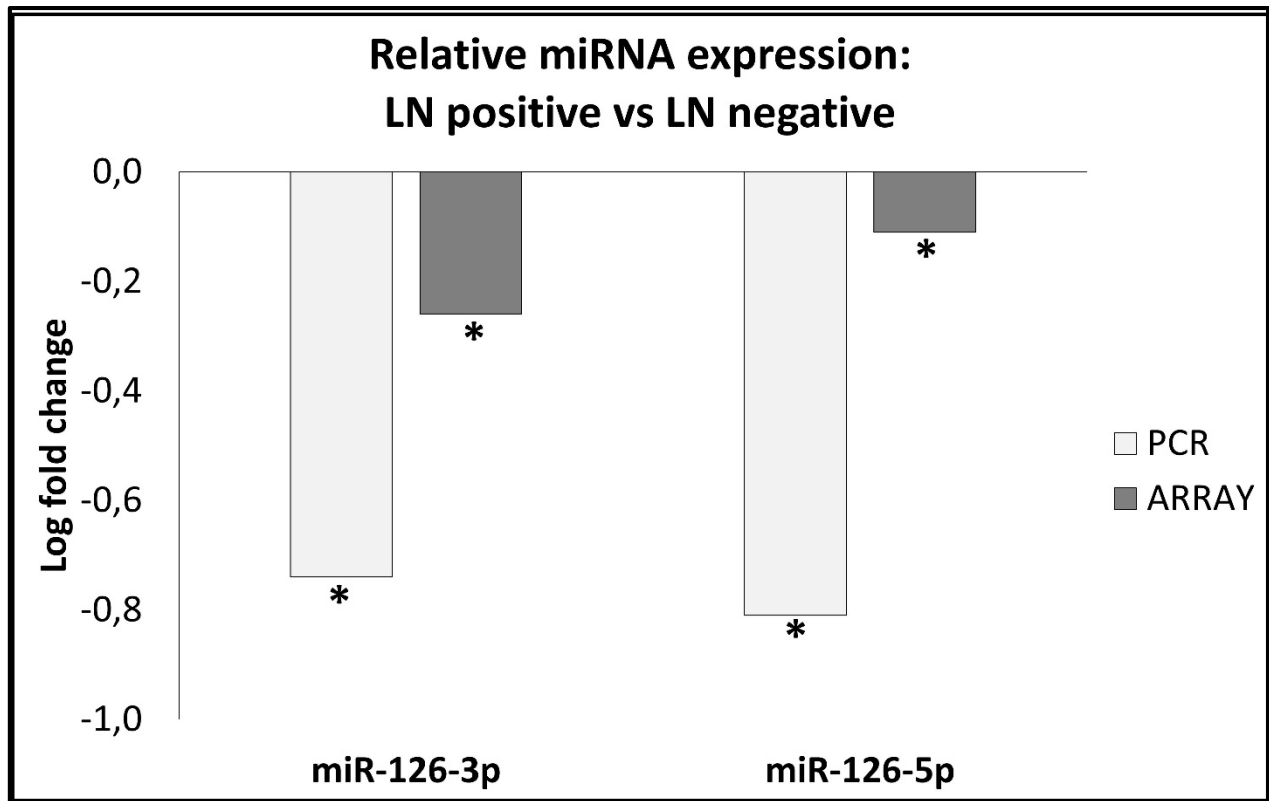


Fig. 5 – Nodal involvement. Differential expression of miR-126-3p and miR-126-5p in cancer patients with nodal involvement compared to patients with no nodal involvement. Results are displayed for both the miRNA microarray and the qPCR validation. Data are displayed as log fold change of nodal involvement vs no nodal involvement, and the annotation * signifies P<0.05.

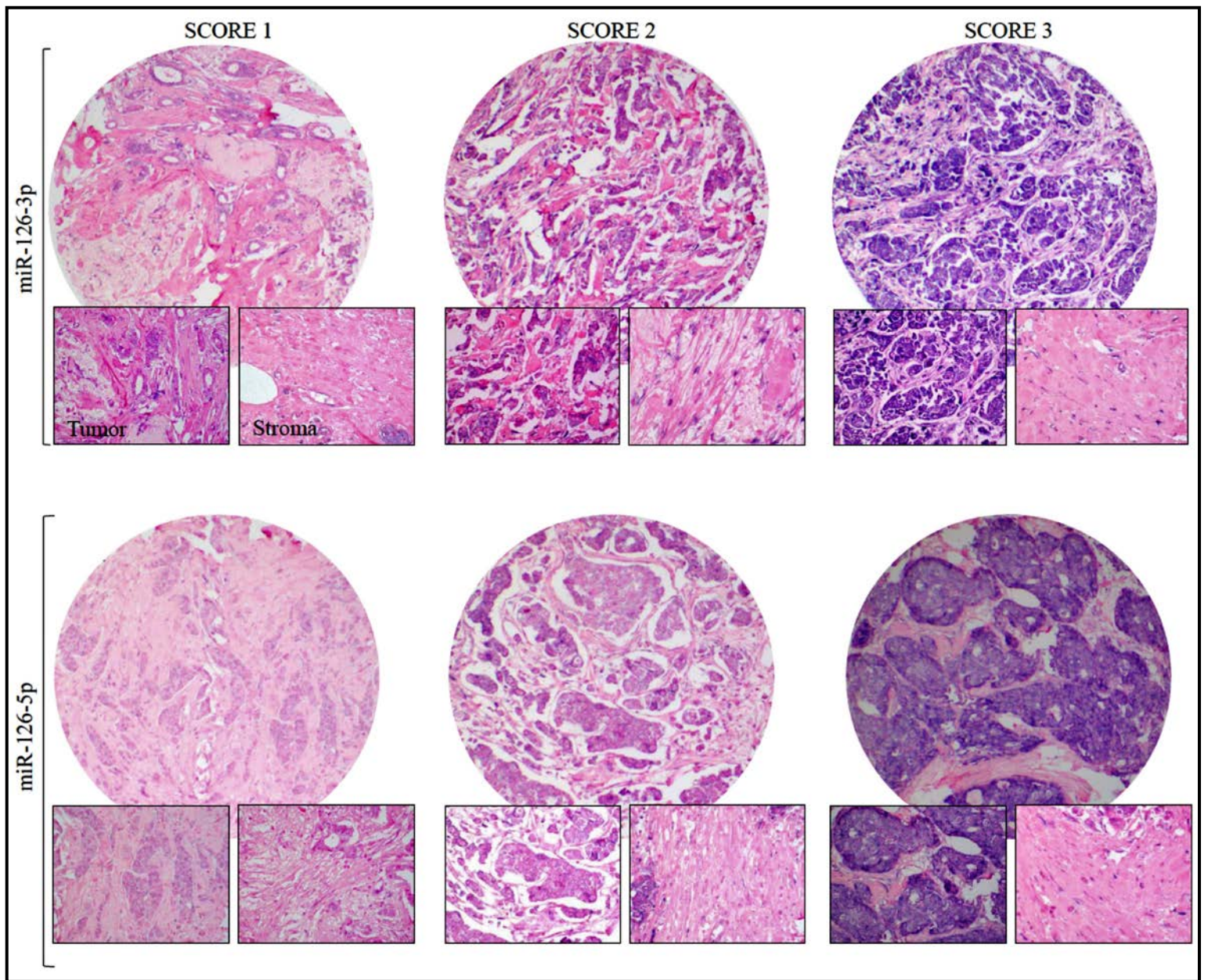


Fig. 6 – Intensities of ISH staining. The *in situ* hybridization staining intensities for miR-126-3p and miR-126-5p in TMA samples. TMA scores were analyzed in both tumor and stroma

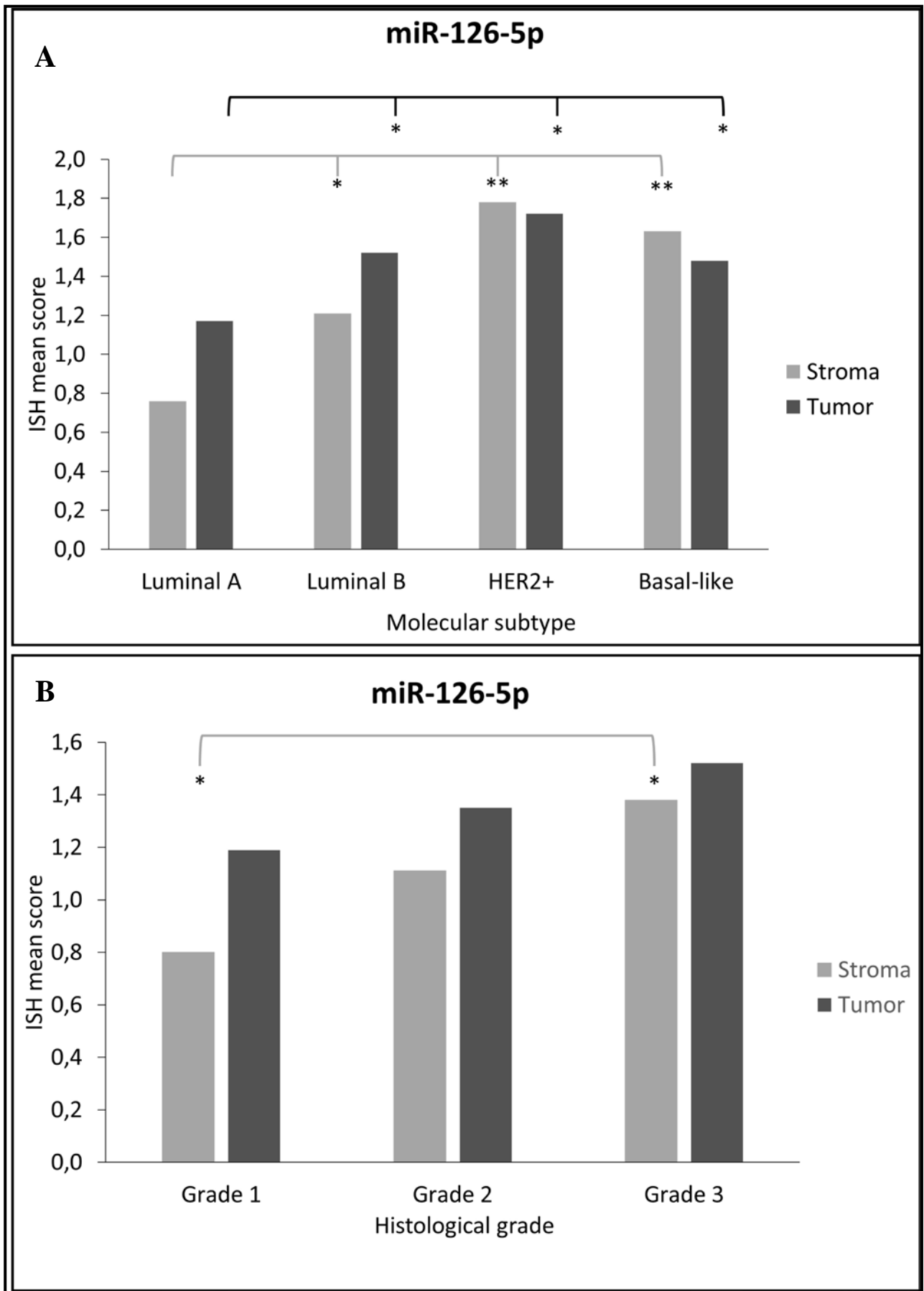


Fig. 7 – TMA subgroup analysis. Differential expression of miR-126-5p in TMA samples for tumor and stroma. Mean value of TMA-scoring stratified into molecular subtype (A) and histological grade (B). The annotation * and ** signifies $P < 0.05$ and $P < 0.01$, respectively.

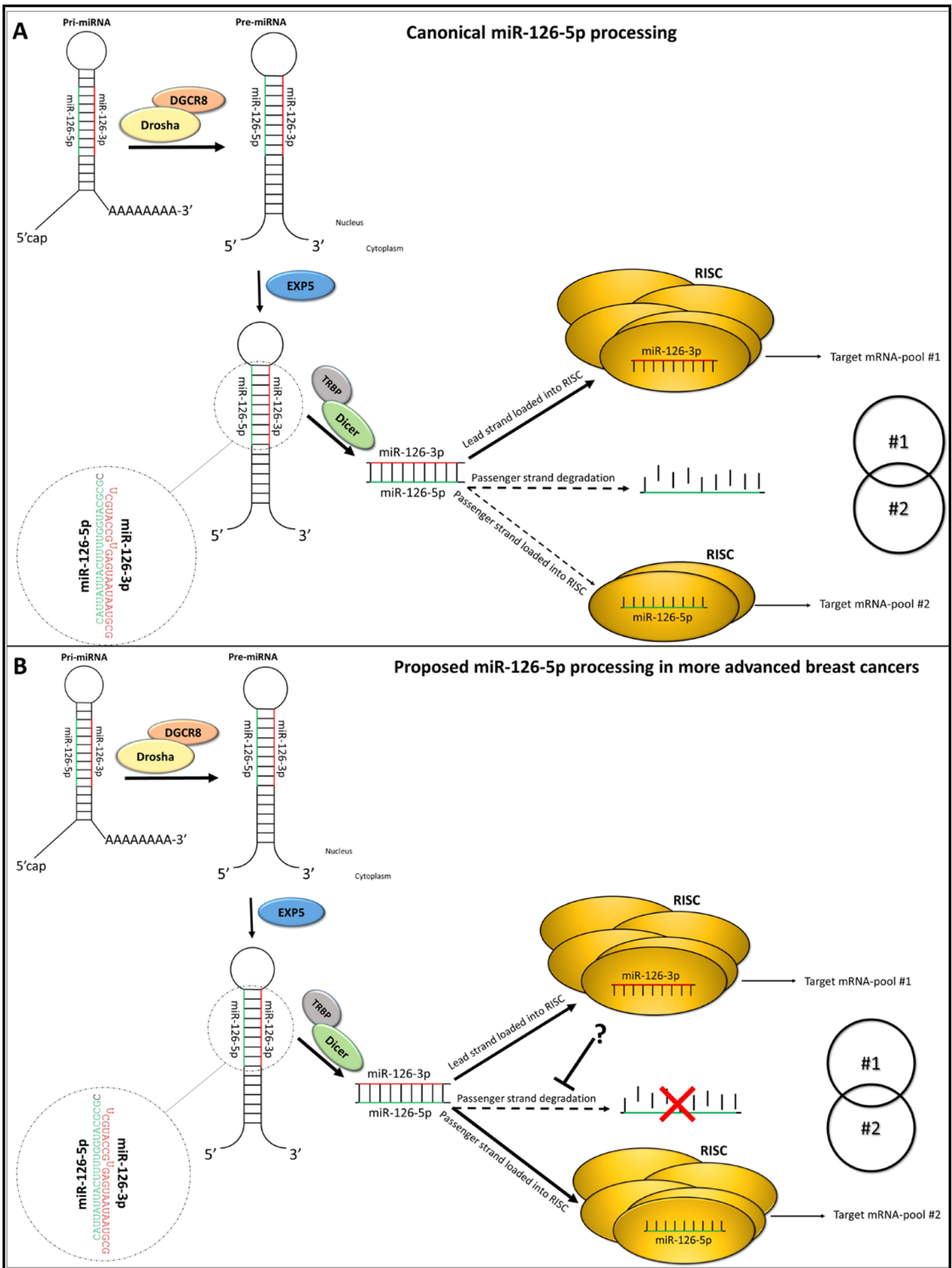


Fig. 8 – miR-126-5p processing in more advanced BC. Canonical processing of miR-126-5p (A), and our proposed miR-126-5p processing in more advanced cancer (B).

Paper III

SCIENTIFIC REPORTS



OPEN

A gender specific improved survival related to stromal miR-143 and miR-145 expression in non-small cell lung cancer

Kaja Skjefstad¹, Charles Johannessen¹, Thea Grindstad¹, Thomas Kilvaer^{2,3}, Erna-Elise Paulsen^{2,3}, Mona Pedersen², Tom Donnem^{2,3}, Sigve Andersen^{2,3}, Roy Bremnes^{2,3}, Elin Richardsen^{1,4}, Samer Al-Saad^{1,4} & Lill-Tove Busund^{1,4}

Micro RNAs (miRNA) are small non-coding RNAs that post-transcriptionally regulate gene expression. Dysregulation of miRNA cluster 143/145 has been reported in several malignancies, but their role in non-small cell lung cancer (NSCLC) remains elusive. This study investigates the prognostic impact of miR-143 and miR-145 in primary tumors and metastatic lymph nodes in NSCLC tissue. Tissue from 553 primary tumors and 143 matched metastatic lymph nodes were collected and tissue microarrays were constructed. *In situ* hybridization was used to evaluate miR-143 and miR-145 expression in tumor epithelial cells and stromal cells in the primary tumors and lymph nodes. *In vivo* data was supplemented with functional studies of cell lines *in vitro* to evaluate the role of miR-143 and miR-145 in NSCLC tumorigenesis. In our cohort, stromal miR-143 (S-miR-143) and miR-145 (S-miR-145) expression in primary tumor tissue were independent prognosticators of improved disease-specific survival (DSS) in female (S-miR-143, HR: 0.53, $p = 0.019$) and male patients (S-miR-145, HR: 0.58, $p = 0.021$), respectively. Interesting correlations between the miR cluster 143/145 and previously investigated steroid hormone receptors from the same cohort were identified, substantiating their gender dependent significance.

Lung cancer remains the leading cancer killer in the world with more than 1.6 million estimated annual deaths, worldwide¹. The predominant histological subtype, non-small cell lung cancer (NSCLC), accounts for 85% of cases and can be further divided into subgroups according to the recent WHO classification; the most frequent being adenocarcinoma and squamous cell carcinoma². Surgical resection is the main curative treatment modality for NSCLC, but unfortunately, the majority of patients are diagnosed in advanced stages and thus not eligible for surgery. Despite development in surgical techniques, diagnostic technologies and the implementation of biologic treatment including immunotherapy, the 5-year survival remains depressing at only 18%³. To optimize therapy and improve the overall survival, it is pivotal to uncover better prognostic and predictive molecular markers.

microRNAs (miRNAs) are small non-coding RNA elements important in various biological processes, including tumorigenesis⁴. They negatively regulate protein translation by binding to the 3'UTR of target messenger RNAs (mRNAs) leading to mRNA degradation or suppression of translation⁵. miRNA expression correlates with biological and clinical characteristics of tumors; differentiation, aggression, tissue type and therapy response⁶. Further, "miRNA replacement therapy" provides a novel treatment opportunity by reintroducing downregulated miRNA into cancer cells⁷. A phase I clinical trial of miRNA replacement therapy in thoracic cancers, based on the miR-15/107 group of miRNAs, was recently completed with promising results⁸.

miR cluster 143/145 consists of two miRNAs, miR-143 and miR-145, transcribed from a gene cluster on chromosome 5. It regulates multiple genes involved in cancer cell growth, including well-established cancer related hormone receptors such as ER α , and is generally regarded as a tumor suppressor^{9–11}. Reports have indicated a

¹Department of Medical Biology, UiT The Arctic University of Norway, Mailbox 6050 Langnes, N-9037, Tromsø, Norway. ²Department of Clinical Medicine, UiT The Arctic University of Norway, Mailbox 6050 Langnes, N-9037, Tromsø, Norway. ³Department of Oncology, University Hospital of North Norway, Mailbox 13, N-9038, Tromsø, Norway. ⁴Department of Clinical Pathology, University Hospital of North Norway, Mailbox 46, N-9038, Tromsø, Norway. Correspondence and requests for materials should be addressed to K.S. (email: kaja.skjefstad@gmail.com)

possible prognostic role in non-small cell lung cancer^{12,13}. The presented study investigates the prevalence and prognostic significance of miR-143 and miR-145 in NSCLC. The utilization of *in situ* hybridization allow both localization of expression according to cell-type and sub-cellular compartment. Further, correlations with steroid hormone receptors progesterone receptor (PR), estrogen receptor alpha (ER α), estrogen receptor beta (ER β) and aromatase enzyme (AR), previously investigated by our group, were explored. The clinicopathological findings were supplied with data from functional *in vitro* studies.

Materials and Methods

Patients. NSCLC patients who underwent radical resection at the Nordland Central Hospital and the University Hospital of North Norway from 1990 to 2011, were retrospectively included in this study. Six-hundred-and-thirty-three patients were identified from the hospital records. Of these, 80 patients were excluded due to (1) inadequate fixation of paraffin-embedded tissue blocks (n = 26), (2) radiotherapy or chemotherapy prior to surgery (n = 15), (3) other malignancy within 5 years ahead of an NSCLC diagnosis (n = 39), leaving 553 patients eligible for inclusion. One-hundred-and-seventy-two of the included patients had confirmed metastatic lymph node tissue disease (LN+). Of these, 143 patients had lymph node specimens available for analysis. The eight edition of the International Union Against Cancer TNM classification was used to re-stage all patients, and the tumors were histologically re-classified according to the 2015 World Health Organization Classification of Lung Tumors^{2,14}. Follow-up data as of October 1st 2013.

Tissue microarray construction. All specimens were embedded in paraffin blocks and examined by two experienced pathologists. Detailed methodology regarding TMA construction has previously been published¹⁵. Briefly, (1) representative areas of stromal and tumor tissue in primary tumors and tumor tissue from lymph nodes were identified and sampled with a 0.6 mm stylet, (2) transferred to the recipient TMA block and (3) cut into 4 μ m sections with a Micron microtome (HM355S) prior to *in situ* hybridization. Normal lung tissue far from the site of the tumor, and lung tissue samples from 20 emphysema patients without any history of neoplastic disease, were used as controls and for comparing biomarker expression level in malignant vs non-malignant tissue.

***In situ* hybridization (ISH).** miR-143 and miR-145 expression was analyzed by *in situ* hybridization (ISH) using the Ventana Discovery Ultra (Ventana Medical Inc, Arizona, USA). Optimization of biomarker detection included: RNA degradation prevention, testing of reagent concentration for the tissue of interest and detection method, and testing of hybridization temperatures for each probe with RNA Tm (melting temperature) as guideline. Digoxigenin (DIG) labeled lock nucleic acid (LNA) probes for miR-145-5p (hsa-miR-145, Prod. No. 88068-15, concentration: 2.5 nM), miR-143-3p (hsa-miR-143, Prod. No. 38515-15, concentration: 10 nM), negative control (Scramble miR, Prod. No. 99004-15, concentration: 10 nM) and positive control (U6 has/mmu/rno, Prod. No. 99002-15, concentration: 0.5 nM) were used in this study. Exiqon validated the LNATM miR probes by CE (Capillary Electrophoresis) or HPLC (High-Performance Liquid Chromatography) and confirmed identity of compound by MS (Mass Spectrometry). A TMA multi organ block was used as positive and negative tissue controls.

4 μ m TMA sections were incubated overnight at 60 °C to attach tissue to Super Frost Plus slides. To ensure good distribution of reagents and protect sections from desiccation, LCS (Liquid Coverslip oil, Roche, 5264839001) was added. Deparaffinization was performed in EZ Prep buffer (Roche 5279755001) at 68 °C (3 \times 12 min). Demasking was done at 95 °C with CC1 buffer (Roche, 6414575001) for 40 minutes. Subsequently, sections were rinsed with Reaction Buffer (Roche 5353955001) and RiboWash, SSPE buffer (Roche 5266262001).

All slides were denaturated for 8 min. at 90 °C. Hybridization with probes was performed for 60 min at 54 °C for miR-145, 55 °C for miR-143, 57 °C for scramble miR and 55 °C for U6. Stringent wash procedures were done at 2 \times 8 min with 2.0X RiboWash, SSPE buffer with the same temperatures as used under hybridization for each probe. Blocking against unspecific bindings followed, with blocking solution (Roche, 5268869001) for 16 min. at 37 °C. Alkaline phosphatase (AP)-conjugated anti DIG (Anti-DIG-AP Multimer, Roche 07256302001) was incubated for 20 min. at 37 °C for immunologic detection. After rinsing, substrate enzymatic reactions were carried out with NBT/BCIP (CromoMap Blue kit, Roche 526661001) for 60 min at 37 °C, to give a blue precipitate to detect the microRNA. Sections were again rinsed and counterstained in 4 min with Red Stain II (Roche 5272017001). Increasing gradients of ethanol solutions was used for dehydration. Finally, all sections were mounted using the Histokitt mounting medium (Assistant-Histokitt, 1025/250 Sondheim/Rhoen Germany).

Scoring of ISH. All tissue samples were independently and semi-quantitatively scored by an experienced pathologist (SAS) and a trained medical doctor (KS). Biomarkers were evaluated by intensity in neoplastic epithelial cells and stromal cells; 0 (no staining), 1 (weak), 2 (intermediate) and 3 (strong) and density in stromal cells; 0 = absent, 1 = 1–5%, 2 = 6–50%, 3 = >50%. Due to homogenous staining in neoplastic epithelial cells, scoring of biomarker density was not deemed necessary. For stromal biomarker expression (S-miR) the mean value of intensity and density combined, was calculated. Staining of fibroblasts, fibrocytes, lymphocytes, smooth muscle cells (SMC) and endothelial cells in blood and lymph vessels were included while scoring tumor stroma. Striking positivity was noted in endothelial cells lining the blood vessels and SMCs, including the smallest capillaries. Each variable was dichotomized for survival analyses based on a minimal p-value approach. A high score was defined as a score \geq mean value for stromal-miR-143 (S-miR-143, mean value: 1.87) and tumor-miR-143 (T-miR-143, mean value: 1.98) and >0 for S-miR-145 and T-miR-145. The same scoring approach was used in PT, LN+, positive and negative tissue controls. For LN+ however, the stromal compartment was not scored due to large numbers of excessively stained lymphocytes. In normal lung tissue from NSCLC patients, collected far from the site of the tumor, miR-143 was prominently expressed in type 2 pneumocytes and macrophages. Collagen and

endothelial cells lining the alveolar wall were mostly negative. miR-145 expression was observed in a few pneumocytes type I, while most were negative. Staining in macrophages was predominantly negative.

Functional studies. Cell cultures. Four lung cancer cell lines were used: the adenocarcinoma cell line A549 (ATCC[®] CCL-185[™]), the squamous cell carcinoma cell line H520 (ATCC[®] HTB182[™]), and the two large cell carcinoma cell lines H460 (ATCC[®] HTB-177[™]) and H661 (ATCC[®] HTB183[™]). All cells were cultured in RPMI-1640 media (# R8758, Sigma-Aldrich, St. Louis, USA) supplemented with 10% fetal bovine serum (# S0415, Biochrom, Berlin, Germany) and 1x penicillin-streptomycin antibiotic mixture (# P0781, Sigma-Aldrich, St. Louis, USA) and incubated at 37 °C in 5% CO₂ humidified atmosphere.

Cell transfection. Cells were transiently transfected with either 100 nM has-miR-143-3p Pre-miR[™] miRNA Precursor (catalog# PM10883, Thermo Fisher Scientific, USA) and/or 100 nM has-miR-145-5p Pre-miR[™] miRNA Precursor (catalog# PM11480, Thermo Fisher Scientific, USA), alongside the Cy3[™] Dye-Labeled Pre-miR Negative Control #1 (catalog# AM17120, Thermo Fisher Scientific, USA) using the transfection reagent Lipofectamine[®] 2000 (catalog# 11668-019, Life Technologies, Waltham, USA). Transfected Cy3[™] Dye-Labeled Pre-miR Negative Control emits fluorescent light when exposed to UV-light, and using a fluorescence microscope, the transfection efficiency was evaluated to be 80–95%.

Total RNA isolation. Total RNA from the cells were isolated using the miRNeasy Mini Kit (cat.# 217004, Qiagen, Hilden, Germany). First, 700 µl QIAzol lysis reagent was used to lyse the cells before homogenization and a 5 minute incubation at room temperature. Second, 140 µl chloroform was added, samples shaken, and then incubated for 3 minutes at room temperature. Third, samples were centrifuged at 12000 G for 15 minutes at 4 °C before the upper aqueous phase was transferred and mixed with 100% ethanol. Finally, the samples were transferred to the RNeasy[®] Mini column and washed in several steps before elution with 50 µl ddH₂O. Samples were stored at –70 °C.

cDNA synthesis. For the first strand cDNA synthesis, the miScript II RT Kit (cat.# 218160, Qiagen, Hilden, Germany) was used. First, 100 ng total RNA was mixed with 4 µl 5X miScript HiSpec buffer, 2 µl 10X Nucleic mix, 2 µl miScript reverse transcriptase mix, and RNase-free water to a final volume of 20 µl. Second, samples were incubated for 1 hour at 37 °C, and then incubated at 95 °C for 5 minutes. Finally, all samples were diluted to a total volume of 200 µl using RNase-free water, and stored at –70 °C.

RT-PCR. Endogenous levels of miR-143 and miR-145 in the cancer cells were quantified relative to the non-cancerous lung cell line NL20 (ATCC[®] CRL-2503[™]), and normalized to the stably expressed reference snRNA RNU6 using real-time PCR and the miScript SYBR[®] Green PCR Kit (catalog# 218073, Qiagen, Hilden, Germany). Primers were miScript Primer Assays Hs_miR-143_1 miScript Primer Assay (catalog# MS00003514, Qiagen, Hilden, Germany), Hs_miR-145_1 miScript Primer Assay (catalog# MS00003528, Qiagen, Hilden, Germany) and Hs_RNU6-2_11 miScript Primer Assay (catalog# MS00033740, Qiagen, Hilden, Germany), according to the manufacturers protocol. In short, a total volume of 25 µl/well in a 96-well plate included 1 µl cDNA mixed with 12.5 µl 2x QuantiTect SYBR Green PCR Master Mix, 2.5 µl 10x miScript Universal Primer, 2.5 µl 10x miScript Primer Assay, and 6.5 µl RNase-free Water. The plate was sealed and centrifuged for 1 minute at 1000 G before it was placed in the 7300 Real-Time PCR System (Thermo Fisher Scientific, Waltham, Massachusetts, USA). Each sample was analyzed in quadruplicates, and two independent experiments were performed.

Proliferation assay. The ability of cancer cells to proliferate was evaluated using the real-time cell analyzer xCELLigence, RTCA DP (catalog#05469759001, ACEA Biosciences, San Diego, USA) fitted with the E-plate 16 (catalog#05469830001, ACEA Biosciences, San Diego, USA). Prior to seeding, cells were trypsinized until detached, resuspended in complete growth media, and counted. In accordance with the manufacturer protocol, cells were seeded in quadruplicates into an E-plate after baseline measurements. The E-plate containing cells was positioned in the RTCA DP instrument, located in an incubator preserving the same conditions as used for routine cultivation of cell lines. The cell index was automatically measured every 30 minutes throughout the experiment duration. Growth curves were calculated with the RTCA software version 1.2.1. A minimum of three independent experiments were performed for each cell line.

Migration assay. The ability of cancer cells to migrate was assessed using ibidi[™] culture inserts (ibidi GmbH, Planegg, Germany). The inserts consist of two 0.22 cm² silicone chambers separated by a 0.5 mm divider. The inserts were positioned into a 12-well tissue culture dish, one insert per well. Roughly 70 µl pre-transfected cell-suspension containing 4–6 × 10⁵ cells/ml were added to each chamber. The cells were left to adhere for 24 hours before the insert was removed and images acquired across the cell-free zone at time points 0 hours and 20 hours. The migration potential into the 0.5 mm gap was calculated using the free online software TScratch, version 1.0 (CSElab, Computational Science and Engineering Laboratory, Switzerland). Initially, the functional experiments for this study were designed using three cell lines; the large cell carcinoma cell line H460, the squamous cell carcinoma cell line H520, and the adenocarcinoma cell line A549. In our experiments, however, the cell lines H460 and H520 did not exhibit migrational properties, leaving only the A549 cell line representing the migration experiment. To strengthen our results, we therefor included the large cell carcinoma cell line H661 in the migration study.

	Overall cohort				Female patients				Male patients			
	N(%)	5 year DSS (%)	Median DSS (mo)	p	N(%)	5 year DSS (%)	Median DSS (mo)	p	N(%)	5 year DSS (%)	Median DSS (mo)	p
Age				0.656				0.637				0.827
≤65	234 (42.3)	58	127		77 (42.8)	62	190		157 (42.1)	56	98	
>65	319 (57.7)	58	NR		103 (57.2)	65	NR		216 (57.9)	44	88	
Sex				0.025								
Female	180 (32.5)	64	190									
Male	373 (67.5)	55	91									
ECOG perf. status				0.009				0.400				0.020
0	324 (58.6)	63	235		112 (62.2)	67	NR		212 (56.8)	60	235	
1	191 (34.5)	52	71		56 (31.1)	60	127		135 (36.2)	48	51	
2	38 (6.9)	52	NR		12 (6.7)	55	NR		26 (7.0)	50	NR	
Smoking				0.069				0.732				0.060
Never	21 (3.8)	50	21		11 (6.1)	64	189		10 (2.7)	33	18	
Present	350 (63.3)	62	235		115 (63.9)	67	NR		235 (63.0)	59	235	
Previous	182 (32.9)	52	84		54 (30.0)	58	NR		128 (34.3)	49	57	
Weightloss				0.971				0.603				0.637
<10%	498 (90.1)	58	190		163 (90.6)	63	190		335 (89.8)	56	91	
≥10%	55 (9.9)	59	NR		17 (9.4)	68	NR		38 (10.2)	54	98	
Surgical procedure				<0.001				0.024				<0.001
Wedge/Lobectomy	411 (74.3)	64	235		148 (82.2)	68	190		263 (70.5)	61	235	
Pulmonectomy	142 (25.7)	42	30		32 (17.8)	42	37		110 (29.5)	42	29	
Margins				0.105				0.088				0.431
Free	506 (91.5)	59	190		166 (92.2)	65	190		340 (91.2)	56	98	
Not free	47 (8.5)	47	57		14 (7.8)	51	64		33 (8.8)	45	47	
Tstage				<0.001				0.009				<0.001
1a	14 (2.5)	93	NR		5 (2.8)	100	NR		9 (2.4)	89	NR	
1b	71 (12.8)	79	NR		30 (16.7)	82	NR		41 (11.0)	77	NR	
1c	95 (17.2)	64	190		33 (18.3)	66	NR		62 (16.6)	63	235	
2a	135 (24.4)	57	88		35 (19.4)	65	NR		100 (26.8)	54	83	
2b	73 (13.2)	48	47		28 (15.6)	60	NR		45 (12.1)	40	40	
3	104 (18.8)	56	NR		36 (20.0)	60	NR		68 (18.2)	54	98	
4	61 (11.1)	31	21		13 (7.2)	23	NR		48 (12.9)	36	19	
Nstage				<0.001				<0.001				<0.001
0	379 (68.5)	70	235		132 (73.3)	74	NR		247 (66.2)	67	235	
1	118 (21.3)	36	35		23 (12.8)	42	47		95 (25.5)	35	27	
2	56 (10.2)	23	21		25 (13.9)	30	35		31 (8.3)	16	15	
Pathological stage				<0.001				<0.001				<0.001
I	232 (42.0)	74	235		78 (43.3)	81	NR		154 (41.3)	70	235	
II	185 (33.4)	59	114		61 (33.9)	66	NR		124 (33.2)	56	91	
IIIA + B	136 (24.6)	28	21		41 (22.8)	29	36		95 (25.5)	27	17	
Histology				0.241				0.431				0.125
SQCC	307 (55.5)	64	235		77 (42.8)	71	NR		230 (61.7)	61	235	
ADC	239 (43.2)	52	73		100 (55.6)	59	190		139 (37.3)	46	57	
Other ^a	7 (1.3)	67	NR		3 (1.6)	50	11		4 (1.0)	75	NR	
Vascular infiltration				<0.001				0.040				<0.001
No	453 (82.0)	62	235		136 (75.6)	68	190		317 (85.0)	60	235	
Yes	97 (17.5)	38	35		42 (23.3)	49	47		55 (14.7)	25	22	
Missing	(0.5)				2 (1.1)				1 (0.3)			

Table 1. Clinical and pathological variables as predictors of disease-specific survival (DSS) in NSCLC patients (univariate analyses; log-rank test; N = 553, 180 and 373, respectively).

Statistical methods. The statistical package IBM SPSS (version 24 IBM Corp., Armonk, NY USA) was used to perform all statistical analyses.

Interobserver reliability between scorers was assessed by a two-way random effects model with absolute agreement definition. Associations between marker expression, and marker expression and

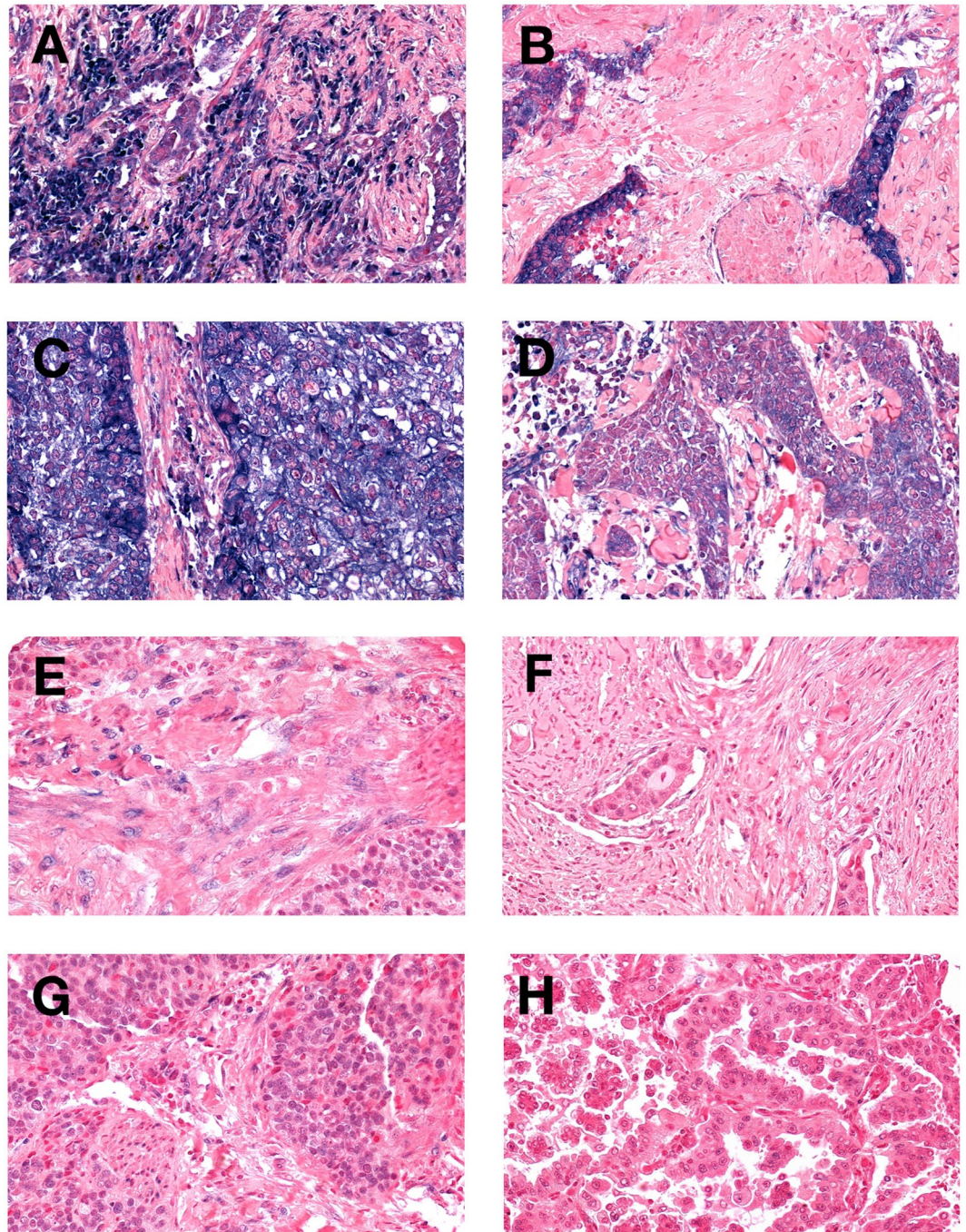


Figure 1. *In situ* hybridization staining of miR-143 and miR-145 in NSCLC. High miR-143 expression: Panel (A) stromal cells, Panel (C) tumor cells. Low miR-143 expression: Panel (B) stromal cells, Panel (D) cancer cells. High miR-145 expression: Panel (E) stromal cells, Panel (G) cancer cells. Low miR-145 expression: Panel (F) stromal cells, Panel (H) cancer cells. 400× magnification.

clinicopathological parameters, were examined by Spearman's rank correlation and χ^2 test or Fisher's exact. Wilcoxon non-parametrical test was used to assess the difference in biomarker expression between lung tumor tissue and non-malignant lung tissue. Statistical significance between proliferation curves was assessed by one-way ANOVA. The Kaplan-Meier method was used to visualize association between marker expression and disease-specific survival (DSS) and the statistical significance between survival curves was tested using the log-rank test. DSS was defined as the time from surgery to lung cancer death. Variables with significant p-values from the univariate analyses were entered into Cox proportional Hazard models. The final models were derived from a backward conditional method with probability for stepwise entry and removal at 0,05 and 0,10.

	Overall cohort				Female patients				Male patients			
	N (%)	5 year (%)	Median (mo)	p	N (%)	5 year (%)	Median (mo)	p	N (%)	5 year (%)	Median (mo)	p
S-miR-143				0.075				0.011				0.589
Low	261 (47.2)	55	104		88 (48.9)	55	127		173 (46.4)	55	104	
High	261 (47.2)	62	235		83 (46.1)	73	190		178 (47.7)	56	98	
Missing	31 (5.6)				9 (5.0)				22 (5.9)			
T-miR-143				0.071				0.699				0.160
Low	198 (35.7)	63	NR		64 (35.6)	65	NR		134 (35.9)	62	NR	
High	320 (58.0)	55	114		106 (58.9)	62	190		214 (57.4)	52	71	
Missing	35 (6.3)				10 (5.5)				25 (6.7)			
S-miR-145				0.130				0.602				0.013
Low	61 (11.1)	46	45		20 (11.1)	63	NR		41 (11.0)	38	32	
High	462 (83.5)	60	190		150 (83.3)	63	190		312 (83.6)	58	235	
Missing	30 (5.4)				10 (5.6)				20 (5.4)			
T-miR-145				0.111				0.068				0.592
Low	69 (12.5)	66	NR		26 (14.4)	76	NR		43 (11.5)	59	NR	
High	432 (78.1)	57	114		139 (77.2)	60	190		293 (78.6)	56	98	
Missing	52 (9.4)				15 (8.4)				37 (9.9)			
S-miR-143/S-miR-145				0.007				0.345				0.004
Low ^a	32 (5.8)	34	32		11 (6.1)	44	45		21 (5.6)	29	21	
High ^b	482 (87.2)	60	190		158 (87.8)	64	190		324 (86.9)	57	114	
Missing	39 (7.0)				11 (6.1)				28 (7.5)			

Table 2. Prognostic Effect of intraepithelial (T) and stromal (S) miR-143 and miR-145 expression in Primary Tumors on Disease-Specific Survival (Univariate Analyses; Log-Rank Test, N = 553, 180 and 373, respectively). Note: Bold numbers indicate $p < 0.05$. Abbreviations: S-miR, stromal miR expression. T-miR, tumor epithelial expression. N, number. NR, not reached. Mo, months. ^aLow: low S/low S. ^bHigh: high S/high S, high S/low S, low S/high.

Ethics. The Regional Committee for Medical and Health Research Ethics (REK Nord), alongside the Norwegian Data Protection have approved this study (protocol ID: 2011/2503). Due to the retrospective study design, the majority of patients were diseased and the tissue specimens over 10 years old. Thus, written patient consent was not deemed necessary by REK Nord. All patients were anonymously included in the database. A trial number for each patient was used when pairing clinical information with the respective patients. Clinical information was reported according to the REMARK guidelines¹⁶. The authors confirm that all experiments were performed in accordance with relevant guidelines and regulations. The database buildup was approved by The Data Protection Official for Research (NSD).

Results

Patient characteristics. Clinical, histopathological and demographic variables and their impact on DSS are presented in Table 1. The median age was 67 years (range, 28–85), 373 patients (68%) were male, and the majority, 532 patients (96%), were current or previous smokers. The median follow-up time of survivors was 86 months (range, 34–267). Postoperative radiotherapy was administered to 76 (14%) patients due to non-radical surgical margins or nodal metastasis. Adjuvant chemotherapy was introduced in Norway in 2005, 43 (8%) patients received this treatment.

Scoring agreement. Scoring agreement between the scorers (SAS and KS) was excellent; ICC were 0.80 ($p < 0.001$) and 0.97 ($p < 0.001$) for miR-143 and miR-145, respectively.

miR-143 and miR-145 expression in NSCLC cells. *ISH expression of miR-143 and miR-145 in NSCLC cells and metastatic lymph nodes.* miR-143 was primarily observed in the cytoplasm of tumor epithelial and stromal cells, while miR-145 was mainly observed in the epithelial and stromal cell nuclei (Fig. 1). Table 2 reports miR-143 and miR-145 expression according to tissue compartment and gender. Neoplastic epithelial and stromal cells had significantly increased levels of miR-143 and miR-145 compared to non-malignant lung tissue (T-miR-143: $p < 0.001$, S-miR-143: $p < 0.001$, T-miR-145: $p = 0.005$, S-miR-145: $p = 0.020$). T-miR-143 expression in PT and LN+ was significantly correlated (0.220, $p < 0.001$). There was a significant correlation between miR-145 expression in neoplastic epithelial cells and stromal cells (0.362, $p < 0.001$). Similarly, miR-145 expression in PT and LN+ was significantly correlated (0.366, $p < 0.001$).

Relative expression of miR-143 and miR-145 in NSCLC cell lines. Endogenous levels of miR-143 and miR-145 in the studied NSCLC cell lines were quantified by qPCR, relative to the non-cancerous lung cell line NL20. Both miR-143 and miR-145 were downregulated in all the selected cell lines, compared to NL20 (Supplementary Fig. 1).

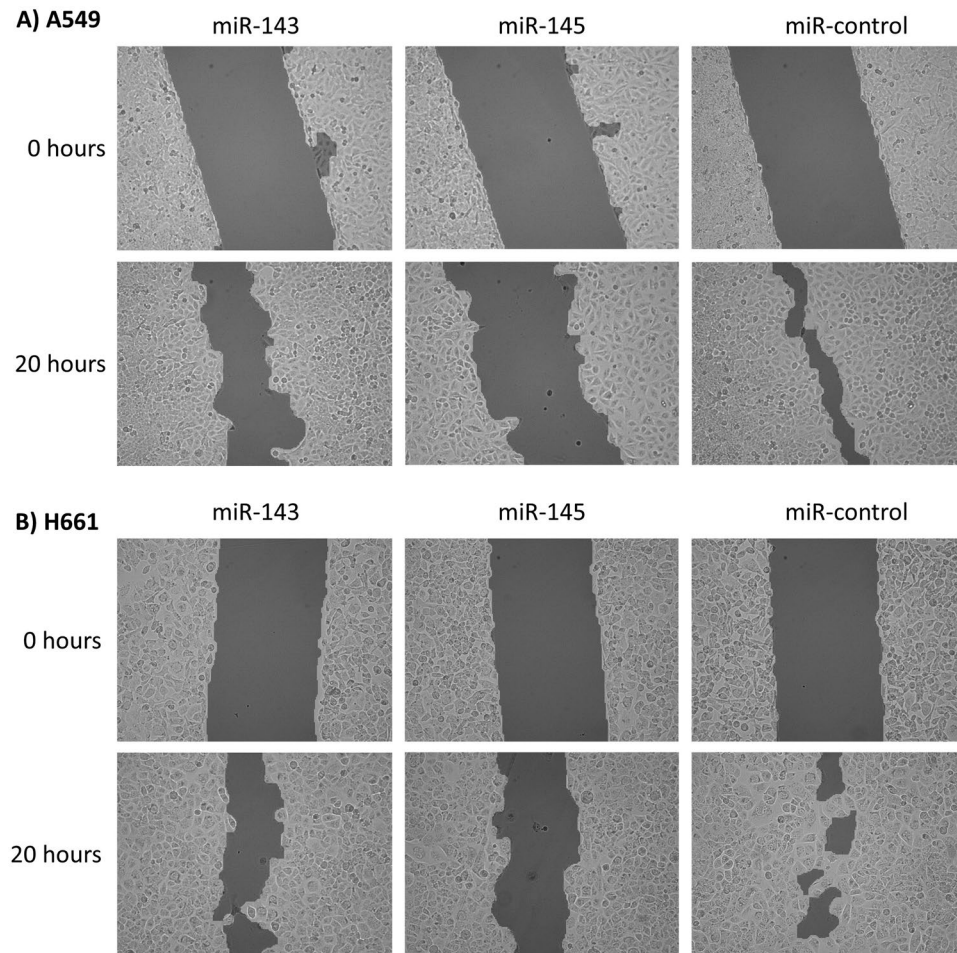


Figure 2. Functional studies on NSCLC cell lines: Migration. (A,B) Show that migration is inhibited in cells transfected with either miR-143 or miR-145 compared to cells transfected with the scrambled negative control. Data was collected at time point 0 and 20.

Functional studies on miR-143 and miR-145 in vitro. To investigate the potential function of miR-143 and miR-145 in NSCLC tumorigenesis, we performed a series of *in vitro* experiments. By transfecting various NSCLC cell lines with miR-143 mimic, miR-145 mimic and miR-143+miR145 mimic, we observed the biomarkers effect on cell migration and proliferation.

miR-143 and miR-145 inhibit NSCLC migration. Transfection with miR-143 and miR-145 inhibited migration in both the A549 and H661 cell line when compared with cells transfected with the negative control miRNA (Fig. 2). The inhibition was strongest for miR-145 in both cell lines.

Inhibition of proliferation by miR-143 and miR-145. Both miR-143 and miR-145 inhibited proliferation in the cell lines H460 and A549, and the inhibition was more evident for cells transfected with miR-145 (Fig. 3A,B). Transfection of miR-143 promoted proliferation in the H520 cell line, whereas miR-145 had an inhibitory effect on proliferation in the same cell line (Fig. 3C). In the cell lines A549 and H460, the inhibitory effects of co-transfection with miR-143 and miR-145 in equal concentrations, were equivalent to that of the miR-145 transfection alone. When co-transfecting the H520 cell line with equal concentrations of miR-143 and miR-145, the inhibitory effects displayed by transfecting miR-145 alone were reduced to a degree where the proliferation-rate was not significantly different to the negative control. Simultaneously, the increase in proliferation caused by the miR-143 transfection alone, was greatly reduced when the H520 cell line was co-transfected with both miR-143 and miR-145 in equal concentrations.

Correlation with clinical variables and other molecular markers. There were no significant associations between miR-143 and miR-145 expression in PT or LN+ and clinicopathological prognosticators listed in Table 1.

Between marker correlations with likely biological significance were as follows: LN+T-miR-143 was positively correlated with PT stromal AR expression ($r=0.494$; $p < 0.001$), and inversely correlated with PT tumor epithelial PGR expression ($-r=0.453$; $p < 0.001$). T-miR-143 in PT was correlated with cytoplasmic ER β in PT ($r=0.215$; $p < 0.001$) and T-miR-145 in PT was correlated with nuclear ER β expression in tumor cells ($r=0.212$; $p < 0.001$). Other significant correlations were also observed (Supplementary Table 1).

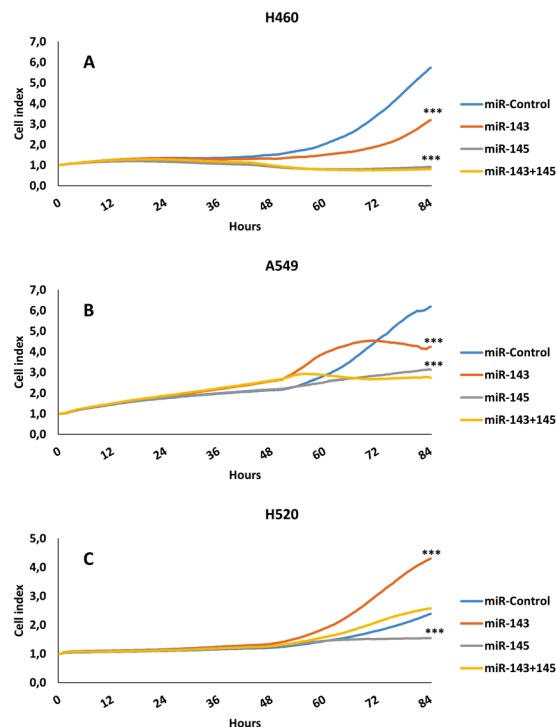


Figure 3. Functional studies on NSCLC cell lines: Proliferation. Panels show proliferation rate in cell lines H460, A549 and H520. Cell Index represents proliferation as a function of time. Panel A-H460: Both miR-143 and miR-145, alone or in combination, inhibits proliferation in H460 cells. The inhibitory effect is strongest in cells receiving the miR-145. Panel B-A549: Same inhibition pattern as panel (A). Panel C-H520: Introducing miR-143 promotes proliferation in this cell line, while transfection with miR-145 inhibits proliferation. *** indicates $p < 0.001$.

Univariate survival analyses. Clinicopathological variables and their impact on DSS are presented in Table 1. The impacts of biomarkers on DSS in PT are presented in Table 2 and Fig. 4. Neither epithelial nor stromal expression of miR-143 or miR-145 showed significant impact on DSS in the overall cohort. Following gender stratification, however, high S-miR-143 was a positive prognosticator in female patients ($p = 0.011$), while high S-miR-145 was a positive prognosticator in male patients ($p = 0.013$). Further, the combination of low S-miR-143 and low S-miR-145 was associated with an unfavorable prognosis in the overall cohort ($p = 0.007$, Fig. 5). In LN+, neither miR-143 nor miR-145 showed impact on DSS in the overall cohort or stratified by gender.

Multivariate analysis. Significant clinicopathological and biomarker variables from univariate analyses were entered into the multivariate analyses. Results are presented in Table 3. In primary tumors (PT), high S-miR-143 (HR: 0.53, 95% CI: 0.31–0.90, $p = 0.019$) and high S-miR-145 (HR: 0.58, 95% CI: 0.37–0.92, $p = 0.021$) were independent, positive prognosticators in female and male patients, respectively. The combination low S-miR-143/low S-miR-145 (overall cohort: HR: 0.57, 95% CI: 0.35–0.94, $p = 0.027$) was independently associated with an unfavorable DSS.

Discussion

In this large retrospective study of 553 NSCLC patients, S-miR-143 and S-miR-145 expression in PT were positive prognosticators in female and male patients, respectively. Further, the combination of low stromal expression of both miR-143 and miR-145 predicted poor DSS in the overall cohort. Cell line studies confirm the tumor suppressive role of miR-143 and miR-145 in NSCLC, further substantiating their importance in lung cancer pathogenesis. We also observe significant correlations with our previously investigated steroid hormone receptors, suggesting that a biological rationale may cause, or contribute to, the gender related survival impact observed.

To our knowledge, this is the first study investigating the prognostic impact of miR-143 and miR-145 in neoplastic epithelial cells, tumor associated stromal cells and matched metastatic lymph nodes in the same NSCLC cohort.

Associations between miR cluster 143/145 and cancer survival have been reported for different malignancies, results are, however, conflicting. In prostate cancer (PCa), Avgeris *et al.*¹⁷ demonstrated a shorter disease-free survival in PCa patients with low miR-145 expression levels. Campayo *et al.*¹⁸ reported similar results for miR-145 in NSCLC patients. These reports confirm our suggestion of high miR-145 expression as a positive prognosticator, herein in NSCLC patients. Contradicting our results, Al Feber *et al.*¹⁹ and Avgeris *et al.*²⁰, both reported associations between high levels of miR-143 and miR-145 and poor overall survival in esophageal and bladder cancer, respectively. Importantly, none of the aforementioned studies have evaluated survival impact according to cellular compartment, as was performed in our study.

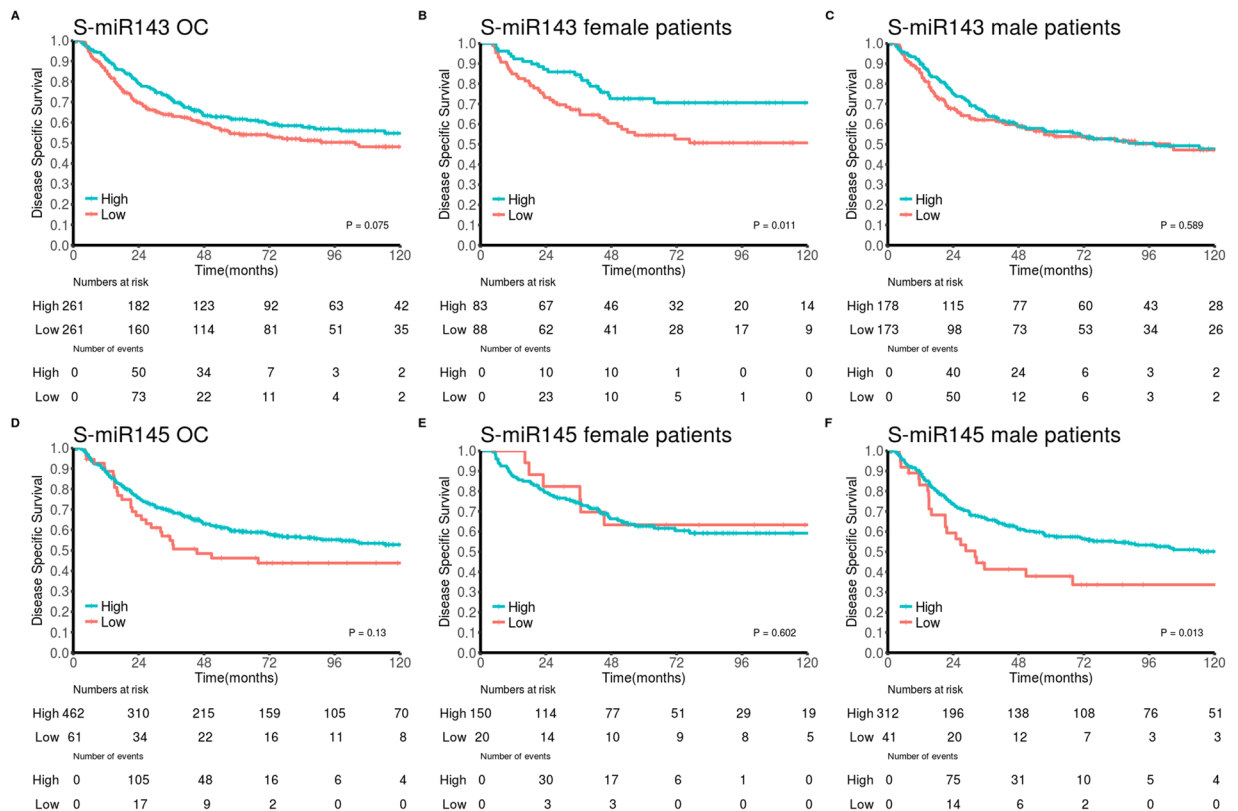


Figure 4. Survival curves. Kaplan-Meier curves showing disease-specific survival (DSS) in relation to stromal miR-143 and miR-145 expression in primary tumor. By dichotomizing biomarker expression level into high vs low, we present an association between improved DSS and high stromal biomarker expression. Overall cohort (OC): panel (A) (miR-143) and panel (D) (miR-145), female patients: panel (B) (miR-143) and panel (E) (miR-145), male patients: panel (C) (miR-143) and panel (F) (miR-145).

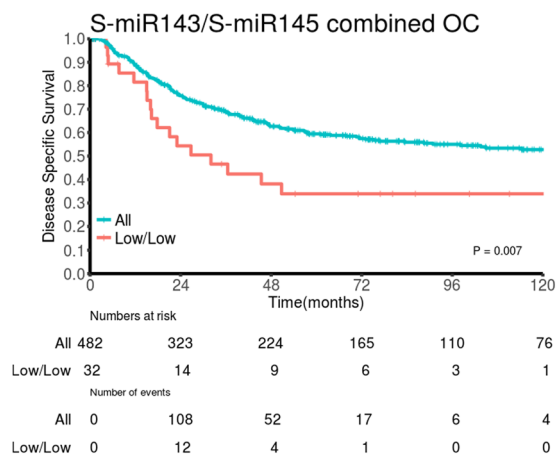


Figure 5. Survival curve. DSS survival curve according to co-expression of stromal miR-143 and stromal miR-145 in primary tumor in the overall cohort (OC). Low/low: low stromal miR-143 expression in combination with low stromal miR-145 expression.

Our findings suggest miR-143 and miR-145 to play protective roles when expressed in stromal cells. This is in concordance with the biomarkers being regarded as tumor suppressors²¹. miR-143 and miR-145 target several important genes involved in tumorigenesis including KRAS²² and ER α ¹¹. However, their biological function in NSCLC remains largely unknown. Functional studies have proposed different roles; Chen *et al.*, 2010 demonstrated that miR-145 inhibited NSCLC proliferation by targeting the transcription factor regulatory gene *c-Myc*¹³, thus confirming the tumor suppressive qualities of this particular miR. In a recent report Zhang *et al.*¹² suggest epidermal growth factor receptor (EGFR) as a downstream target of miR-143, contributing to tumor suppression.

	Overall cohort		Female patients		Male patients	
	HR (95% CI)	p	HR (95% CI)	p	HR (95% CI)	p
Pstage		<0.001		<0.001		<0.001
I	1 (ref)		1 (ref)		1 (ref)	
II	1.47 (1.03–2.09)	0.033	1.80 (0.92–3.55)	0.088	1.45 (0.96–2.18)	0.075
IIIA + IIIB	3.82 (2.69–5.44)	<0.001	5.02 (2.64–9.55)	<0.001	3.36 (2.28–5.06)	<0.001
Vascular infiltration		0.001		0.049		0.001
No versus Yes	1.82 (1.30–2.57)		1.75 (1.00–3.06)		2.10 (1.37–3.22)	
Sex		0.010	NE		NE	
Female versus Male	1.50 (1.10–2.04)					
ECOG perf. status		0.028	NE			0.050
0	1 (ref)				1 (ref)	
1	1.45 (1.09–1.93)	0.012			1.51 (1.08–2.11)	0.017
2	1.57 (0.82–3.03)	0.176			1.47 (0.71–3.08)	0.301
Primary tumors						
S-miR143				0.019	NE	
Low vs High	NE		0.53 (0.31–0.90)			
S-miR145	NE					0.021
Low vs High					0.58 (0.37–0.92)	
S-miR143/S-miR145		0.027	NE			0.027
Low vs High	0.57 (0.35–0.94)				0.50 (0.27–0.92)	

Table 3. Results of Cox regression analysis summarizing significant independent prognostic factors for disease-specific survival (DSS) in primary tumors (PT) in the overall cohort and stratified by gender (N = 553, 180 and 373, respectively). Abbreviations: S-miR, stromal miR expression. CI, confidence interval. ECOG perf. status, Eastern Cooperative Oncology Group performance status. HR, Hazard ratio. NE, not entered.

Consistent with our findings, Zhang *et al.*¹² demonstrated an inhibition of migration and proliferation of NSCLC cells following transfection with miR-143. Surprisingly, when we transfected the squamous cell carcinoma cell line H520 with miR-143, proliferation was dramatically increased (Fig. 3C). This is in contrast to most studies reporting on the effects of miR-143 on proliferation^{23–27}. However, there are studies depicting alternative roles for the miR cluster 143/145²⁸, and members of our research group have reported similar findings using breast cancer cell lines²⁹. Interestingly, when co-transfecting miR-143 and miR-145 in equal concentrations, the proliferative capacity was markedly reduced (Fig. 3A,B), meaning the net effect of co-transfecting is tumor suppressive.

The use of verified laboratory techniques with meticulously prepared protocols for biomarker handling is a strength with regards to reliability and reproducibility of our results. Our patient cohort is large with an extensive follow-up time, which further substantiate our results. The retrospective study design may represent a weakness with inaccurate clinical patient data.

In line with previous reports, we detect downregulation of both miR-143 and miR-145 in four independent cancer cell lines relative to levels in a non-cancerous cell line (Supplementary Fig. 1)^{30,31}. Thus, extending the general sense of miR-143/miR-145 downregulation in cancer, including NSCLC²¹. Interestingly, this is in contrast with our ISH-results, reporting significantly increased expression of miR-143/miR-145 in tumor cells and adjoining stromal cells in comparison to non-malignant tissue. To our knowledge, this is the first large-scale miRNA *in situ* NSCLC tissue hybridization analysis reporting an upregulated miR-143/miR-145 expression. These findings are conflicting with the smaller study (n = 48) by Shen *et al.*³¹, reporting a downregulation of miR-145 expression in NSCLC, by the use of ISH technique. We present a thorough and comprehensive study of miR-143 and miR-145 expression in appropriate cell types by the use of several acknowledged techniques, giving an optimal account of miR-expression in the tumor environment. Due to contributions from stromal cells in tumor growth, it is pivotal to consider the stromal compartment when elucidating biological mechanisms in epithelial cancers³². We found that miR-143 was primarily observed in the cell cytoplasm, while miR-145 was mainly observed in the nuclei of epithelial and stromal cells. Further, we report an abundant positivity of miR-143 and miR-145 in fibroblasts and SMCs lining the blood and lymph vessels, consistent with previous reports^{9,33}. miRs are traditionally considered to act within the cell cytoplasm, regulating gene expression post-transcriptionally³⁴. However, a number of miRNAs have been localized in the nuclei, although their nuclear functions remain elusive³⁵.

In an extensive meta-analysis, Kent *et al.*⁹ highlighted the crucial importance of cell-type localization of miRNAs, and how a lack of consideration of specific cellular expression of miRNAs may lead to a general misconception that miRNAs are downregulated in neoplastic tissue. Chivukula *et al.*³⁶, Dimitrova *et al.*²⁸ and Akao *et al.*³⁷ all published results indicating that neither miR-143 nor miR-145 are expressed in tumor epithelial cells, causing the latter group to conclude that these miRNAs are downregulated in malignant tissue. Similar results have been published by other groups investigating a variety of malignancies^{21,38,39}. However, only one²⁸ of the previous studies has focused on the histological cell-type localization of miR-143/miR-145. These factors, combined with the lung cancer cell lines lack of stroma, inflammatory cells and vascularization, may contribute to the discrepancy observed between miR-143/miR-145 expression in cell lines and tissue samples.

In this study, we present interesting correlations between miR-143/miR-145 and steroid hormone receptors expressed in the NSCLC tissue. The finding of gender specific survival significance of miR-143 and miR-145, forces us to consider sex hormones as a relevant factor. Delfino *et al.*⁴⁰ reported a gender-specific miRNA targeting of molecules related to glioblastoma survival. Further, Duttagupta *et al.*⁴¹ reported differential miRNA expression levels in a gender specific manner. Mounting evidence confirms activation of hormone receptors to be of utmost importance in lung cancer pathogenesis and several interesting cross-talk pathways between steroid hormones and miR-143/miR-145 have been found^{42–46}. Both miRNAs play a critical role in ovarian functioning, and a recent report presents miR-143 affecting estradiol production in granulosa cells by targeting KRAS^{47,48}. Further, Spizzo *et al.*, 2011 reported that miR-145 downregulates ER α expression in breast cancer¹¹. We found correlations between miR-143/miR-145 and AR, the rate limiting enzyme in estradiol production, suggesting the miRs may interact with regional estradiol production and ER signaling in the lung, as observed in breast tissue. In 2012, Paris *et al.* presented a study on estrogen effects in breast cancer, showing a direct regulation of miRNA expression and ER β signaling⁴⁹. Herein, ER β expression correlated with miR-143/miR-145 expression, suggesting a similar link may exist in NSCLC. The aforementioned reports, assembled with our findings, provide a compelling rationale for a biological cross-talk between miR-143/miR-145 and hormone receptors. If validated in larger, confirmatory studies, this may in fact represent new possibilities for targeted therapy for NSCLC patients, using gender, miRNA and hormone receptor expression as therapy selection criteria.

Conclusion

We present high stromal expressions of miR-143 and miR-145 as positive prognosticators in a gender specific manner in early stage NSCLC patients. Our findings indicate that miR-143/miR-145 acts as tumor suppressor molecules in lung cancer, suggesting that these miRNAs may be useful in miRNA based therapy in NSCLC. Further, we highlight the complexity of miR expression, and stress the importance of cell-type specific expression profiling. By accentuating the correlation between miRNA expression and hormone receptor expression, we emphasize the importance of exploring multi-targeted therapies in the treatment of NSCLC patients, as anti-hormonal therapy is highly accessible.

References

1. Ferlay, J. *et al.* Cancer incidence and mortality worldwide: sources, methods and major patterns in GLOBOCAN 2012. *International journal of cancer* **136** (2015).
2. Travis, W. D., Brambilla, E., Burke, A., Marx, A. & Nicholson, A. G. *WHO classification of tumours of the lung, pleura, thymus and heart.* (International Agency for Research on Cancer, 2015).
3. Siegel, R. L., Miller, K. D. & Jemal, A. Cancer statistics, 2016. *CA: a cancer journal for clinicians* **66**, 7–30 (2016).
4. Bartel, D. P. MicroRNAs: genomics, biogenesis, mechanism, and function. *Cell* **116**, 281–297 (2004).
5. Doench, J. G. & Sharp, P. A. Specificity of microRNA target selection in translational repression. *Genes & development* **18**, 504–511 (2004).
6. Calin, G. A. & Croce, C. M. *MicroRNA signatures in human cancers.* **6**, 857, <https://doi.org/10.1038/nrc1997> (2006).
7. Wiggins, J. F. *et al.* Development of a lung cancer therapeutic based on the tumor suppressor microRNA-34. *Cancer research* **70**, 5923–5930 (2010).
8. Reid, G. *et al.* Clinical development of TargomiRs, a miRNA mimic-based treatment for patients with recurrent thoracic cancer. *Epigenomics* **8**, 1079–1085 (2016).
9. Kent, O. A., McCall, M. N., Cornish, T. C. & Halushka, M. K. Lessons from miR-143/145: the importance of cell-type localization of miRNAs. *Nucleic acids research* **42**, 7528–7538 (2014).
10. Zhang, J. *et al.* Loss of microRNA-143/145 disturbs cellular growth and apoptosis of human epithelial cancers by impairing the MDM2-p53 feedback loop. *Oncogene* **32**, 61 (2013).
11. Spizzo, R. *et al.* miR-145 participates with TP53 in a death-promoting regulatory loop and targets estrogen receptor- α in human breast cancer cells. *Cell death and differentiation* **17**, 246 (2010).
12. Zhang, H. B., Sun, L. C., Ling, L., Cong, L. H. & Lian, R. miR-143 suppresses the proliferation of NSCLC cells by inhibiting the epidermal growth factor receptor. *Experimental and Therapeutic Medicine* **12**, 1795–1802 (2016).
13. Chen, Z. *et al.* miRNA-145 inhibits non-small cell lung cancer cell proliferation by targeting c-Myc. *Journal of Experimental & Clinical Cancer Research* **29**, 1 (2010).
14. Goldstraw, P. *et al.* The IASLC Lung Cancer Staging Project: proposals for revision of the TNM stage groupings in the forthcoming (eighth) edition of the TNM classification for lung cancer. *Journal of Thoracic Oncology* **11**, 39–51 (2016).
15. Bremnes, R. *et al.* High-throughput tissue microarray analysis used to evaluate biology and prognostic significance of the E-cadherin pathway in non-small-cell lung cancer. *Journal of Clinical Oncology* **20**, 2417–2428 (2002).
16. McShane, L. M. *et al.* REporting recommendations for tumour MARKer prognostic studies (REMARK). *British journal of cancer* **93**, 387–391 (2005).
17. Avgeris, M., Stravodimos, K., Fragoulis, E. & Scorilas, A. The loss of the tumour-suppressor miR-145 results in the shorter disease-free survival of prostate cancer patients. *British journal of cancer* **108**, 2573–2581 (2013).
18. Campayo, M. *et al.* Low miR-145 and high miR-367 are associated with unfavourable prognosis in resected nonsmall cell lung cancer. *European Respiratory Journal* **41**, 1172–1178 (2013).
19. Feber, A. *et al.* MicroRNA prognostic signature for nodal metastases and survival in esophageal adenocarcinoma. *The Annals of thoracic surgery* **91**, 1523–1530 (2011).
20. Avgeris, M. *et al.* Uncovering the clinical utility of miR-143, miR-145 and miR-224 for predicting the survival of bladder cancer patients following treatment. *Carcinogenesis* **36**, 528–537 (2015).
21. Das, A. V. & Pillai, R. M. Implications of miR cluster 143/145 as universal anti-oncomiRs and their dysregulation during tumorigenesis. *Cancer cell international* **15**, 92 (2015).
22. Kent, O. A. *et al.* Repression of the miR-143/145 cluster by oncogenic Ras initiates a tumor-promoting feed-forward pathway. *Genes & development* **24**, 2754–2759 (2010).
23. Wang, Q., Cai, J., Wang, J., Xiong, C. & Zhao, J. MiR-143 inhibits EGFR-signaling-dependent osteosarcoma invasion. *Tumour Biol* **35**, 12743–12748, <https://doi.org/10.1007/s13277-014-2600-y> (2014).
24. Xia, H. *et al.* miR-143 inhibits NSCLC cell growth and metastasis by targeting Limk1. *Int J Mol Sci* **15**, 11973–11983, <https://doi.org/10.3390/ijms150711973> (2014).
25. Liu, J. *et al.* MiR-143 inhibits tumor cell proliferation and invasion by targeting STAT3 in esophageal squamous cell carcinoma. *Cancer letters* **373**, 97–108, <https://doi.org/10.1016/j.canlet.2016.01.023> (2016).

26. Xu, Y. F. *et al.* Identification of miR-143 as a tumour suppressor in nasopharyngeal carcinoma based on microRNA expression profiling. *Int J Biochem Cell Biol* **61**, 120–128, <https://doi.org/10.1016/j.biocel.2015.02.006> (2015).
27. Zhang, W., Wang, Q., Yu, M., Wu, N. & Wang, H. MicroRNA-145 function as a cell growth repressor by directly targeting c-Myc in human ovarian cancer. *Technology in cancer research & treatment* **13**, 161–168, <https://doi.org/10.7785/tcrt.2012.500367> (2014).
28. Dimitrova, N. *et al.* Stromal Expression of miR-143/145 Promotes Neoangiogenesis in Lung Cancer Development. *Cancer Discov* **6**, 188–201, <https://doi.org/10.1158/2159-8290.CD-15-0854> (2016).
29. Johannessen, C. *et al.* Expression and function of the miR-143/145 cluster *in vitro* and *in vivo* in human breast cancer. *PLoS One* **12**, e0186658, <https://doi.org/10.1371/journal.pone.0186658> (2017).
30. Takagi, T. *et al.* Decreased expression of microRNA-143 and -145 in human gastric cancers. *Oncology* **77**, 12–21 (2009).
31. Shen, H. *et al.* Low miR-145 expression level is associated with poor pathological differentiation and poor prognosis in non-small cell lung cancer. *Biomedicine & Pharmacotherapy* **69**, 301–305 (2015).
32. Almeida, M. I. & Calin, G. A. The miR-143/miR-145 cluster and the tumor microenvironment: unexpected roles. *Genome medicine* **8**, 29 (2016).
33. Cordes, K. R. *et al.* miR-145 and miR-143 regulate smooth muscle cell fate decisions. *Nature* **460**, 705 (2009).
34. Roberts, T. C. The MicroRNA Biology of the Mammalian Nucleus. *Molecular therapy. Nucleic acids* **3**, e188, <https://doi.org/10.1038/mtna.2014.40> (2014).
35. Liao, J. Y. *et al.* Deep sequencing of human nuclear and cytoplasmic small RNAs reveals an unexpectedly complex subcellular distribution of miRNAs and tRNA 3' trailers. *PLoS one* **5**, e10563, <https://doi.org/10.1371/journal.pone.0010563> (2010).
36. Chivukula, R. R. *et al.* An essential mesenchymal function for miR-143/145 in intestinal epithelial regeneration. *Cell* **157**, 1104–1116 (2014).
37. Akao, Y., Nakagawa, Y. & Naoe, T. MicroRNAs 143 and 145 are possible common onco-microRNAs in human cancers. *Oncology reports* **16**, 845–850 (2006).
38. Lui, W.-O., Pourmand, N., Patterson, B. K. & Fire, A. Patterns of known and novel small RNAs in human cervical cancer. *Cancer research* **67**, 6031–6043 (2007).
39. Szczyrba, J. *et al.* The microRNA profile of prostate carcinoma obtained by deep sequencing. *Molecular cancer research* **8**, 529–538 (2010).
40. Delfino, K., Serão, N., Southey, B. & Rodriguez-Zas, S. Therapy-, gender- and race-specific microRNA markers, target genes and networks related to glioblastoma recurrence and survival. *Cancer Genomics-Proteomics* **8**, 173–183 (2011).
41. Duttagupta, R., Jiang, R., Gollub, J., Getts, R. C. & Jones, K. W. Impact of cellular miRNAs on circulating miRNA biomarker signatures. *PLoS one* **6**, e20769 (2011).
42. Weinberg, O. K. *et al.* Aromatase inhibitors in human lung cancer therapy. *Cancer research* **65**, 11287–11291 (2005).
43. Mah, V. *et al.* Aromatase expression predicts survival in women with early-stage non-small cell lung cancer. *Cancer research* **67**, 10484–10490 (2007).
44. Márquez-Garbán, D. C., Chen, H.-W., Fishbein, M. C., Goodglick, L. & Pietras, R. J. Estrogen receptor signaling pathways in human non-small cell lung cancer. *Steroids* **72**, 135–143 (2007).
45. Skjefstad, K. *et al.* Prognostic relevance of estrogen receptor α , β and aromatase expression in non-small cell lung cancer. *Steroids* **113**, 5–13, <https://doi.org/10.1016/j.steroids.2016.05.008> (2016).
46. Skjefstad, K. *et al.* The prognostic role of progesterone receptor expression in non-small cell lung cancer patients: Gender-related impacts and correlation with disease-specific survival. *Steroids* **98**, 29–36 (2015).
47. Zhang, L. *et al.* MiRNA-143 mediates the proliferative signaling pathway of FSH and regulates estradiol production. *Journal of Endocrinology* **234**, 1–14 (2017).
48. Hossain, M., Sohel, M., Schellander, K. & Tesfaye, D. Characterization and importance of microRNAs in mammalian gonadal functions. *Cell and tissue research* **349**, 679–690 (2012).
49. Paris, O. *et al.* Direct regulation of microRNA biogenesis and expression by estrogen receptor beta in hormone-responsive breast cancer. *Oncogene* **31**, 4196 (2012).

Acknowledgements

This study was funded by the Northern Norway Health Region Authority (Helse Nord RHF) and The Norwegian Cancer Society. The authors would like to thank them for supporting their work. The funders had no role in study design, data collection and analysis, decision to publish, or preparation of the manuscript. The publication charges for this article have been funded by a grant from the publication fund of UiT The Arctic University of Norway.

Author Contributions

Everyone included in the author list have been involved in the development and design of this study and manuscript. K.S. prepared the first manuscript draft, revisions and finalization was a collaboration between all co-authors. Statistical analysis and interpretation of results was performed by K.S. and C.J., with special contributions from T.G., S.A.S., and L.T.B. E.E.P., T.D., S.A.S., T.K., M.P. and K.S. have contributed to acquisition of data, enabling conduction of this study. C.J. has prepared Figures 2 and 3, T.K. has prepared Figures 4 and 5.

Additional Information

Supplementary information accompanies this paper at <https://doi.org/10.1038/s41598-018-26864-w>.

Competing Interests: The authors declare no competing interests.

Publisher's note: Springer Nature remains neutral with regard to jurisdictional claims in published maps and institutional affiliations.



Open Access This article is licensed under a Creative Commons Attribution 4.0 International License, which permits use, sharing, adaptation, distribution and reproduction in any medium or format, as long as you give appropriate credit to the original author(s) and the source, provide a link to the Creative Commons license, and indicate if changes were made. The images or other third party material in this article are included in the article's Creative Commons license, unless indicated otherwise in a credit line to the material. If material is not included in the article's Creative Commons license and your intended use is not permitted by statutory regulation or exceeds the permitted use, you will need to obtain permission directly from the copyright holder. To view a copy of this license, visit <http://creativecommons.org/licenses/by/4.0/>.

© The Author(s) 2018